Università degli Studi di Ferrara

DOTTORATO DI RICERCA IN
"Biochimica, Biologia Molecolare e Biotecnologie"

CICLO XXVI

COORDINATORE Prof. FRANCESCO BERNARDI

Mitochondrial calcium uptake and release mechanisms as key regulators of cell life or death

Settore Scientifico Disciplinare **MED/04**

Dottorando
Dott.ssa De Marchi Elena

Tutore
Prof. Pinton Paolo

Cotutore
Prof. Wieckowski Mariusz R.

Anni 2011/2013

TABLE OF CONTENTS

ABBREVIATIONS

Ca^{2+}	Calcium
$[Ca^{2+}]_c$	Cytoplasmic calcium concentration
$[Ca^{2+}]_m$	Mitochondrial calcium concentration
acetyl-CoA	acetyl coenzyme A
ADP	Adenosine 5’ diphosphate
ANT	Adenine Nucleotide Translocase
ATP	Adenosine 5’ triphosphate
$[ATP]_m$	mitochondrial ATP
ATP5A	ATP synthase, H+ transporting, mitochondrial F1 complex, alpha subunit
Bcl-2	B cell leukemia/lymphoma 2
CaM	Ca^{2+}-calmodulin
CaMK	Ca^{2+}-calmodulin kinase
Cdk	Cyclin-dependent kinase
CsA	Cyclosporine A
DAG	Diacylglycerol
DOA	Dominant Optic Atrophy
DRP1	Dynamin Related Protein 1
EMRE	Essential MCU Regulator
ER	Endoplasmic Reticulum
ETC	Electron Transport Chain
FACS	Fluorescence-Activated Cell Sorting
FAD	Flavin Adenine Nucleotide
FCCP	Carbonyl Cyanide –p- trifluoromethoxyphenylhydrazone
GFP	Green Fluorescent Protein
HIF1α	Hypoxiainducible Factor 1α

HA	Hemagglutinin
HK	Hexokinase II
HtrA2	High temperature requirement protein A2
IAP	Inhibitor of Apoptosis Protein
IB	Intracellular Buffer
IMM	Inner Mitochondrial Membrane
IMS	Intermembrane Space
IP_3	Inositol 1,4,5-trisphosphate
MAM	Mitochondria Associated Membrane
MCU	Mitochondrial Calcium Uniporter
MCUR1	Mitochondrial Calcium Uniporter Regulator 1
MEFs	Mouse Embryonic Fibroblasts
mgluR1	matabotropic glutamate Receptor
MICU1	Mitochondrial Calcium Uptake 1
ψ_m	Mitochondrial membrane potential
MPT	Mitochondrial Permeability Transition
mPTP	mitochondrial Permeability Transition Pore
mtGFP	mitochondrial Green Fluorescent Protein
NCLX	mitochondrial Na^+/Ca^{2+} antiporter
OMM	Outer Mitochondrial Membrane
pHH3	phosphohistone H3
PI	Propidium Iodide
PiC	inorganic Phosphate Carrier
Pin1	Peptidyl-prolyl cis/trans isomerase
PIP_2	Phosphatidylinositol-4,5-biphosphate
PPIF	Peptidyl Prolyl Isomerase F

RNA pol II	RNA polymerase II
RNS	Reactive Nitrogen Species
ROS	Reactive Oxygen Species
siRNA	short interfering RNA
TCA	Citric Acid Cycle
TSPO	Peripheral Benzodiazepine Receptor
VDAC	Voltage-Dependent Anion Channels

INTRODUCTION

Mitochondrial structure and functions

Mitochondria

Mitochondria are organelles with complex structures and functions. They are derived from an α-proteobacterium-like ancestor, due to an ancient "invasion" that occurred more than a billion years ago [1] The acquisition of mitochondria (and plastids) was a key event in the evolution of the eukaryotic cell, supplying it with bioenergetic and biosynthetic factors.

At subcellular resolution mitochondria are composed of an outer membrane (OMM), mostly permeable to ions and metabolites up to 10 kDa, and a highly selective inner mitochondrial membrane (IMM), characterized by invaginations called cristae. The space between these two structures is called the intermembrane space (IMS). Together, the OMM and IMM enclose the mitochondrial matrix. The IMM is further subdivided into two compartments: the peripheral inner boundary membrane and the cristae [2]. Cristae are not simply random folds, but rather internal compartments formed by profound invaginations originating from very tiny "point-like structures" in the inner membrane. These narrow tubular structures, called cristae junctions, can limit the diffusion of molecules from the intra-cristae space towards the IMS, thus creating a microenvironment where mitochondrial electron transport chain (ETC) complexes (as well as other proteins) are hosted and protected from random diffusion. The inner boundary membrane is enriched with structural proteins and components of the import machinery of mitochondria [3].

Mitochondrial morphology in living cells is heterogeneous and can range from small spheres to interconnected tubules. This heterogeneity results from the balance between fusion and fission processes, and represents a phenomenon termed mitochondrial dynamics [4]. A growing body of evidence indicates that mitochondrial morphology is critical for the physiology of the cell and changes in mitochondrial shape have been related to many different processes such as development, neurodegeneration, calcium (Ca^{2+}) signalling, reactive oxygen species (ROS) production, cell division, and apoptotic cell death [5].

Mitochondrial shape is controlled by the recently identified "mitochondria-shaping proteins", which regulate the fusion-fission equilibrium of the organelle. In mammals, key components of the fusion machinery include the homologues MFN1 and MFN2 [6]. The only dynamin-like GTPase currently identified in the IMM is OPA1, a fusion protein that

is mutated in dominant optic atrophy (DOA), the most common cause of inherited optic neuropathy. Post-transcriptional mechanisms, including proteolytic processing, tightly regulate OPA1 activity. In mammalian cells, mitochondrial division is regulated by DRP1 and FIS1 [7, 8]. The large GTPase DRP1 is a cytosolic dynamin-related protein, whose inhibition or downregulation results in a highly interconnected mitochondrial network. The same phenotype is caused by the downregulation of FIS1, a protein of the OMM, proposed to act as a mitochondrial receptor for DRP1 [9]. For example, mitochondrial dynamics seem to influence production of ROS and cellular longevity. DRP1-dependent fragmentation of the mitochondrial reticulum is a crucial component for accumulation of ROS in pathological conditions [10]. How mitochondrial fission is required for ROS production and lifespan remains unclear, although a link between the two processes seems plausible. Hence, factors other than mitochondrial metabolism *per se* could have a role in the pathogenesis of ROS-related diseases. Interestingly, many ROS (as well as Reactive Nitrogen Species, RNS) sources and targets are localized in the mitochondria and ER with are relevant consequences for different pathways [11].

Within cells, energy is provided by oxidation of “metabolic fuels” such as carbohydrates, lipids and proteins. It is then used to sustain energy-dependent processes, such as the synthesis of macromolecules, muscle contraction, active ion transport or thermogenesis. The oxidation process results in free energy production that can be stored in phosphoanhydrine “high-energy bonds” within molecules such as nucleoside diphosphate and nucleoside triphosphate (*i.e.*, adenosine 5' diphosphate and adenosine 5’ trisphosphate, ADP and ATP, respectively), phosphoenolpyruvate, carbamoyl phosphate, 2,3-bisphosphoglycerate, and other phosphates like phosphoarginine or phosphocreatine. Among them, ATP is the effective central link-the exchange coin-between energy producing and the energy demanding processes that effectively involve formation, hydrolysis or transfer of the terminal phosphate group.

In general, the main energy source for cellular metabolism is glucose, which is catabolized in the three subsequent processes: glycolysis, tricarboxylic acid cycle (TCA or Krebs cycle), and finally oxidative phosphorylation to produce ATP. In the first process, when glucose is converted into pyruvate the amount of ATP produced is low. Subsequently, pyruvate is converted to acetyl coenzyme A (acetyl-CoA) which enters the TCA cycle, enabling the production of NADH. Finally, NADH is used by the respiratory chain complexes to generate a proton gradient across the inner mitochondrial membrane, necessary for the production of large amounts of ATP by mitochondrial ATP synthase. In

addition, it should be mentioned that acetyl-CoA could be generated also by lipid and protein catabolism.

Citric Acid Cycle, Respiratory Chain and Oxidative Phosphorylation

The citric acid cycle (TCA) was elucidated by Sir Hans Krebs in 1940 [12]. The triose deriving from glycolysis is completely oxidized into three molecules of CO_2 during a sequence of reactions that allow the reduction of cofactors NAD and flavin adenine nucleotide (FAD), providing energy for the respiratory chain in the form of electrons. In 1949 Kennedy and Lehningher demonstrated that the entire cycle occurs inside mitochondria [12]. The first reaction of the citric acid cycle is the condensation of one Acetyl-CoA and a molecule of citrate to generate oxaloacetate and is catalysed by citrate synthase. Citrate is then transformed into isocitrate by aconitase through the formation of cis-aconitate. This step is reversible and could lead to the formation of both citrate and isocitrate. Only the fast consumption of isocitrate by its dehydrogenase can force the reaction to the proper direction. Isocitrate dehydrogenase catalyses the first irreversible oxidation leading to the decarboxylation of isocitrate, generating CO_2 and α-ketoglutarate. The second carbon leaves the cycle in the following step, when the newly generated α-ketoglutarate is immediately decarboxylated by the α-ketoglutarate dehydrogenase complex in a reaction similar to the pyruvate decarboxylation. In fact, both these complexes share high similarities in enzyme amino acid composition and in the organization of the different subunits. Energy released from both oxidations is used to generate NADH from NAD that directly feeds into the respiratory chain.

The following step is catalysed by succinyl-Coa synthetase and utilizes the energy derived from the CoA removal to phosphorylate GDP (or ADP) to GTP (or ATP). Selectivity for the nucleotide is determined by the isozyme involved. It has been well established that at least two isozymes of succinyl-CoA synthetase are expressed in animal tissues [13] and the proportion between them seems to be tissue specific.

The succinate generated in the previous step is the 4 carbon compound that is then converted, by three sequential reactions, to oxaloacetate to conclude the cycle. The first of these steps is the oxidation of succinate to fumarate by succinate dehydrogenase. This enzyme, tightly bound to the inner mitochondrial membrane (IMM), catalyses FAD reduction to $FADH_2$ that provides electrons for the respiratory chain. Fumarate is then hydrated by fumarate hydratase to L-malate. Both succinate dehydrogenase and fumarate

hydratase are oncosuppressor genes and their inactivation leads to the accumulation of succinate and fumarate that spread in the cytosol and promote hypoxiainducible factor 1α (HIF1α) accumulation by inactivating prolyl hydroxilase enzymes (promoter of HIF1α degradation); HIF1α, promotes a pseudo-hypoxic condition that favours tumour development [14]. The last event that completes the citric acid cycle is the oxidation of L-malate to oxaloacetate. This reaction is performed by L-malate dehydrogenase, which induces the reduction of another molecule of NAD to NADH. The resulting molecule of oxaloacetate is suitable for starting another cycle through condensation with an acetyl group.

During all these processes, only one molecule of ATP (or GTP) is produced, but three molecules of NADH and one of $FADH_2$ (plus one molecule of NADH from pyruvate dehydrogenase), which provide electrons for respiratory chain, are also generated and subsequently result in the production of large amounts of ATP [15].

The mitochondrial respiratory chain comprises a series of protein complexes and fat-soluble compounds which act as electron carriers and the majority of which are integral membrane proteins containing prosthetic groups capable of accepting or donating one or two electrons. It is located in the IMM and is able to produce an electrochemical potential across the mitochondrial membrane by creating a concentration gradient of H^+ ions between the two sides of the membrane. This potential is exploited to activate the transport channels present on the membrane and to promote the synthesis of ATP by ATP synthase.

The electron carriers of the respiratory chain are organized in separated supramolecular intramembrane complexes, and each of them represents a fraction of the respiratory chain (**Fig. 1**).

The complexes of the respiratory chain are:

- Complex I: NADH dehydrogenase
- Complex II: Succinate dehydrogenase
- Complex III: cytochrome c reductase
- Complex IV: Cytochrome c oxidase

All complexes are formed by multiple subunits and contain all the proteins encoded by nuclear DNA that is mitochondrial, except the Complex II which is entirely encoded by nuclear DNA. Coenzyme Q (ubiquinone) transfers the electrons previously transported in complex I and complex II from NADH and $FADH_2$ to complex III, and hence they will be conducted to complex IV by cytochrome c. It eventually transfers electrons directly to oxygen, leading to H_2O production.

Coenzyme Q (also called ubiquinone) is located between Complex I and Complex III and can accept only one electron, becoming a semiquinone radical, or two electrons acquiring the fully reduced ubiquinol form. Since ubiquinone is small in size and hydrophobic, it is freely diffusible in the lipid bilayer of the IMM and can act as a bridge between less mobile electron carriers in the same membrane.

The cytochrome c is also an essential part of the ETC. It is a peripheral membrane protein of 12.5 KDa soluble in water and weakly associated with the external surface of IMM due to interaction with cardiolipin [16]. This protein transfers electrons between complexes III and IV. Like all cytochromes it has a prosthetic group (heme group) and it is constituted by a tetrapyrrolic ring with an iron atom covalently bonded to the center. Cytochrome c allows the passage of electrons through the oscillation of the iron from the ferric form Fe^{3+} to the ferrous form Fe^{2+}.

The chemical mechanism which couples the proton flow with the phosphorylation is called Chemiosmotic Model and it was proposed by Peter Mitchell [17]. In agreement with this model the electrochemical energy contained in the difference of proton concentration and in the charge separation across the IMM leads to the synthesis of ATP when the proton flow reverses its direction and protons back into the matrix through a proton channel associated to the ATP synthase. The mechanism of action of ATP synthase was elucidated by the Nobel Prizes Paul Boyer and John Walker. ATP synthase could be divided in two main components: F_o that allows the channelling of protons, and F_1 that catalyses ATP phosphorylation. The F_o is embedded in the IMM, while the F_1 resides in the mitochondrial matrix and is bound to the F_o through a γ subunit (which drives conformational changes) and a b2δ dimer (that holds F_o and F_1 together). The protons flow from the intermembrane space to the matrix through the F_o inducing its rotation; the movement is transmitted from the γ subunit to the F_1 causing conformational rearrangements. The F_o region consists of three main subunits a (ATP6 gene), b (ATP5F1 gene) and c (ATP5G1, ATP5G2 and ATP5G3 genes), and in humans six additional subunits d, e, f, g, F6 and 8. The F_1 has a trimeric structure consisting of αβ dimers. The sequential changes are linked to the binding of substrates, phosphorylation and release of ATP. The three available dimers are never in the same conformational state and the conformational changes in one dimer drive rearrangements in the other [18]. This region consists of different protein subunits, α (ATP5A1 and ATPAF2 genes), β (ATP5B, ATPAF1 and C16orf7 genes), γ (ATP5C1 gene), δ (ATP5D gene) and ε (ATP5E gene). It has been calculated that for the synthesis of one ATP molecule, 4 protons are required [19]. Once synthetized, ATP can locate inside mitochondrial matrix or be transported into the IMS by the nucleotide exchanger adenine

nucleotide translocase (ANT) that passively exchanges ATP with ADP. Once in the IMS, ATP can freely pass the OMM through the voltage dependent anion channel (VDAC).

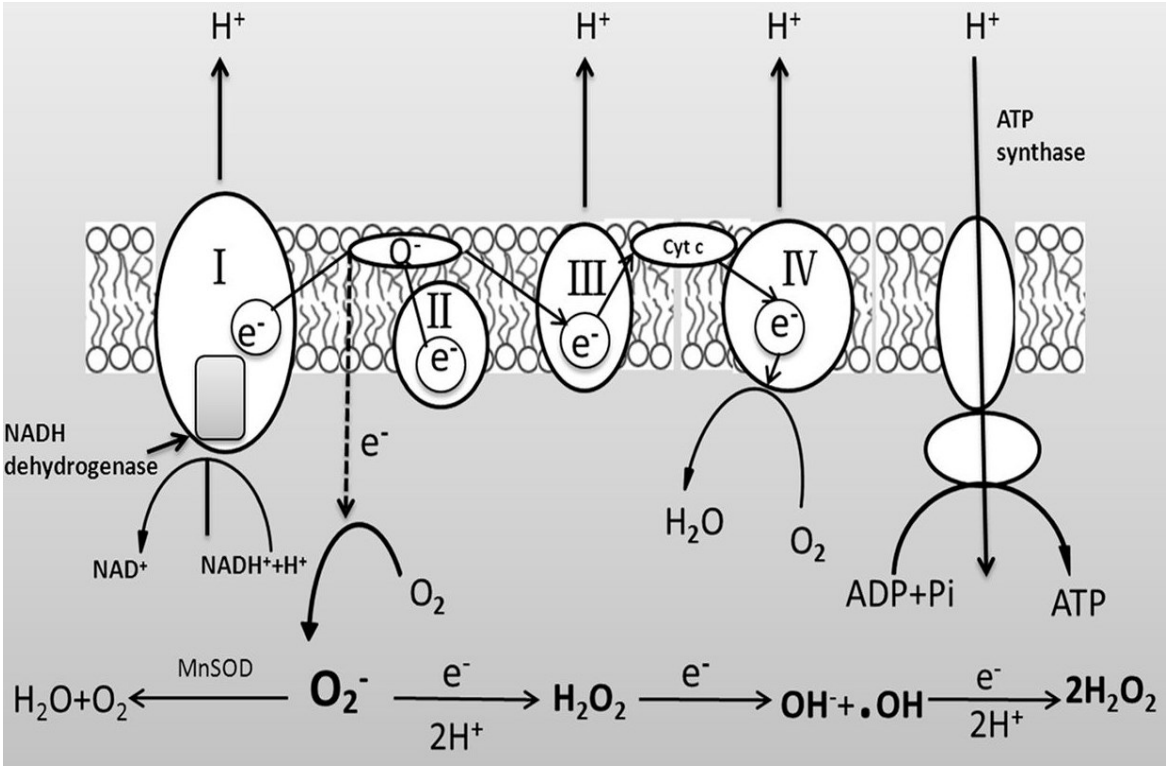

Figure 1: Schematic representation of mitochondrial electron transport chain [20].

A recent our work by Bonora et al. suggested moreover that the c subunit of the F_o ATP synthase constitutes a critical component of the mitochondrial Permeability Transition Pore (mPTP) and that it is required for the MPT, mitochondrial fragmentation and cell death induced by oxidative stress or mitochondrial Ca^{2+} overload [21]. However this part will be discussed more extensively in the thesis.

The concentration gradient of H^+ ions that is created between the two sides of the membrane is equivalent to a proton motive force and this is defined mitochondrial transmembrane potential which corresponds to -150/-180 mV in the cytosol [22]. This is essential for many processes, including the production of ATP by ATP synthase and the accumulation of Ca^{2+}. Dysfunction of the respiratory chain are associated with mitochondrial disorders and affect tissues that require a large amount of energy as the brain, heart and skeletal muscle [23].

Mitochondrial DNA encodes thirteen polypeptides, each of which is an integral subunit of respiratory chain complexes [24].

Mitochondria and cell fate

Mitochondria are also important checkpoints of the apoptotic process, as they may release caspase cofactors [25].

Apoptosis, or programmed cell death, is a highly regulated cellular event that plays an extremely important role in the tissue homeostasis and in the development of multicellular organisms. Defects in regulation of apoptosis are often associated with pathological conditions such as neurodegenerative diseases, tumorigenesis, autoimmune syndromes and viral infections. Apoptosis occurs through two pathways: the extrinsic pathway and the intrinsic or mitochondrial mitochondrial pathway, and it requires the action of specific enzymes (caspases) and regulatory proteins (such as those of the family Bcl-2). From the biochemical point of view, apoptosis is a proteolytic event generated by the activation of a large family of proteases called caspases (cysteine aspartate-specific proteases), generally present in the cytoplasm in the form of inactive enzymes.

The main player in the apoptotic activation process is cytochrome c. The majority of cytochrome c is tightly bound to mitochondrial inner membrane, thanks to its electrostatic interactions with acidic phospholipids, but a small fraction probably exists loosely attached to inner mitochondrial membrane and available for mobilization.

This protein is an irreplaceable component of the mitochondrial electron transport chain, shuttling electrons from complexes III to IV, and is thus essential to life: the disruption of its only gene is embryonic lethal [26]. Once released in the cytoplasm, this protein drives the assembly of a caspases activating complex together with Apaf-1 (apoptosis–protease activating factor 1) and caspase 9, the so-called ‘apoptosome’. Cytochrome c, once in the cytosol, induces the rearrangement and heptaoligomerization of Apaf-1: each of these complexes can recruit up to seven caspase molecules, leading to their proteolytic self-processing and consequent activation [27]. Mitochondria contain several other proapoptotic, intermembrane space-resident proteins, such as Smac/ DIABLO, HtrA2/Omi, AIF and EndoG. DIABLO (direct inhibitor of apoptosis-binding protein with a low isoelectric point) and HtrA2 (high temperature requirement protein A2) both have an N-terminal domain that can interact and inhibit IAPs (inhibitor of apoptosis proteins).

Another event that accompanies apoptosis is the loss of mitochondrial membrane potential caused by the opening of the PTP. The opening may be triggered by several factors, such as an excessive accumulation of Ca^{2+}, ATP depletion, oxidative stress, increased fatty acids or inorganic phosphate. PTP opening causes mitochondrial depolarization, followed immediately by mitochondria swelling, rupture of the OMM, release of cytochrome c and

other apoptotic factors, caspases activation and cell death by apoptosis. It is interesting to underline the important role of Ca^{2+} in this event, demonstrating how the mitochondrial Ca^{2+} signal represents a complex signaling pathway that mitochondria can translate in different biological consequences.

Moreover, mitochondria are the most important source of intracellular reactive oxygen species and leak from the electron transfer chain is supposed to be the main route [28]. An unexpected pathway has emerged that involves p66Shc in mitochondrial reactive oxygen species production. Intriguingly, upon phosphorylation by PKCβ and peptidyl–prolyl cis/trans isomerase (Pin1) recognition, p66Shc translocates to mitochondria [29] where it exerts its own oxidoreductase activity [30]. As a consequence, p66shc directly oxidizes cytochrome c (thus allowing electron to escape mitochondrial electron transport chain) and generates H_2O_2, leading to mPTP opening and in turn cell death [31] (**Fig. 2**).

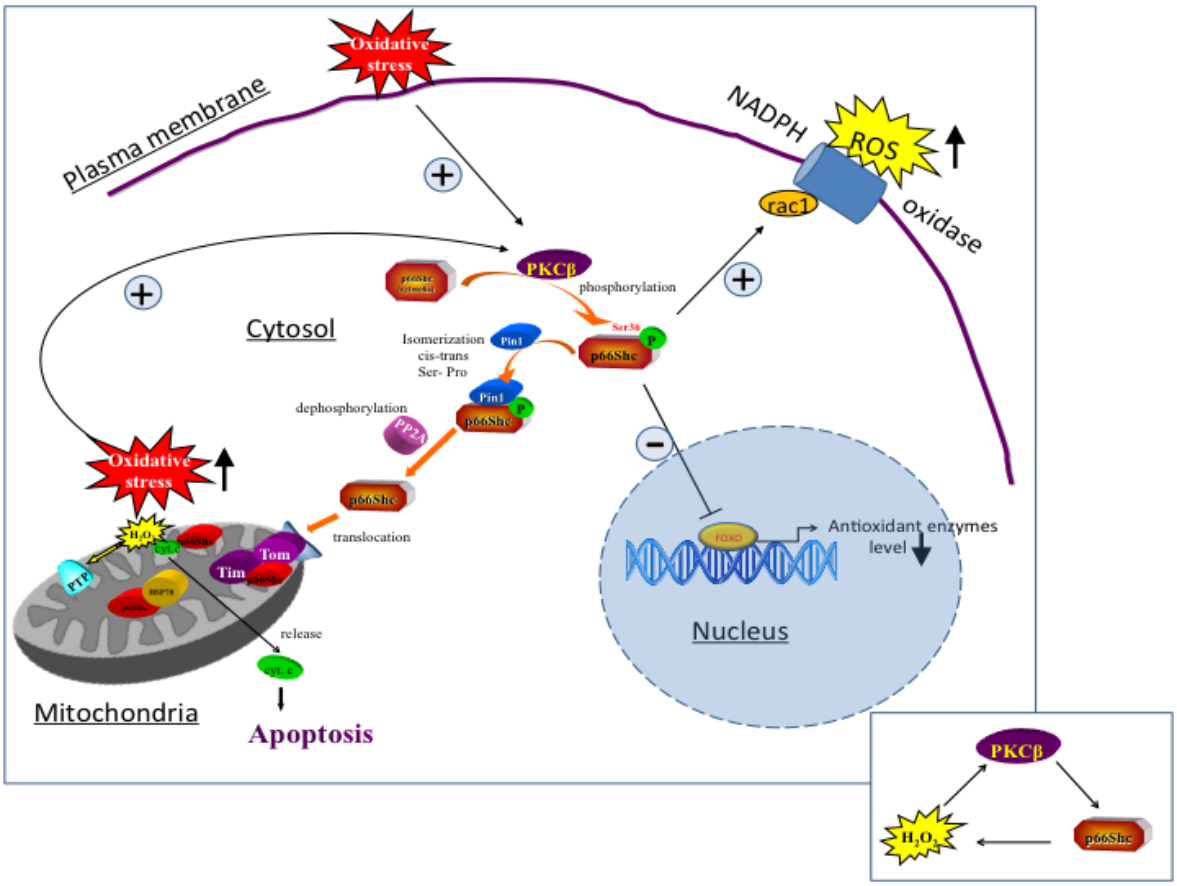

Figure 2: Signal transduction pathway of p66Shc in oxidative condition [31].

The study of Ca^{2+} homeostasis in apoptotic process has highlighted some important regulators of apoptosis, such as proteins of Bcl-2 family, which are located in compartments deeply involved in the intracellular Ca^{2+} levels regulation (mitochondria and

endoplasmic reticulum (ER)). Indeed, Bcl-2 was found to be associated to OMM, ER and nucleus; there is also a cytoplasmic form of Bcl-2 [32]. The Bcl-2 protein family controls the intrinsic pathway of apoptosis.

Proapoptotic Bax and Bak proteins exist as inactive monomers in viable cells with Bax localizing in the cytosol, loosely attached to membranes, and Bak residing in mitochondrial fraction. Upon apoptosis induction, Bax translocate to mitochondria where it homo-oligomerizes and inserts in the outer membrane; similarly, also Bak undergoes a conformational change, which induces its oligomerization at the outer mitochondrial membrane. Together, these events trigger OMM permeabilization, the crucial process mediating the release of intermembrane space-resident caspase cofactors into the cytoplasm [33].

Mitochondria also undergo a more 'macroscopic' remodelling of their shape during the programed cell death. Indeed, after apoptosis induction, mitochondria become largely fragmented, resulting in small, rounded and numerous organelles. This process occurs quite early in apoptotic cell death, soon after Bax/Bak oligomerization, but before caspase activation.

Mitochondrial and ER networks are also fundamental for the maintenance of cellular homeostasis and for the determination of cell fate under stress conditions [34]. The communication between the two organelles takes place via a zone of close contact between ER and mitochondria, called MAM (mitochondria associated membrane) [35], involved in bioenergetics and cell survival.

The intracellular Ca^{2+} signalling

In resting cells the $[Ca^{2+}]_c$ is carefully maintained at extremely low levels (100 nM), while the concentration of the ion in the extracellular space is about 1 mM. There are also intracellular organelles, such as the ER and secretory granules, which contain one to ten thousand fold greater concentrations of Ca^{2+} than the cytoplasm. There is an electric gradient between the two sides of the plasma membrane, which stands on values between -10 and -70 mV. The cell then spends a significant proportion of this energy against electrochemical gradient to maintain the concentration of this ion on such low values. However, in response to different stimuli the amount of the cation may increase significantly, up to 1-3 μM. The rapid increase in $[Ca^{2+}]$ in the cytoplasm is therefore one of the main features of the complex Ca^{2+} signal at the cellular level. The effect of this increase was correlated with an increasing number of physiopathological events. Muscle

contraction, hormone secretion, synaptic transmission, as well as the proliferation and apoptosis are just a few examples of Ca^{2+}-mediated processes. The fundamental question is how it is possible that different events may be regulated by a single messenger. The answer is found in the versatility of the Ca^{2+} signal.

In recent decades the huge amount of research done in this field has in fact revealed that the differences in amplitude, speed, and spatio-temporal characteristics of the $[Ca^{2+}]$ increase play an essential role in different events mediation.

This versatility is ensured by the great complexity of the systems to regulate the Ca^{2+} homeostasis: a lot of proteins (channels, pumps, receptors, enzymes, etc.) in fact collaborate in calcium signal activation, shutdown, and translation, and by the interaction with each other create many different spatio-temporal profiles of the signal responsible for the versatility and flexibility of the tasks of this intracellular messenger.

The processes that shape the Ca^{2+} signalling in all its complexity can be schematically divided into four functional units [36]:

- stimuli that produce messengers able to mobilize Ca^{2+} ions;
- the consequent Ca^{2+} signalling activation that feed Ca^{2+} into the cytoplasm;
- the role of Ca^{2+} as a second messenger;
- the OFF mechanisms of Ca^{2+} signalling, composed of pumps and exchangers that remove Ca^{2+} from the cytoplasm to restore resting conditions.

It is very important to discuss now the role of Ca^{2+} signalling in mitochondria. In the sixties in fact a lot of studies conducted in isolated organelles have demonstrated the ability of energized mitochondria to accumulate Ca^{2+} [37]. This has quickly found an explanation in the chemiosmotic theory that was becoming popular in those years. It became clear that the proton gradient generated by the activity of the respiratory chain may be used not only for the synthesis of ATP, but also to accumulate cations in the matrix.

Precisely the proton gradient determines the mitochondrial potential of about -180 mV (negative inside the organelle), which provides the driving force necessary to support the Ca^{2+} influx into the mitochondria. It has been calculated that the equilibrium would be reached only if the $[Ca^{2+}]$ in the matrix reached values 10^6 times higher than those present in the cytosol. Furthermore, the inhibition of the respiratory chain or the collapse of the membrane potential blocks the ability of mitochondria to accumulate the cation.

The development of new indicators such as aequorin allowed to demonstrate that the increase in $[Ca^{2+}]_c$ in live and intact cells induced by physiological stimuli is always accompanied by a parallel increase in mitochondrial matrix $[Ca^{2+}]$, where it reaches levels

much higher than in the cytosolic compartment (up to 500 μM in chromaffin cells). We can say that mitochondria play an active role in the signaling pathway of Ca^{2+}.

Mitochondrial Ca^{2+} uptake plays a key role in the regulation of many cellular functions, ranging from ATP production to cell death. Increases in mitochondrial calcium activate several dehydrogenases and carriers, inducing an increase in the respiratory rate, H^+ extrusion, and ATP production necessary for the correct energy state of the cell. However, prolonged increase in $[Ca^{2+}]_m$ leads to the opening of the mitochondrial permeability transition pore (mPTP), a critical event driving to cell death by apoptosis [38].

Although it is generally accepted that cellular energy metabolism, survival and death are controlled by mitochondrial Ca^{2+} signals, the underlying molecular mechanisms have been completely elucidated yet.

The mitochondrial Ca^{2+} uptake and release mechanisms are based on the utilization of gated channels for Ca^{2+} uptake and exchangers for release that are dependent upon the negative mitochondrial membrane potential, which represents the driving force for Ca^{2+} accumulation in the mitochondrial matrix [39].

There are several proteins involved in mitochondrial Ca^{2+} influx and efflux, such us the mitochondrial calcium uniporter (MCU) [40, 41] and the mitochondrial Na^+/ Ca^{2+} antiporter (NCLX) [42]. It is mostly accepted that Na^+/Ca^{2+} exchange activity is relevant for excitable cells [43] and that NCLX inhibition or silencing does not completely arrest Ca^{2+} efflux [42], which indicates that other mechanisms are involved in this process. Two mechanisms have been proposed to supplement Ca^{2+} efflux, one based on the H^+/Ca^{2+} antiporter [44] and another based on the mPTP [45], but evidence supporting the latter remains elusive (**Fig. 3**).

In particular this thesis focuses the attention on MCU and mPTP complex that are involved in the maintenance of mitochondrial Ca^{2+} homeostasis and more details are shown below.

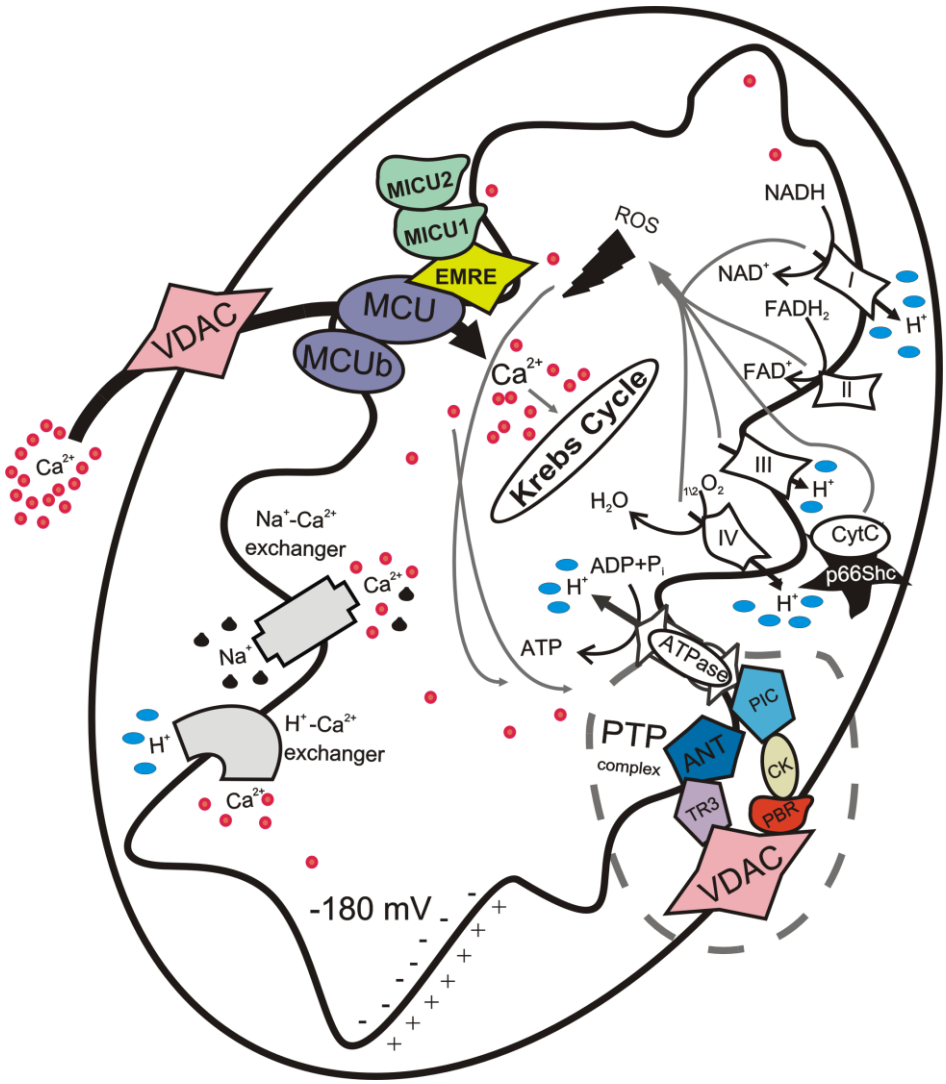

Figure 3: Schematic representation of mitochondrial calcium signalling.

Ca^{2+} signalling and cell cycle

Ca^{2+} signalling plays a crucial role in every cellular process, such us the origin of life, the fertilization and cell death. Several lines of evidence suggest that the intracellular Ca^{2+} concentration influences mitogenic signals that control the progression of the cell cycle. Despite these strong indications, little attention is paid to the role that Ca^{2+} has on this process [46].

In eukaryotes, Ca^{2+}-calmodulin (CaM) is one of the proteins more sensitive to Ca^{2+}, which constitutes a family of Ser/Thr kinases that are able to stimulate the Ca^{2+}-calmodulin kinase (CaMK). These proteins are involved in cell cycle regulation, in particular the G1/S phase progression and the exit from mitosis are dependent on changes in the concentration of CaM. The Ca^{2+} binding induces a modification of CaM and this is able to activate

several targets, such as ion channels and protein kinases. The selective inhibition of CaMKI leads to a block in the G1 phase due to a decrease in the cyclin D levels, an increased phosphorylation of pRb and prevention of the activation of cyclin-dependent kinases (Cdk) 4. The other isoform CaMKII is implicated in the progression into S phase, but also in the G2 and M phases [47].

Another protein involved in Ca^{2+} signalling is calcineurin, a heterodimer composed by the catalytic subunit calcineurin A and the regulatory, Ca^{2+}-binding subunit calcineurin B. This protein is activated as a result of changes in intracellular [Ca^{2+}] and it controls the cell cycle progression with the proteins of the CaMK family. In particular, in the G1 phase inhibition of both proteins stops the cycle before the activation of the cyclin D1/Cdk4 complex. During the G1/S transition, the inhibition of calcineurin and CaMK leads to the accumulation of p21 and p27 respectively, the increase of the levels of these proteins is sufficient to inactivate Cdk2 and to block the cell cycle. Finally, CaMKII is the target of CaM during the G2/M transition and also during the metaphase/anaphase transition [48].

Changes in the mRNA of CaM are associated with a transition of cells from G1 phase to the quiescent phase. CaMs are also capable of activating DNA polymerase α and δ, indicating a role in the PCNA transcription. Ca^{2+} and CaM are involved also in the breakdown of the nuclear envelope, cytokinesis and in the contraction of myosin's ring [46].

MCU, the Mitochondrial Calcium Uniporter

Ca^{2+} accumulation into mitochondria plays a fundamental role in many cellular processes and occurs through the uniporter, thanks to a mechanism driven by the membrane potential generated by the respiratory chain. The activity and biochemical properties of the MCU have been characterized for years, but the molecular identity of the channel has remained unknown for a long time [49].

The molecular characterization of MCU was a major challenge for several reasons, including the lack of a selective inhibitor (the uniporter was inhibited not specifically by ruthenium red) and a yeast homolog of the uniporter.

MCU has a low affinity for Ca^{2+}; in fact, MCU takes up Ca^{2+} in the micromolar range and experiments in permeabilized cells report a K_d of the uniporter of 10 μM [50]. In addition, a biphasic effect of calcium on the MCU has been reported: beyond a certain level, cytosolic Ca^{2+} inactivates the uniporter, preventing further Ca^{2+} uptake and this process might avoid an excessive accumulation of the cation in mitochondria [51].

Initially the candidates proposed for the MCU were the uncoupling proteins UCP2/3 [52], but this suggestion was then retired [53]. Recently, Perocchi and colleagues [54] demonstrated that MICU1 (mitochondrial calcium uptake 1) has a key role in regulating the classically defined uniporter.

Finally in 2011 it has been discovery the molecular identity of MCU, the coiled-coil domain-containing protein 109A (CCDC109A) [40, 41, 55].

The nuclear MCU gene, located on chromosome 10, encodes for a protein of 40 kDa but it loses its target sequence when it is imported into the mitochondria. The result is a mature 35-kDa protein expressed in all tissues, capable of oligomerization, giving rise to a complex of higher molecular weight [41].

From the topological point of view, the MCU is located in the IMM, with the N-terminal and the C-terminus facing the matrix; there is a linker of 9 aa (the DIME domain) facing in the IMS between the two transmembrane domains. The DIME domain is essential for the Ca^{2+} transport because mutations inside it render the protein non-functional [41].

The overexpression of MCU increases mitochondrial Ca^{2+} uptake and sensitizes cells to apoptotic stimuli, and the employment of short interfering RNA (siRNA) silencing of MCU strongly reduced mitochondrial Ca^{2+} uptake. This reduction is specific for mitochondria, does not induce impairment of the electrochemical gradient or change in mitochondrial morphology and the induction of specific mutations at the level of the putative pore-forming region reduce the mitochondrial calcium uptake and blocks the channel activity of the protein [40]. Recently it was shown that miR-25, a small (22 nucleotides) noncoding regulatory RNA overexpressed in several human cancers, decreases mitochondrial Ca^{2+} uptake through selective MCU downregulation, conferring resistance to apoptotic challenges. MCU appears to be downregulated in human colon cancer samples, and accordingly, miR-25 is aberrantly expressed, indicating the importance of mitochondrial Ca^{2+} regulation in cancer cell survival [56].

About MICU1, previously identified as regulator of MCU, recently it has been shown that it is a 54-kDa single-pass membrane protein containing two highly conserved EF-hand Ca^{2+}-binding domains. Through [57] or independently [58] of these domains MICU1 stabilizes the closed state of the MCU complex limiting mitochondrial Ca^{2+} entry.

MICU1 has two paralogues (MICU2 and MICU3) possessing N-terminal mitochondrial targeting sequences. MICU2 localizes in mitochondria, it has a highly conserved EF-hand domain and interacts with MICU1 and MCU [59].

It was also recently discovered another isoform of MCU, called MCUb. It is a protein of 33 kDa that shares 50% of similarity with MCU. Its topology and structure is very similar to

that of MCU. It has two transmembrane domains with the N-terminal and the C-terminus facing the IMS but it has a lower level of expression and a different expression profile compared to the MCU. MCUb might be a dominant-negative isoform and the insertion of one or more MCUb subunits in the multimer might alter the permeability to Ca^{2+} [60]. However the mRNA levels of MCUb are very low when compared to MCU levels; this mRNA is highly expressed in the heart and lungs and little expressed in skeletal muscle. Variations of tissue-dependent accumulation of mitochondrial Ca^{2+} have been reported, and the Ca^{2+} influx in skeletal muscle is 28-fold greater than in cardiac mitoplasts [61].

In 2012 it has been identified also a regulator of MCU, CCDC90A or MCUR1 (mitochondrial calcium uniporter regulator 1), an integral membrane protein required for MCU-dependent mitochondrial Ca^{2+} uptake [62]. MICUR1 interacts with MCU but not with MICU1 and these three proteins do not exist in the same complex [62].

It has been identified also an essential MCU regulator (EMRE), it is a component of the uniporter complex and it interacts with MICU1 at IMS and with MCU oligomers in the inner membrane. [63].

Therefore the uniporter complex (uniplex) seems to be composed of MCU holomers, MCUb, MICU1, MICU2 and EMRE [63, 64].

The latest work by Patron et al. shows also that MICU1 and MICU2 finely tune the MCU by exerting opposite effects on MCU activity; at low [Ca^{2+}] MICU2 largely shuts down MCU activity, at higher [Ca^{2+}] MICU1 allows the response of mitochondria to Ca^{2+} signals generated in the cytoplasm [65].

Thus, MCU complex is important for mitochondrial Ca^{2+} uptake and the equilibrium of all the components manteins the normal cellular bioenergetics (**Fig. 4**).

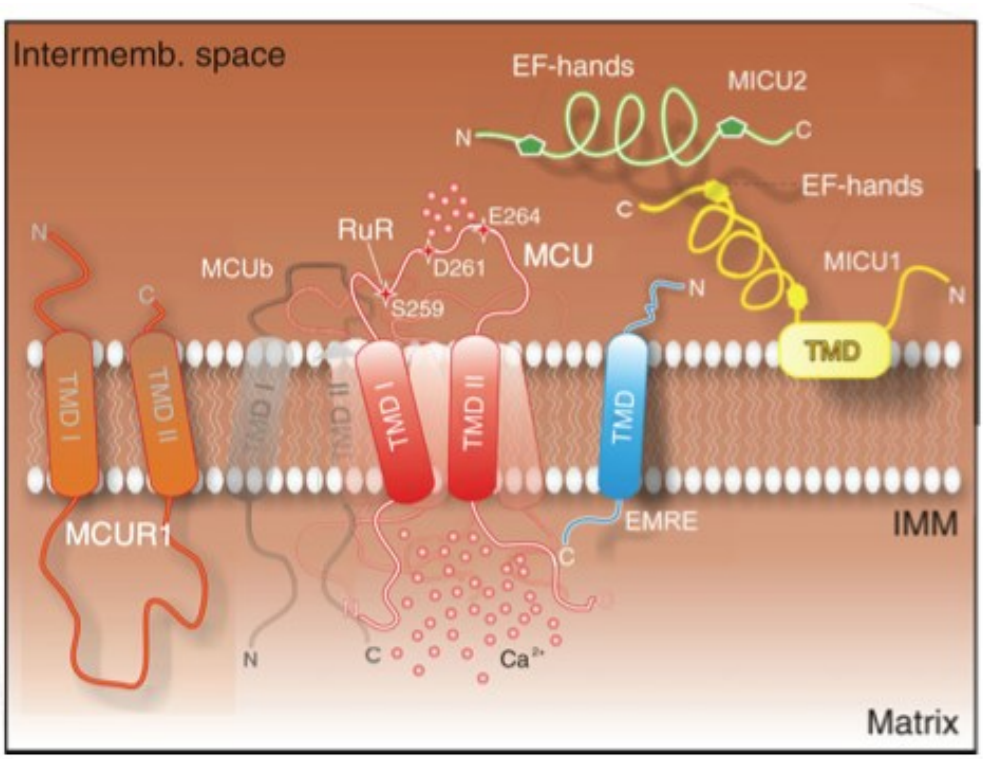

Figure 4: Schematic representation of the different components of the uniporter complex [64].

mPTP, the mitochondrial Permeability Transition Pore

The mPTP is a high-conductance channel located at the contact sites between the inner and outer mitochondrial membranes. This channel is responsible for the non-selective permeability state of the mitochondrial inner membrane. The transition to this state for small molecules is referred to as the MPT. Due to osmotic forces, MPT results in a massive influx of water into the mitochondrial matrix, eventually leading to the structural break-down of the organelle [25, 66].

The molecular composition of the mPTP is not yet clear, but several proteins have been shown to be components that participate in mPTP activity, including VDAC [67], ANT [68], the inorganic phosphate carrier (PiC) [69], peptidyl prolyl isomerase F (PPIF) [70, 71], the peripheral benzodiazepine receptor (TSPO) [72], hexokinase II (HKII) [73] and several members of the Bcl-2 family. Both pro- and anti-apoptotic BCL-2 family members, including BAX, BID, BCL-2 and BCL-X_L [74-76] have been shown to physically bind to- and hence modulate the function of-PTPC components, indicating that the molecular machineries mediating MPT-driven and primary MOMP do not operate in a mutually exclusive manner.

Ca^{2+} ions, prooxidant and proapoptotic proteins, a decrease in the mitochondrial membrane potential, pH variations and adenine nucleotides all sensitize the opening of the pore [25, 77].

MPT resulting from mPTP opening is usually considered a transducer event in between Ca^{2+} or oxidative signal and different type of cell death [78, 79].

Recently, we suggested that, similar to PPIF, the c subunit of the F_O ATP synthase constitutes a critical component of the mPTP and that it is required for the MPT, mitochondrial fragmentation and cell death induced by oxidative stress or mitochondrial Ca^{2+} overload [21] (discussed later) (**Fig. 5**).

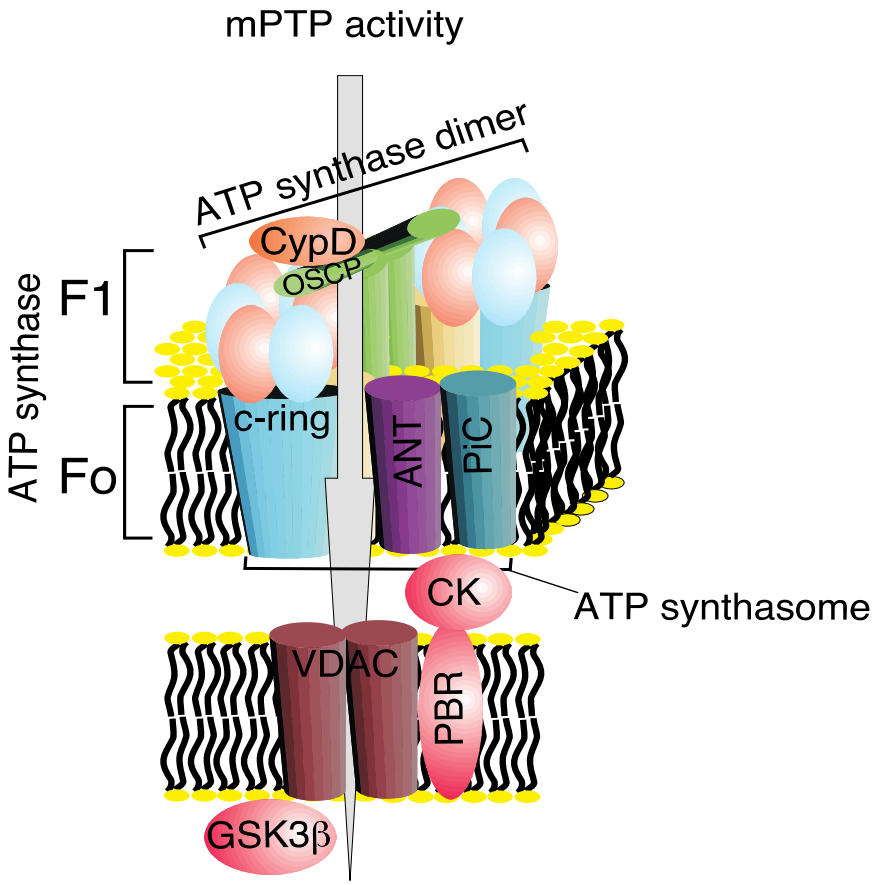

Figure 5: Schematic representation of the different components of the mPTP complex.

Nonetheless several observations have suggested that mPTP is a component of the Ca^{2+} efflux mechanism [80, 81] proposing a physiological role for this ambiguous complex. Unfortunately a different amount of studies have proposed the exact opposite [82, 83] leaving this supposition still unresolved.

In this thesis I will focus also my attention on the role of mPTP in mitochondrial Ca^{2+} homeostasis in a non-pathological context.

[Ca^{2+}] measurements by the photoprotein Aequorin

At the beginning of the nineties, due to the rapid development of molecular biology techniques, the aequorin cDNA was cloned and this opened the possibility to transfect the gene and obtain the expression of this protein in live cells. It was then possible to specifically localise it within the cell by including defined targeting signals in the amino acid sequence to measure variations in [Ca^{2+}] in well-defined subcellular compartments in a highly specific manner [84].

Aequorin was extracted and purified in 1962 by the luminescent jellyfish Aequorea Victoria [85]. It consists of a monomeric apoprotein of 189 amino acids and a hydrophobic prosthetic group (coelenterazine) of 400 Da. The ability of the bioluminescent protein is closely related to the presence of the prosthetic group. The probe has three high affinity EF-hand regions able to bind Ca^{2+}. When the cation binds aequorin there is a conformational change of the protein resulting in the bond breaking between apoprotein and coelenterazine, irreversible oxidation of the latter and photon emission (**Fig. 6**). In nature, the detachment of the prosthetic group in the form of celenteramide is irreversible and in vitro an active aequorin can be obtained by incubating the apoprotein with coelenterazine in the presence of oxygen and 2-mercaptoethanol. Reconstitution of an active aequorin (expressed recombinantly) can be obtained also in living cells by simple addition of coelenterazine to the medium.

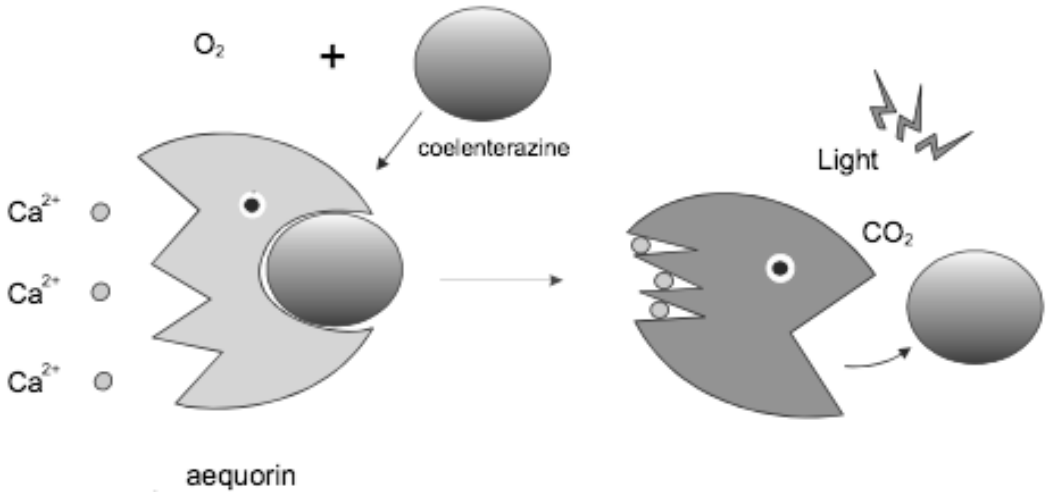

Figure 6: Scheme of the Ca^{2+} induced photon emission process.

The rate of photons emission is measured by a photomultiplier and it can be converted to $[Ca^{2+}]$: under known conditions of pH, $[Mg^{2+}]$, ionic strength and temperature and aequorin exposure to solutions containing known amounts of Ca^{2+} it is possible to draw a sigmoidal calibration curve which correlates the $[Ca^{2+}]$ with the ratio of light emitted at any istant by the photoprotein and measured by the photomultiplier (L) and the light emitted from the same aequorin in the presence of saturating $[Ca^{2+}]$ (Lmax). [86] (**Fig. 7**).

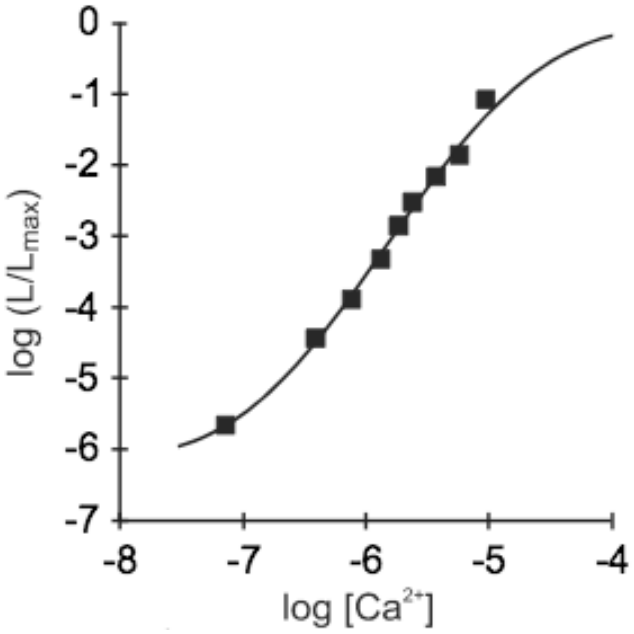

Figure 7: Relationship between the free Ca2+ concentration and the rate of aequorin photon emission [86].

The rate of aequorin luminescence is independent of $[Ca^{2+}]$ at very high ($>10^{-4}$ M) and very low $[Ca^{2+}]$ ($< 10^{-7}$ M). However it is possible to expand the range of $[Ca^{2+}]$ that can be monitored with aequorin.

Until now, different recombinant aequorins were obtained, each characterized by a precise subcellular localization, by including specific targeting sequencing in the engineered cDNAs, and all targeted aequorins synthesized in our laboratory include modifications of the photoprotein N-terminal. As demonstrated by Watkins and Campbell in fact, the C-terminal proline residue of aequorin is essential for the long-term stability of the bound coelenterazine so it is not possible to alterate it [87].

It is also possible to introduce a point mutation in one of three sites able to bind Ca^{2+} (AEQmut) to reduce the affinity of the protein for the cation and thus to obtain accurate measurements in a wider range of concentrations (between 1 and 200 μM). Finally, for

higher [Ca^{2+}] it is possible to use a modified,prosthetic group, the coelenterazine n, which has lower affinity for the cation [88].
Below I briefly describe the constructs that I used in this thesis.

Cytoplasm (cytAEQ)

An unmodified aequorin cDNA encodes a protein that, in mammalian cells is located in the cytoplasm and, given its small size, also diffuses into the nucleus. An alternative construct was also available that is located on the outer surface of the ER and of the Golgi apparatus. This construct was intended to drive the localization of aequorin to the inner surface of the plasma membrane given that it derives from the fusion of the aequorin cDNA with that encoding a truncated metabotropic glutamate receptor (mgluR1). The encoded chimeric protein, however, remains trapped on the surface of the ER and Golgi apparatus, with the aequorin polypeptide facing the cytoplasmic surface of these organelles. The cytoplasmic signal revealed by this chimeric aequorin is indistinguishable from that of a cytoplasmic aequorin, but it has the advantage of being membrane bound and excluded from the nucleus (**Fig. 8**).

Mitochondria (mtAEQ)

All mitochondrial proteins, but the 13 encoded by the organellar genome, are synthesized on cytoplasmic ribosomes and then imported into the organelle. In most cases, import depends on the presence of a cleavable signal at the N-terminus of a precursor protein. This signal (rich in basic and hydroxylated residues, and devoid of acidic ones) usually referred to as mitochondrial presequence, is removed after import by matrix proteases [89]. When added to a heterologous protein, a mitochondrial presequence is sufficient to drive its import into mitochondria. MtAEQ was the first targeted aequorin generated in the laboratory, which has been successfully employed to measure the [Ca^{2+}] of the mitochondrial matrix of various cell types. This construct includes the targeting presequence of subunit VIII of human cytochrome c oxidase fused to the aequorin cDNA [84] (**Fig. 8**).

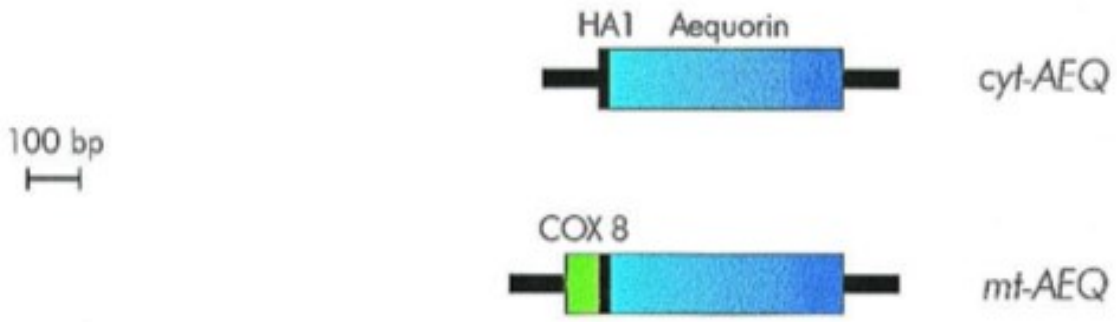

Figure 8: Schematic representation of aequorin chimeras.

Luminescence detection

The aequorin detection system is derived from that described by Cobbold and Lee [90] is based on the use of a low noise photomultiplier placed in close proximity (2-3 mm) of aequorin expressing cells. The cell chamber, which is on the top of a hollow cylinder, is adapted to fit 13-mm diameter coverslip. The volume of the perfusing chamber is kept to a minimum (about 200 µl). The chamber is sealed on the top with a coverslip, held in place with a thin layer of silicon. Cells are continuously perfused via a peristaltic pump with medium thermostated via a water jacket at 37°C. The photomultiplier (EMI 9789 with amplifier-discriminator) is kept in a dark box. During manipulations on the cell chamber, the photomultiplier is protected from light by a shutter. During aequorin experiments, the shutter is opened and the chamber with cells is placed in close proximity of the photomultiplier. The output of the amplifier-discriminator is captured by an EMIC600 photon-counting board in an IBM compatible microcomputer and stored for further analysis.

Recently it has been extensively explained with a specific protocol the subcellular Ca^{2+} measurements in mammalian cells using aequorin-based probes [91].

MCU involvement in cell cycle

Introduction

Cell cycle, cyclins and cyclin-dependent kinases

Cell division is a universal process for living organisms and it ensures reproduction, growth and development of the organism. The regulation of this process is the basis of cell ability to maintain genetic integrity, which is important to cell survival and proliferation [92]. At present proteins alterations involved in cell cycle regulation are of considerable interest, because they are directly involved in the tumor development. Therefore, understanding all the mechanisms that regulate cell proliferation becomes increasingly indispensable.

In mammals cell cycle consists of two main phases: interphase and mitosis. The interphase occupies most of the time of cell division and can be further divided into:

- G1 phase, which prepares the cell for the genetic material division with a size increase and synthesis of numerous proteins and organelles such as mitochondria and ribosomes. At a certain point - the restriction point - the cell is committed to division and moves into the S phase.
- S phase, during which DNA synthesis replicates the genetic material. Each chromosome now consists of two sister chromatids.
- G2 phase, which runs from the completion of S phase until the phase of mitotic division. It is characterized by a high metabolic activity and the synthesis of the mitotic spindle;
- G0 phase or "quiescent state" is the phase in which cells do not divide because they are already differentiated and do not continue in the division cycle, or it may be a waiting phase to proceed the division later. They are busy carrying out their functions in the organism. e.g., secretion, attacking pathogens. Most of the lymphocytes in human blood are in G0. However, with proper stimulation, such as encountering the appropriate antigen, they can be stimulated to reenter the cell cycle at G1.

  The mitotic phase includes the most significant events of cell division and can be divided into two phases: mitosis and cytokinesis. During interphase, chromosomes are not visible individually but they are condensed in the form of chromatin, an association

of DNA and protein present in the nucleus, in the step of division the chromatin coils in individual chromosomes that will then be divided.

The mechanism of division involves the diploid somatic cells (2n): they consist of two pairs of homologous chromosomes that carry both genes that control the same characteristics.

A class of proteins directly involved in cell cycle progression are cyclins, discovered in 1983 by Tim Hunt and his colleagues [93]. Cyclins levels vary drastically through the phases of the cell cycle as a result of transcriptional changes and degradation mediated by the proteasome.

There are eight cyclins involved in cell cycle progression: cyclin A1 and A2, B1-B2-B3, C, D1-D2-D3, E1-E2, F, G1-G2, H. All these show a 150 amino acid residues region called cyclin box; this domain consisting of five helices [94] is responsible for the binding of the N-terminal part of specific Cdk [95].

The fluctuation of the expression levels of these proteins has been demonstrated by the fact that cyclins A and B are accumulated at the beginning of S phase and in the late G2 phase respectively, while in G1 phase cyclin D1 levels increase and remain high until the mitosis. While cyclins A and B contain a "destruction box", cyclins D and E contain a PEST sequence, or a segment of amino acid residues rich in proline (P), glutamic acid (E), serine (S) and threonine (T), these sequences are required for efficient proteolysis ubiquitization-mediated in the end of each phase of the cell cycle [96]. Cyclin H forms complexes with Cdk7 to constitute an enzyme known as CAK (kinase activated by Cdk); CAK is involved in the activation of CDC2 and Cdk2, respectively, by phosphorylation of residues Thr 160 and Thr 161. Together with the Cdk 7 and MAT-1 (protein menage-a - trois- 1), cyclin H form a tertiary complex which modulates transcription by acting on the activity of RNA polymerase II (RNA pol II). Cyclin T does not seem to be directly involved in cell cycle regulation, but his bond with the Cdk9 makes active in various processes such as transcription, signal transduction and differentiation [95].

Cyclin F has some similarities with cyclins A and B, it seems interact with the cyclin B and Cdk1 to form a trimeric complex. Cyclins G (G1-G2) are the p53 target and they appear to be involved in the arrest of the cycle in G2/M phases after DNA damage.

Cyclins activate specific Cdks, a family of serine/threonine protein kinases [95], and the activation occurs in specific phases of the cell cycle [96].

The formation of specific complexes cyclin/Cdk ensures the progression of the cell cycle; cyclins have a high expression at particular times and then they are degraded, ensuring the

periodic activation of the Cdk, which on the contrary have expression levels constant (**Fig. 9**).

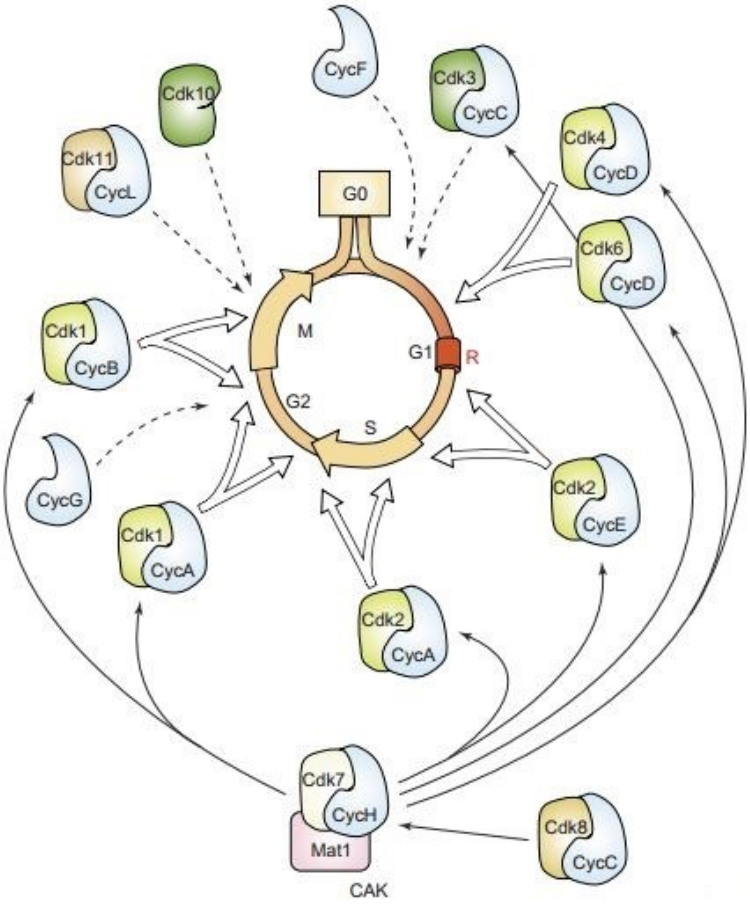

Figure 9: Schematic representation of the complex cyclin/Cdk during different phases of the cell cycle [94].

So the cell cycle is one of the most regulated mechanisms of the cell.

It has long been known the role of Ca^{2+} as a second messenger which can be influenced by a large number of effector proteins and as explained previously mitochondrial Ca^{2+} homeostasis is crucial for the destiny of the cell.

Therefore it was interesting to investigate a possible link between mitochondrial Ca^{2+} homeostasis and cell cycle. On the other hand, mitochondrial Ca^{2+} uptake by MCU has a great importance for the regulation of cell life and energy production. It will be particularly interesting to investigate if MCU could be a pivotal regulator of cell cycle.

After an optimization of synchronization's protocol for cells derived from primary culture (mouse embryonic fibroblast, MEFs), we studied the expression of MCU in different phases of cell cycle in synchronized MEFs cells, showing an increased expression of this protein in G0 and S-G2 phases.

Moreover, we measured mitochondrial and cytosolic Ca^{2+} response after agonist stimulation in each phase of cell cycle, and mitochondrial membrane potential, the driving force for the Ca^{2+} accumulation within the mitochondria.

Finally we checked also the effect of MCU overexpression on cell cycle phases.

Our data show that MCU expression positively correlates with the mitochondrial membrane potential but, surprisingly, it also opposite correlates with agonist-dependent mitochondrial and cytosolic Ca^{2+} response. MCU overexpression instead does not alter cell cycle phases.

Results and discussion

Results

The first step of this work was an optimization of a cellular synchronization protocol to correctly discriminate the different phases of the cell cycle in MEFs cells. The synchronization procedure is based on the Serum Starvation (0.1% FBS) to allow the cells to enter in the stationary phase G0. Then the serum addiction leads the cells to re-enter in the cell cycle. The correct synchronization was assessed by western blot, using specific markers of the cycle. In particular, Cyclin A is a marker of S-G2 phase (as described previously), p27 or Cyclin-dependent kinase inhibitor 1B is a cell cycle inhibitor protein that controls the cell cycle progression at G1, phosphohistone H3 (pHH3) is a marker of M phase and Skp1 is used as protein loading control. Asynchronous cells were used as control and each cellular homogenate was taken together with the corresponding homogenate in synchronized cells. (**Fig. 10A**).

We have then evaluated endogenous MCU expression in each phase of cell cycle, and we use a specific antibody for the protein of interest. In this case and in the next experiments, we use only a single control in asynchronous cells, corresponding to the beginning of cell cycle in synchronized cells. It seems evident that MCU is more expressed in G0 and S-G2 phases, and this expression is specific for MCU. Indeed the expression of another mitochondrial protein, ATP5A, coding for α-subunit of F_1 ATP synthase, does not change in different phases of cell cycle (**Fig. 10B**).

We also have studied the MCU involvement in cell cycle by the blockade of its degradation through the use of MG-132, an inhibitor of the proteasome. We have treated MEFs cells with 10 μM MG-132 3 h before the end of each phase of cell cycle.

There are no appreciable differences in the markers of cell cycle, but it is evident that MCU is not degraded because its expression remains constant during all the phases. With these results we deduce that the non-degradation of MCU and therefore its complete stabilization has not effect on cell cycle progression (**Fig. 10C**).

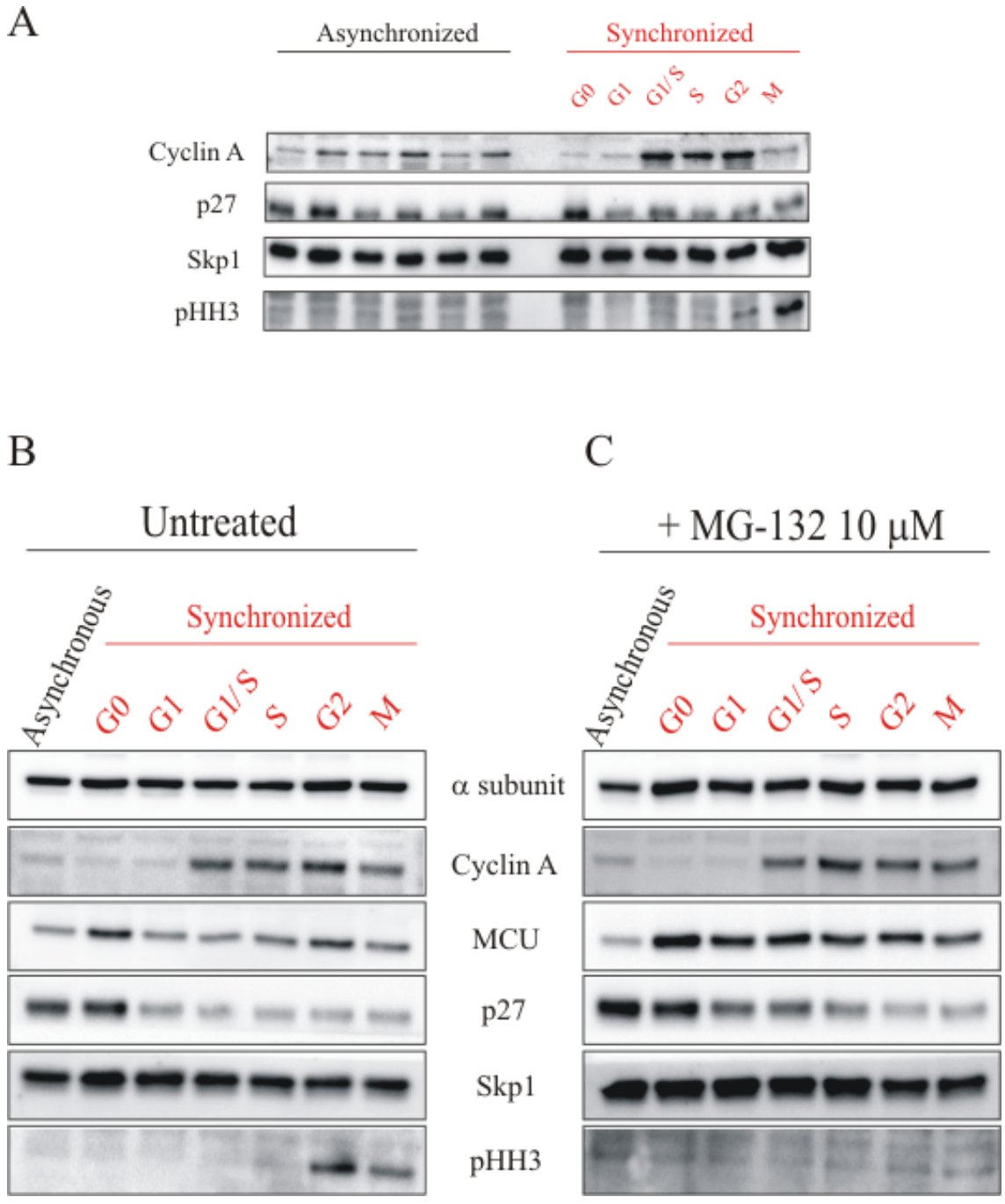

Figure 10: (A) Western Blot of MEFs cells synchronization. On the left asynchronous MEFs cells are used as control. Cyclin A is a marker of S-G2 phases, p27 is a marker of G0-G1 phase, pHH3 is a marker of M phase, Skp1 is used as protein loading control. (B) Western Blot of MCU expression in cell cycle. (C) Proteasome inhibition by MEFs cells treatment with MG-132 10 µM for 3 h before the end of each cell cycle phase.

Therefore it is interesting to investigate a possible link between mitochondrial Ca^{2+} homeostasis and cell cycle. On the other hand, mitochondrial Ca^{2+} uptake by MCU has a great importance for the regulation of cell life and energy production.

Ca^{2+} is in fact a second messenger able to control multiple cellular processes such as gene transcription, muscle contraction, cell proliferation [97], learning, memory, fertilization, development and secretion [98].

The intracellular Ca^{2+} concentration influences signals that control cell cycle progression, despite these strong indications, little attention is paid to the role of Ca^{2+} in the cell cycle [46].

There are a lot of proteins that are modulated by the Ca^{2+} signal, due to its versatility and ability to diffuse, as the CaMK, activated by CaM, which are regulators of the G1/S transition and regulators of the exit from mitosis [92]; calcineurin also plays a role in mediating the entry into G1 phase and the continuation in the S phase [48].

In order to carry out its functions, Ca^{2+} undergoes fluctuations that alter its concentration during the resting state: normally Ca^{2+} ions are stored in mitochondria, ER and Golgi Apparatus and only in response to stimulation they are released to be poured into the cytosol. Mitochondrial and ER networks are also fundamental for the maintenance of cellular homeostasis and for the determination of cell fate under stress conditions [34]. The communication between the two organelles takes place via a zone of close contact between ER and mitochondria, called MAM [35], involved in bioenergetics and cell survival.

In particular, ER is constituted by a network of connections between cisterns and tubular structures that represent an extension of the nuclear envelope. During the cell cycle this structure undergoes specific changes: during interphase it is presented as a series of tubules and cisterns, while at the time of mitosis, it only highlights the extensive network of cisterns. This alteration is due to the depolymerization of microtubules that occurs during the M phase; once anaphase occurred, cisterns are able to provide the making of the nuclear envelope, even before the appearance of the tubular structure [99].

For $[Ca^{2+}]$ measurements in different intracellular compartments, we infected MEFs cells with the adenovirus for the mitochondrial and cytosolic aequorin. This experiment was conducted in asynchronous and synchronized cells. MEFs cells are stimulated with 100 μM ATP to enable Ca^{2+} mobilization. This agonist selectively binds the membrane receptor coupled to a trimeric G protein: in particular, the α subunit is able to activate phospholipase C which hydrolyzes phosphatidylinositol-4,5-bisphosphate (PIP_2) generating diacylglycerol (DAG) and inositol 1,4,5-trisphosphate (IP_3). The IP_3 binding to

its receptor on the ER causes an increase of the $[Ca^{2+}]$ in the cytoplasm and in the mitochondrial matrix.

So $[Ca^{2+}]_m$ measured after agonist stimulation is 37.33 ± 1.68 µM in asynchronous cells, 28.76 ± 2.85 µM in G0 phase cells, 32.4 ± 2.57 µM in G1 phase cells, 58.17 ± 4.33 µM in G1/S phase cells, 50.12 ± 4.13 µM in S phase cells, 48.44 ± 8.09 µM in G2 phase cells and 65.0 ± 6.86 µM in M phase (n=15). (**Fig. 11A and 11B**)

Instead $[Ca^{2+}]_c$ measured after agonist stimulation is 2.27 ± 0.11 µM in asynchronous cells, 1.65 ± 0.1 µM in G0 phase cells, 2.41 ± 0.09 µM in G1 phase cells, 1.97 ± 0.08 µM in G1/S phase cells, 1.97 ± 0.08 µM in S phase cells, 1.77 ± 0.06 µM in G2 phase cells and 1.95 ± 0.07 µM in M phase (n=15). (**Fig. 11C and 11D**)

Our data suggest that, surprisingly, MCU expression opposite correlates with agonist-dependent mitochondrial and cytosolic Ca^{2+} response.

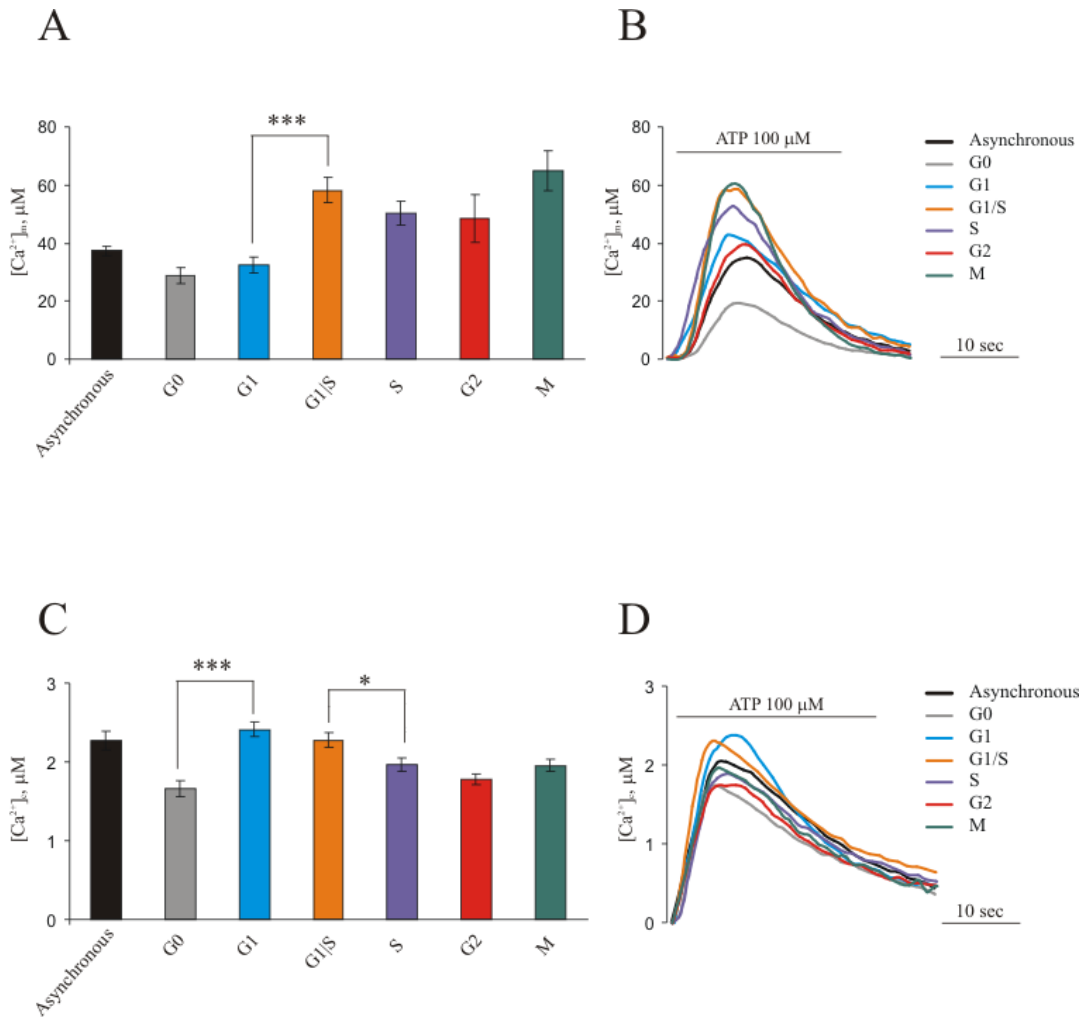

Figure 11: Measurements of $[Ca^{2+}]$ using recombinant aequorin upon agonist (100 µM ATP) stimulation in mitochondria (A and B) and cytosol (C and D) in MEFs cells. The data are presented as means ± SEM *p<0.05, ***p<0.001.

We then questioned about the possible effect of the phase-specific expression of MCU on the mitochondrial membrane potential (Ψm), since it represents the driving force for the Ca^{2+} accumulation within mitochondria. To measure this parameter we use the fluorescent probe Tetramethylrhodamine, methyl ester (TMRM), a cell-permanent, cation, red-orange fluorescent dye that is readily sequestered by active mitochondria, in asynchronous and synchronized MEFs cell.

The percentage of arbitrary fluorescence units (AFU) measured are -42.37 ± 1.72 in asynchronous cells, -43.27 ± 1.82 in G0 phase cells, -42.1 ± 1.79 in G1 phase cells, -28.08 ± 1.46 in G1/S phase cells, -32.38 ± 1.29 in S phase cells, -38.31 ± 1.74 in G2 phase cells and -31.35 ± 1.28 in M phase (n=80) (**Fig.12**).

Our data show that MCU expression in this case positively correlates with the mitochondrial membrane potential.

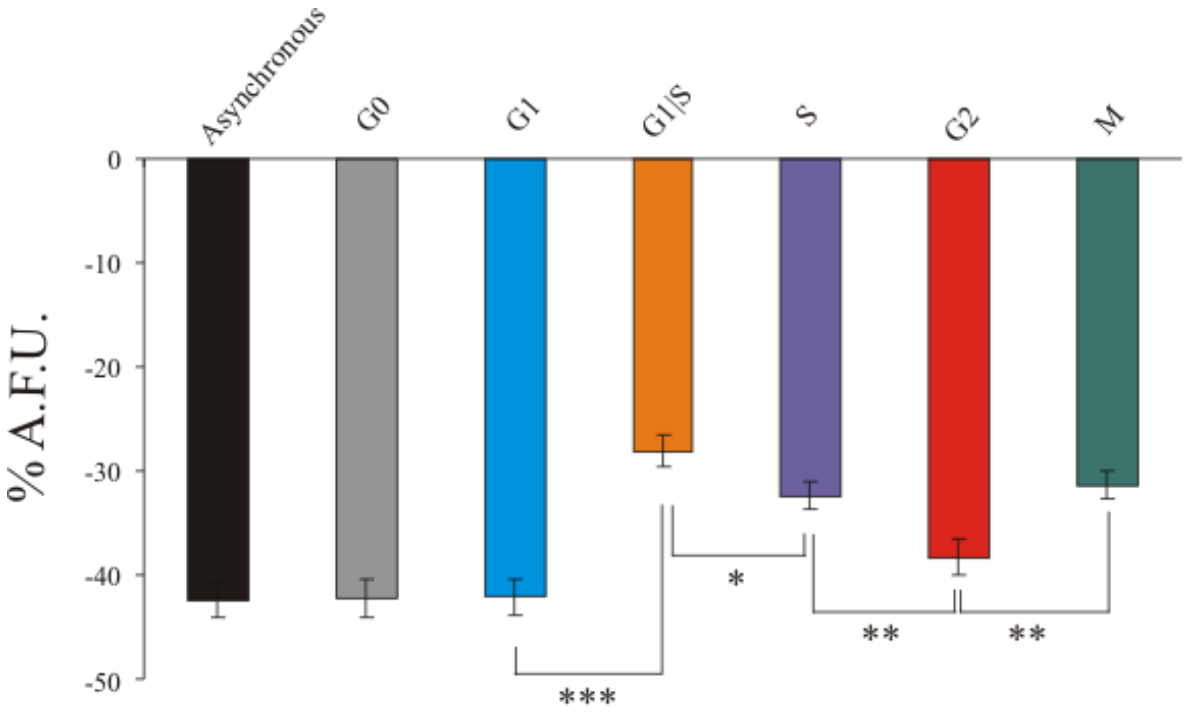

Figure 12: Measurements of ΔΨm with potentiometric dye TMRM in MEFs cells. The data are presented as means ± SEM *p<0.05, **p<0.01, ***p<0.001.

To evaluate the possible role of MCU in cell cycle, we decided to investigate the effects of its overexpression in the different phases.

The overexpression was achieved by cells infection with an adenovirus expressing MCU. Cell cycle was analyzed by the Tali® Image-Based Cytometer and we meausured control cells without infection (**Fig. 13A**), cells infected with an adenovirus expressing a

mitochondrial Green Fluorescent Protein (mtGFP) (**Fig. 13B**) and cells expressing MCU-GFP (**Fig. 13C**).

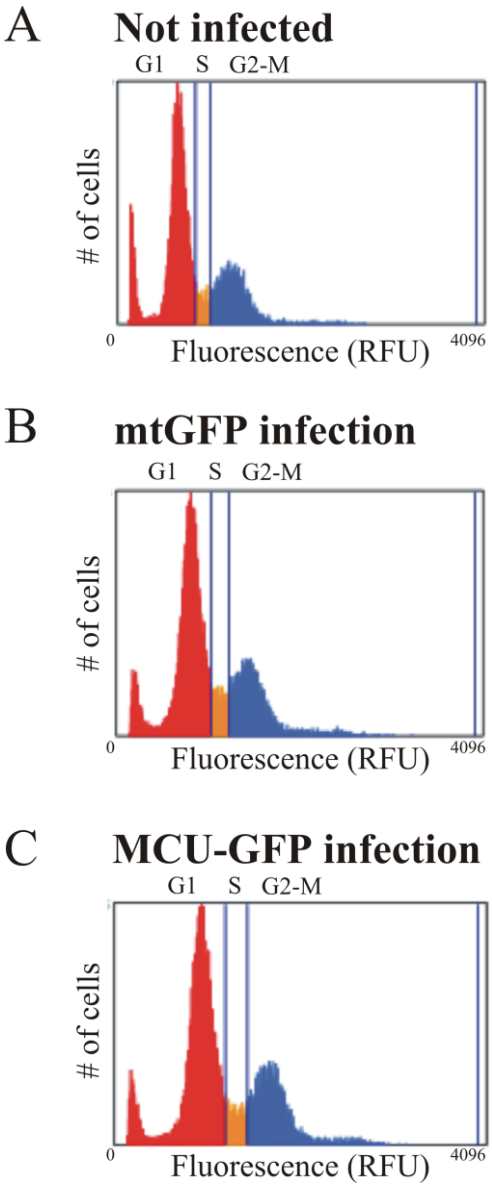

Not infected

PHASE	% CELLS
G1 phase	65%
S phase	5%
G2-M phase	30%

mtGFP infection

PHASE	% CELLS
G1 phase	62%
S phase	7%
G2-M phase	31%

MCU-GFP infection

PHASE	% CELLS
G1 phase	63%
S phase	7%
G2-M phase	29

Figure 13: Cell cycle analysis in not incedcted (A), mtGFP infected (B) and MCU-GFP infected (C) MEFs cells by Tali® Image-Based Cytometer. The percentage of cells is referred to the number of cells in each phase of cell cycle.

MCU overexpression does not alter cell cycle progression, as the percentage of cells in each phase of cell cycle does not change.

The effects of MCU overexpression were also evaluated by use of FACS (Fluorescence-Activated Cell Sorting), which has a high sensitivity and precision and it is perfectly

indicated for this type of analysis. As for the previous experiment, we meausured control cells without infection (**Fig. 14A**), cells infected with an adenovirus expressing mtGFP (**Fig. 14B**) and cells expressing MCU-GFP (**Fig. 14C**).

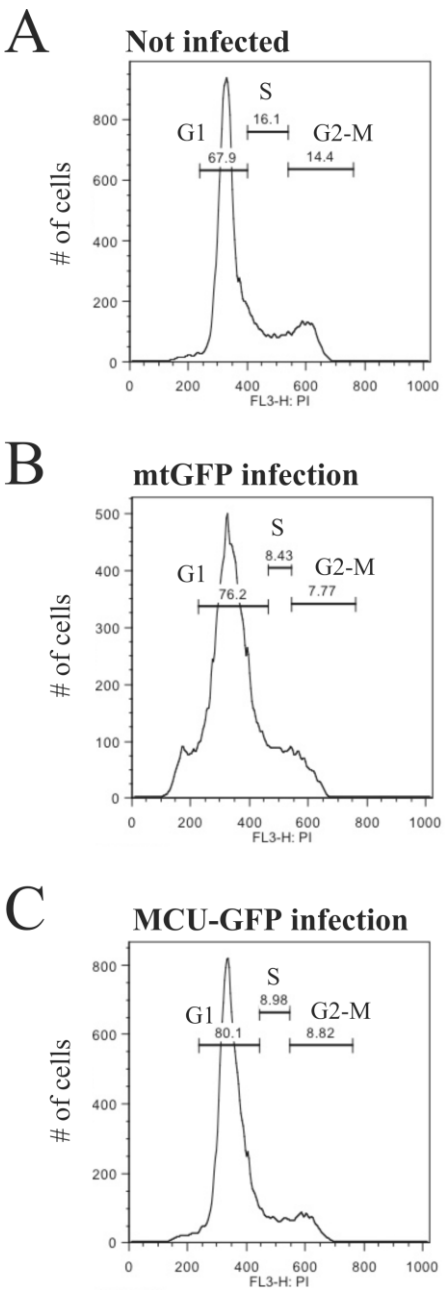

Figure 14: Cell cycle analysis in not incedcted (A), mtGFP infected (B) and MCU-GFP infected (C) MEFs cells by FACS. The percentage of cells is referred to the number of cells in each phase of cell cycle.

These results confirm our previous data, the overexpression of MCU does not seem to affect cell cycle. Minor variations in cellular distribution are present only between infected and not infected cells, maybe due to the cell transfection.

Discussion

The cell cycle is the series of events leading to cell division and duplication of its genetic material. It is an evolutionarily conserved process in the succession of the events and in their regulation [95].

The proper development of an organism is due to the precise regulation and the respect of the order of cell cycle progression. Proteins alterations can trigger an uncontrolled proliferation that often leads to tumor formation, thus it is so important that all the events of the cycle are regulated on multiple levels.

The control system is constituted by the complex cyclin/Cdk. Cyclins are proteins with different expression in the cell cycle phases, as a result of transcriptional changes and proteasome degradation [96].

Cdks are a family of serine/threonine protein kinase that form specific complexes with cyclins and ensure the cell cycle progression. In fact cyclins expression in well-determined phases allows the periodic activation of the Cdk that, instead, show constant levels of expression [96].

A lot of Ca^{2+}-binding proteins (CaM, CaMK and calcineurin) are involved in the regulation of certain phases of the cell cycle [47]. Recently, it has been identified the mitochondrial Ca^{2+} uniporter MCU, a protein of 40 kDa expressed in all tissues, which is located in the IMM, with the N-terminal and the C-terminus facing the matrix [40, 41]. MCU is a low affinity-channel but it has been shown that mitochondria are exposed to microdomains with high $[Ca^{2+}]$, which represent the contact sites between mitochondria and ER [100].

Given the high importance of this protein in the regulation of cell life, the aim of this work is the investigation of a possible MCU involvement in the cell cycle. At the beginning the attention was focused on the development of cell cycle synchronization protocols for primary cultures (MEFs cells) in order to discriminate the different phases of the cycle.

We then evaluate endogenous expression of MCU in each phase of the cell cycle by western blot. MCU is more expressed in G0 and S-G2 phases, and this is specific for the protein of interest as the expression of another mitochondrial protein, ATP5A, coding for α-subunit of F_1 ATP synthase, does not change in different phases of cell cycle.

We also have investigated the MCU involvement in cell cycle by the blockade of its degradation through the use of MG-132, an inhibitor of the proteasome. It is evident that MCU is not degraded because its expression remains constant during all the phases. We can deduce that the non-degradation of MCU and therefore its complete stabilization has not effect on cell cycle progression.

At this point, given the important role of the MCU in the Ca^{2+} homeostasis, we measured mitochondrial and cytosolic Ca^{2+} concentrations after agonist stimulation in each phase of cell cycle, so as to be able to understand if the phase-specific expression of MCU is related to a different Ca^{2+} accumulation into mitochondria. Surprisingly, MCU expression opposite correlates with agonist-dependent mitochondrial and cytosolic Ca^{2+} response.

The Ca^{2+} accumulation gradient into mitochondria is governed by the strongly electronegative potential inside so we proceeded with mitochondrial membrane potential measurement in the different phases of the cell cycle. To measure this parameter we use the fluorescent probe TMRM, a cell-permanent, cation, red-orange fluorescent dye that is readily sequestered by active mitochondria, in asynchronous and synchronized MEFs cell.

Data reveal a positive correlation with the phase-specific expression of the MCU, suggesting a compensatory effect of the expression of the protein of interest.

At this point, it was interesting to understand if MCU overexpression could have influence on cell cycle progression and we took advantage of the use of flow cytometry, in particular a specialized type of this technology, the fluorescence-activated cell sorting (FACS). It provides fast, objective and quantitative recording of fluorescent signals from individual cells as well as physical separation of cells in each phase of cell cycle.

MEFs cells were infected with an adenovirus expressing mtGFP or with an adenovirus expressing MCU-GFP, cells not infected were used as control. The percentage of cells in each phase of the cell cycle remains constant in all the experimental conditions, to indicate that the overexpression of MCU does not alter cell cycle progression.

Numerous other works are still in progress and not included in this thesis.

We are trying to modulate the mitochondrial membrane potential using two compounds known for their ability to alter it. The first one is FCCP (Carbonyl cyanide -p-trifluoromethoxyphenylhydrazone), a chemical uncoupler of electron transport and oxidative phosphorylation, that permeabilizes the IMM to protons, destroying the proton gradient and, in doing so, uncouples the electron transport system from the oxidative phosphorylation system. Thus electrons continue to pass through the electron transport system and reduce oxygen to water, but ATP is not synthesized in the process.

The second compound is the methyl succinate, a putative cell permeable complex II-linked substrate that, on the contrary, hyperpolarizes the mitochondrial membrane.

We are also investigating the correlation between cell cycle, MCU and cancer: it is known that miR-25 (a microRNA overexpressed in colon cancer cells) decreases mitochondrial Ca^{2+} uptake through selective MCU downregulation, conferring resistance to apoptotic challenges. MCU appears to be downregulated in human colon cancer samples, and

accordingly, miR-25 is aberrantly expressed, indicating the importance of mitochondrial Ca^{2+} regulation in cancer cell survival [56]. Therefore it is evident that MCU has a great importance in the regulation of cell fate and for this reason we are moving on a tumor cell line.

In conclusion, these experimental evidences suggest that the only activity of MCU is not sufficient for the regulation of the cell cycle.

In the light of the latest discovery about the different components of the uniporter complex [54, 59, 60, 62, 63], it is now interesting to investigate the possible involvement of these proteins in cell cycle, and preliminary data show that also in this case there is a different phase-specific protein expression. Our data suggest moreover that MCU could have a possible compensatory role in mitochondrial Ca^{2+} homeostasis.

Future experiments will then be directed to study the roles of all MCU's interactors in the cell cycle progression, with a more thorough investigation in tumor cell line.

Role of the c subunit of the Fo ATP synthase in mitochondrial permeability transition

Introduction

MPT refers to an alteration in the permeability of the IMM; the MPT was first characterized in 1979 [101] and then linked to cell death [102].

More recently, it was hypothesized that the permeability transition state is caused by a high permeability channel [103] termed the mPTP. Several studies have examined the molecular structure of the pore and revealed its complex organization, which includes proteins located in all of the mitochondrial sub-districts. Although all of these elements exhibit regulatory activity, a complete model for mPTP activity is lacking. Some proteins formerly believed to be crucial for PTP, have been excluded after experiments with the use of transgenic knockout animals, is the case of the ANT [104], and VDAC [105]. Several lines of evidence suggest that mitochondrial ATP synthase is linked to mPTP. Specifically, i) a selective inhibitor of mitochondrial ATP synthase, oligomycin, is able to prevent MPT and cell death induced by TNF-alpha [106], staurosporine [107] or pro-apoptotic Bax protein [108]; ii) both mPTP and ATP synthase display sensitivity to Mg^{2+} [109, 110] and iii) cyclophilin D, a fundamental regulator of mPTP [111, 112] interacts with the lateral stalk of ATP synthase and regulates its activity [113], similar to the cell death and mPTP regulator Bcl-xL [114]. Here, we demonstrate that the c-subunit of mitochondrial ATP synthase is present in mPTP and plays a determinant role in MPT activity. This finding suggests that the c-subunit plays a direct role in the core-forming element of mPTP, thus establishing the c-subunit as an important player in the processes of crucial physiopathological relevance.

Results and Discussion

The F_O portion of ATP synthase requires 3 different subunits for its proton pumping activity: a, b and c [115]. A-subunit is encoded by the mitochondrial DNA, while b- and c-subunits are encoded by nuclear DNA. Recently, mPTP opening activity has been demonstrated in cells deprived of mitochondrial DNA, indicating that a-subunit does not participate in mPTP opening [116]. Conductive properties have been indicated for c-subunit [117] but not for b-subunit. In addition, a peptide with a high level of similarity to c-subunit has been proposed as a regulator of mPTP [118]. Thus, we focused our attention to c-subunit.

The MPT perturbs several aspects of mitochondrial physiology by inducing a decrease in $\Delta\Psi_m$, the release of mitochondrial proteins, network fragmentation, and impaired Ca^{2+} uptake in the mitochondrial matrix. The manipulation of c-subunit levels was thus expected to impair several of these features if it is involved in mPTP. C-subunit is encoded by *ATP5G1*, *2* and *3*. Each gene possesses a different mitochondrial targeting sequence that is cleaved by matrix peptidases to generate the same mature protein [119]. We used a mixture of siRNAs directed against the three isoforms of the c-subunit to down-regulate the levels of c-subunit protein (**Fig. 15B**) and a vector expressing *ATP5G1* cDNA to increase c-subunit levels (**Fig. 15A and 15B**). We measured ATP levels within the mitochondrial matrix using recombinant mitochondrial targeted firefly luciferase (mtLuc) as previously described [120]. In the presence of luciferin, HeLa cells expressing mtLuc emit light proportionally to [ATP] in the mitochondrial matrix ($[ATP]_m$). ATP production can be stimulated by a transient increase in $[Ca^{2+}]_m$, which promotes the activity of the Krebs cycle. In our cell model, histamine-induced Ca^{2+} uptake within mitochondria resulted in a slight increase in luminescence (**Fig. 15Ci**); this is to be expected in HeLa cells, which do not rely heavily on respiration [120]. The simultaneous silencing of all 3 c-subunit isoforms did not induce much variation in ATP levels, confirming the glycolytic nature of the chosen cell model. Overexpression of the c-subunit magnifies this increase, indicating more efficient ATP synthesis (**Fig. 15Cii**). Together with the increase in ATP levels, c-subunit overexpression led also to a reduction in $\Delta\Psi_m$, as revealed by TMRM staining (**Fig. 15Di**) due to ATP synthesis-related depolarization (state 3 of respiration). Under these conditions, mitochondrial Ca^{2+} uptake can be monitored through the use of recombinant aequorin. C-subunit silencing induced only a weak, non-significant reduction in $\Delta\Psi_m$ (Fig. 1Dii), this was likely due to the regulatory effects of c-subunit silencing on respiratory chain complexes, as previously demonstrated [121].

An analysis of mitochondrial morphology using 3D imaging deconvolution in HeLa cells expressing mtGFP indicated that c-subunit overexpression promotes network fragmentation, which was manifested as a large increase in the number of objects composing the mitochondrial network (**Fig. 15E**). This result suggests that c-subunit overexpression-related increase in the rate of ATP production dictates mitochondrial morphology [122]. On the other hand, c-subunit silencing did not induce relevant alterations in the network morphology (**Fig. 15E**). The effect on mitochondrial number is not due to variations in the total mitochondrial mass as indicated by western blotting for the mitochondrial VDAC, ATP synthase a-subunit, ATP synthase alpha-subunit and cytochrome c levels, which do not correlate with c-subunit levels (**Fig. 15B**).

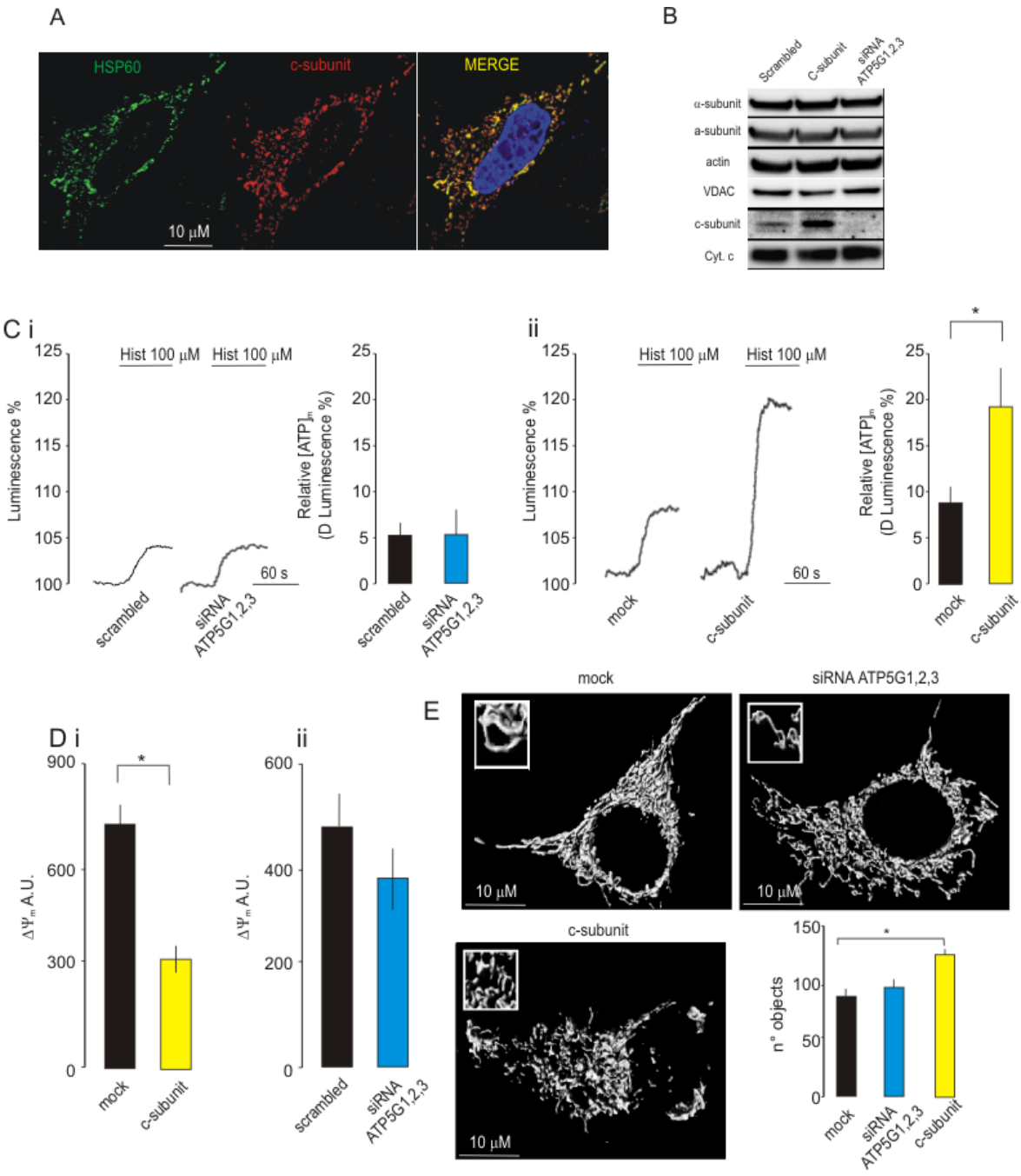

Figure 15: (A) Colocalization between overexpressed c-subunit encoding plasmid (red) and the mitochondrial marker HSP60 (green). (B) Immunoblot analysis of mitochondrial proteins in HeLa cells, transfected with scrambled siRNA, c-subunit encoding plasmid or siRNA *ATP5G1, 2, 3*. (C) Effect of histamine agonist on $[ATP]_m$ measured by using mitochondrial targeted luciferase construct (mtLuc) in scrambled-transfected and *ATP5G1, 2, 3* silenced HeLa cells (Ci) and mock-transfected, c-subunit overexpressing (Cii). Luminescence data are expressed as a percentage of the initial value. (D) Basal intensity of TMRM loaded HeLa cells during c-subunit overexpression (Di) or siRNA *ATP5G1, 2, 3* (Dii). (E) Analysis of mitochondrial structure in HeLa cells co-transfected with a green fluorescent protein targeted to mitochondria (mtGFP) together with scrambled siRNA or siRNA *ATP5G1, 2, 3* or c-subunit encoding plasmid. Data represent mean ± SEM of mitochondrial number. *p<0.05.

The manipulation of c-subunit levels has more significant effects when mPTP opening is induced. To monitor the live opening of the mPTP, we used the calcein-cobalt assay with our cell model system. Calcein generates common cytoplasmic staining in the absence of cobalt. When cobalt is added, cytosolic calcein is quenched whereas mitochondrial calcein is protected due to the impermeability of the IMM [123]. The stimulation of the MPT by 1 μM ionomycin permits cobalt entry into the mitochondrial matrix, which quenches mitochondrial calcein at a very high rate (**Fig. 16A**). If the cells are exposed to 1 μM Cyclosporine A (CsA), the rate of calcein quenching is drastically reduced. The inhibition of the calcein quenching rate by c-subunit silencing was similar to that which was induced by CsA exposure (**Fig. 16A**), while c-subunit overexpression dramatically increased the quenching rate compared with mock transfected cells (**Fig. 16B**). Within 10 min of exposure to ionomycin, calcein was typically completely quenched whereas CsA almost completely prevented this phenomenon (**Fig. 16B**).

We then analyzed the mitochondrial morphology alterations under the same conditions, a process that was previously demonstrated to be dependent on mPTP activity [29]. The mitochondrial networks were dramatically fragmented after ionomycin treatment, reaching a maximal fragmentation after 10 min (**Fig. 16C**). This phenomenon was significantly inhibited in CsA-pretreated cells and after c-subunit silencing (**Fig. 16C**). On the contrary, cells overexpressing the c-subunit displayed a faster and more extensive network fragmentation (**Fig. 16D**).

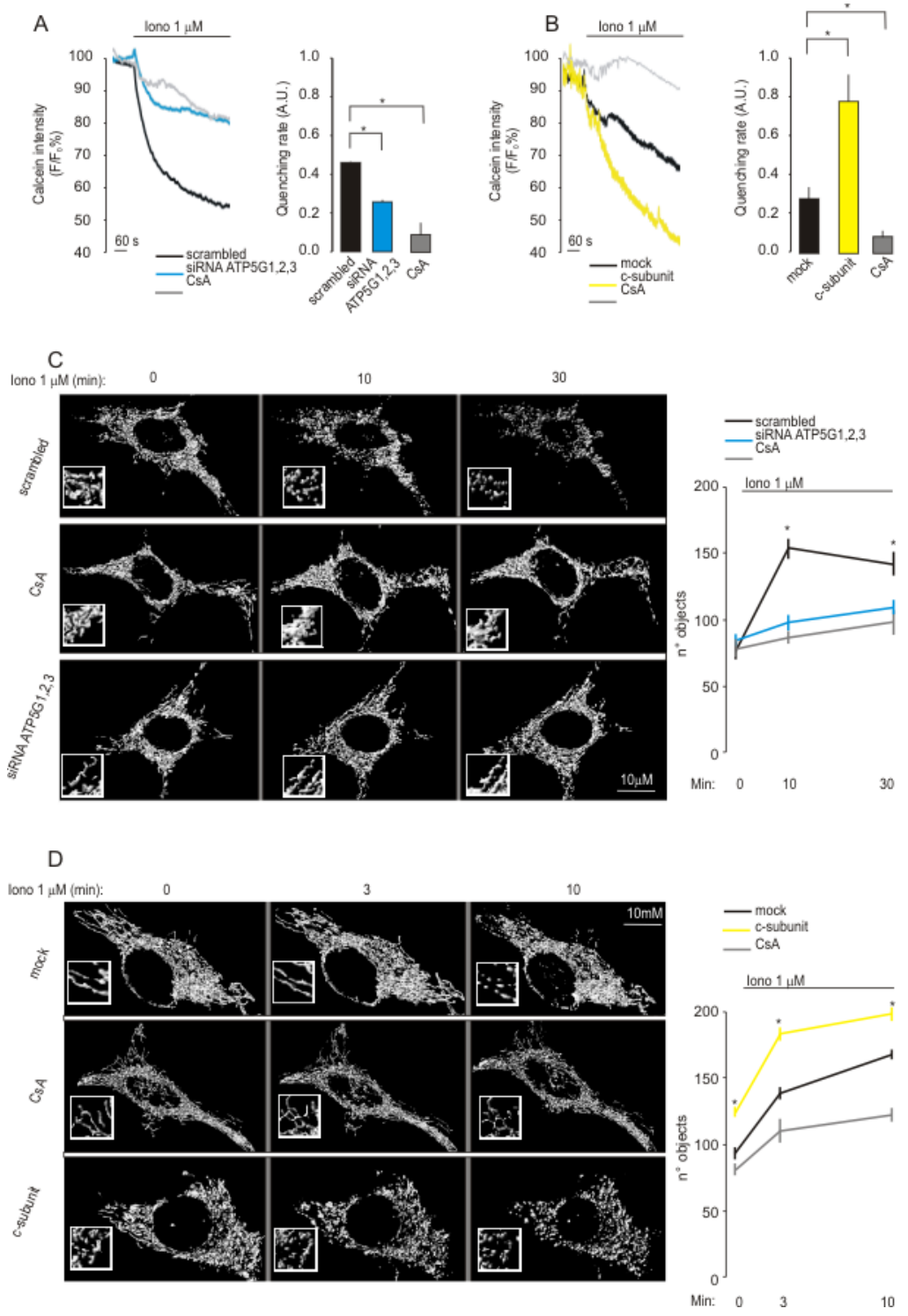

Figure 16: (A) Representative Calcein assay during ionomycin 1 µM (Iono) induced mPTP opening in cells transfected with scrambled siRNA or siRNA *ATP5G1, 2, 3* and (B) after transfection with mock or c-subunit encoding plasmid. CsA 1 µM was used as negative control. (C) Time course of mitochondrial fragmentation in HeLa cells expressing mtGFP following ionomycin 1 µM induced mPTP opening. Fragmentation was monitored for 30 min in cells co-trasfected with scrambled siRNA or siRNA *ATP5G1, 2, 3*. (D) Time-laps were reduced to 10 min in HeLa transfected with mock or c-subunit encoding plasmid. Where indicated, before experiments, cells were treated with CsA 1 µM for 30min. Data represent mean ± SEM *p<0.05.

Mitochondria transfected with a control siRNA and exposed to high dose of the prototypic pro-oxidant hydrogen peroxide H_2O_2 underwent an irreversible depolarization. The $\Delta\Psi_m$ of cells depleted of the F_o c subunit dissipated upon the administration of high-dose H_2O_2 with a delayed kinetics (**Fig. 17A**). As expected, cells overexpressing the c-subunit also depolarized dramatically faster also at low concentrations of H_2O_2 (**Fig. 17B**).

Prolonged MPT has been demonstrated as an event linked to the release of mitochondrial proteins preceding different types of cell death [26].

A cytosol isolation experiment in which digitonin was used to permeabilize the plasma membrane without disrupting mitochondrial integrity indicated that cytochrome c release is inducible by H_2O_2 in cells transfected with scrambled siRNA, but this process was strongly inhibited by c-subunit silencing (**Fig. 17C**).

H_2O_2- and ionomycin-induced cell death (as measured by PI positivity) was dramatically inhibited by c-subunit silencing (**Fig. 17D**), whereas simple overexpression of the c-subunit was able to induce an increase in PI positivity in untreated cells that was further dramatically increased by H_2O_2 exposure compared with mock-transfected cells (**Fig. 17E**).

Mitochondrial ATP synthase activity is closely linked to the amount of regulators of mPTP opening such as ADP and inorganic phosphate (Pi). The specific effects of these elements on pore opening are still a matter of intense debate [69, 124]; nonetheless, the indirect modulation of the mPTP by the impairment of ATP synthase activity could be expected.

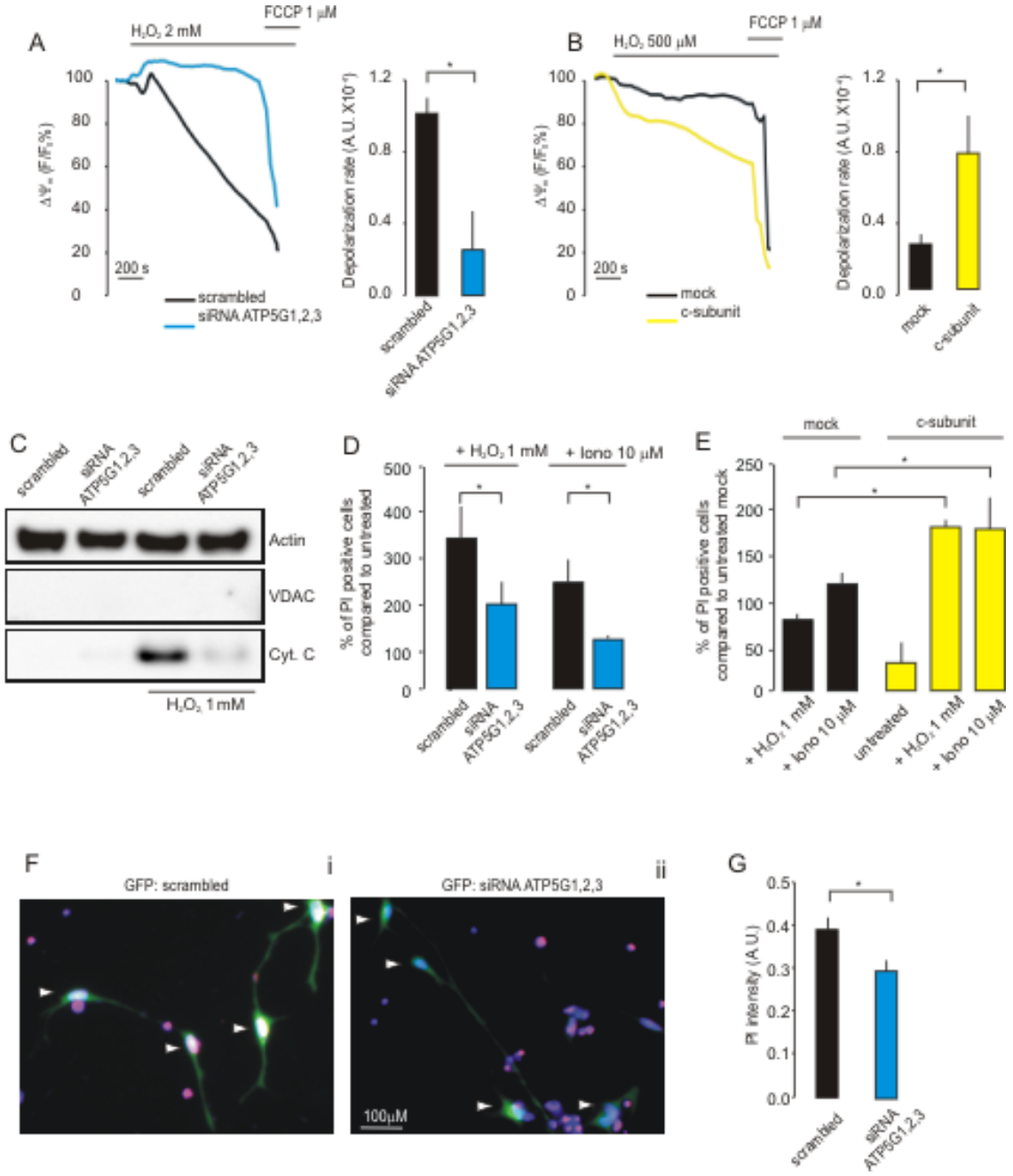

Figure 17: (A) Representative TMRM assay during hydrogen peroxide (H_2O_2) induced mPTP opening. H_2O_2 was used at 2 mM concentration in cells transfected with scrambled siRNA or siRNA *ATP5G1, 2, 3* or (B) at 500 µM during transfection with mock or c-subunit encoding plasmid. (C) Cytosolic extracts from HeLa cells showing amounts of cytochrome c (Cyt. c) released from mitochondria, after apoptotic induction (H_2O_2 1 mM, 2h), in scrambled-transfected and *ATP5G1, 2, 3* silenced HeLa cells. (D) Percentage of PI positive cells after treatment with H_2O_2 1 mM and ionomycin 10 µM in scrambled siRNA or a siRNA *ATP5G1, 2, 3* transfected cells referred to untreated scrambled transfected cells. (E) Percentage of PI positive cells after treatment with H_2O_2 1 mM and ionomycin 10 µM in c-subunit overexpressing cells referred to untreated mock-transfected cells. (F) Extent of cell death in neurons co-trasfected with GFP and scrambled siRNA (Fi) or siRNA *ATP5G1, 2, 3* (Fii) upon excitotoxicity challenge. (G) PI intensity was measured only in nuclei of GFP positive cells (indicated by the white arrows in representative images). Data represent mean ± SEM *p<0.05.

To avoid this misinterpretation, we silenced the α-subunit of mitochondrial ATP synthase, which is mainly involved in the organization of the F_1 portion and contains nucleotide-binding sites that are fundamental for the catalysis of ATP synthesis [125]. As previously demonstrated for c-subunit silencing, α-subunit siRNA (**Fig. 18A**) did not significantly impair ATP synthesis in HeLa cells (**Fig. 18B**). However, while c-subunit depletion severely impaired mPTP opening, α-subunit depletion did not alter the rate of calcein quenching (**Fig. 18C**) or the network fragmentation induced by ionomycin (**Fig. 18D**). Finally, HeLa cells transfected with α-subunit siRNA and exposed to H_2O_2 or ionomycin displayed the same level of PI positivity as HeLa cells transfected with scrambled siRNA (**Fig. 18E**). Overall these data indicate that c-subunit manipulation directly impairs mPTP as opposed to causing secondary effects due to the alteration of mitochondrial ATP synthase activity.

To further demonstrate the functionality of the c-subunit as a strategic element in the mPTP and MPT-induced cell death, we examined a more complex and physiologically relevant system. Glutamate-induced neurotoxicity is dependent on mPTP opening [126], and mitochondrial physiology has become a focus of research for several neurodegenerative diseases. Glutamate induces Ca^{2+} entry from the extracellular milieu, causing $[Ca^{2+}]_m$ overload and the MPT during excitotoxicity [127]. When cultured rat neurons stained with TMRM were exposed to 500 μM glutamate (**Fig. 18F**), progressive mitochondrial depolarization was detectable in 64% of cells; however, only 50% of c-subunit-silenced cells displayed depolarization (**Fig. 18Fi**). Moreover, depolarization occurred at a significantly lower rate in silenced neurons (**Fig. 18Fii**). To examine the extent of excitotoxicity after 30 min of exposure to glutamate, the neurons were washed and allowed to recover for 24 h prior to staining with PI. PI intensity, as detected by fluorescence microscopy, appeared significantly higher in neurons transfected with scrambled siRNA compared to those transfected with siRNAs targeting *ATP5G1, 2,* and *3* indicating that c-subunit is fundamental for glutamate-induced excitotoxicity and the MPT in neuronal cells (**Fig. 18G**).

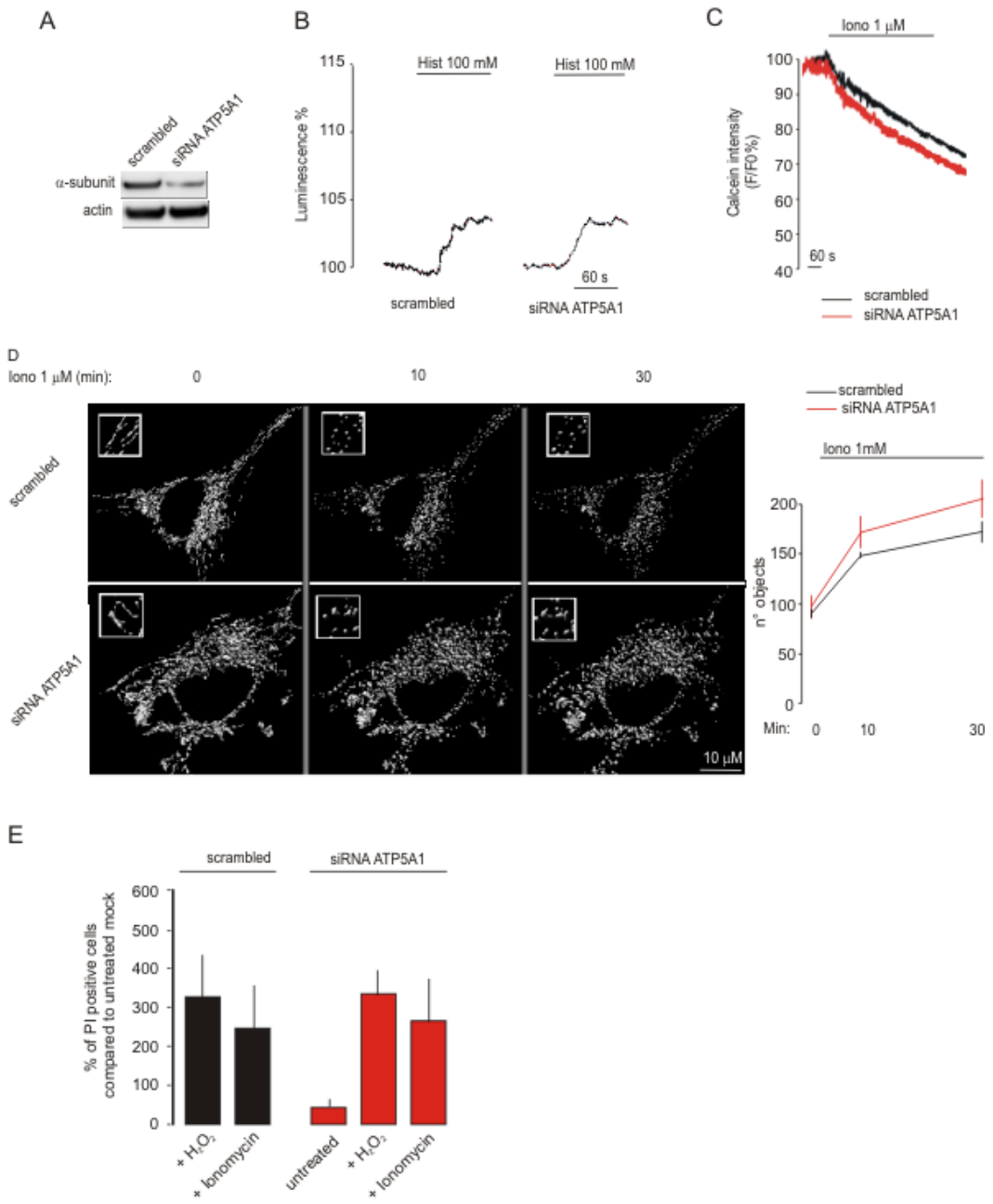

Figure 18: (A) HeLa cells were transfected for 48 hours with either scrambled or siRNA *ATP5A*1. Cells were harvested, total proteins were extracted and endogenous α-subunit was detected by western blotting using MitoProfile Total OXPHOS Human Antibody Cocktail. Actin was blotted as loading control. (B) Effect of histamine agonist on $[ATP]_m$ measured by using mitochondrial targeted luciferase construct (mtLuc) in scramble-transfected and α-subunit silenced HeLa cells. Luminescence data are expressed as a percentage of the initial value. (C) Calcein assay during ionomycin 1 µM (Iono) induced mPTP opening in cells transfeted with scrambled siRNA or siRNA *ATP5A*1. (D) Mitochondrial number, as deduced by calculating object number. HeLa cell were transfected with a green fluorescent protein specifically targeted to the mitochondria (mtGFP), scrambled siRNA, or siRNA *ATP5A*1. Images were acquired at the indicated time points before and after treatment with ionomycin. (E) Percentage of PI positive cells after treatment with H_2O_2 1 mM and ionomycin 10 µM in scrambled siRNA or a siRNA *ATP5A*1 transfected cells referred to untreated scrambled transfected cells. Data represent mean ± SEM *p<0.05.

Overall, these data indicate that the c10 ring of the mitochondrial ATP synthase is a key player in the MPT and strongly suggest that it participates in the core-forming element of the mitochondrial permeability transition pore also on the light that, in vesicles enriched in F_1F_O ATP synthase [114], a regulated non-selective leak conductance, sensitive to ATP and increased by pharmacological or genetic inhibition of Bcl-xL has been recorded.

The mitochondrial permeability transition pore is a dispensable element for mitochondrial calcium efflux

Introduction

Mitochondria are intracellular organelles involved in several cellular functions such as ATP production, fatty acid oxidation, Ca^{2+} signaling and cell death [36, 78, 128]. Under pathological conditions, mitochondria are able to adapt by fusion or fission processes and modulate respiratory substrate utilization to regulate ATP production [15]. Furthermore, in cases of severe damage, mitochondria are eliminated by autophagy, and cell death can occur [129]. Thus, these organelles are master regulators of danger signaling [130, 131].

A key signaling messenger that is able to transduce life or death signals to mitochondria is intracellular Ca^{2+} [38, 132]. The mitochondrial Ca^{2+} uptake and release mechanisms are based on the utilization of gated channels for Ca^{2+} uptake and exchangers for release that are dependent upon the negative ψ_m, which represents the driving force for Ca^{2+} accumulation in the mitochondrial matrix [39]. MCU, which is encoded by the recently discovered gene ccdc109a [40, 41], is responsible for Ca^{2+} influx, while NCLX [42] is responsible for Ca^{2+} efflux. In spite of this information, the mitochondrial Ca^{2+} efflux mechanism has not been completely elucidated. It is mostly accepted that Na^{+}/Ca^{2+} exchange activity is relevant for excitable cells [43] and that NCLX inhibition or silencing does not completely arrest Ca^{2+} efflux [42], which indicates that other mechanisms are involved in this process. Two mechanisms have been proposed to supplement Ca^{2+} efflux, one based on the H^{+}/Ca^{2+} antiporter [44] and another based on the mPTP [45], but evidence supporting the latter remains elusive.

The mPTP is a high-conductance channel that is located at the contact sites between the inner and outer mitochondrial membranes. This channel is responsible for the non-selective permeability state of the mitochondrial inner membrane. The transition to this state for small molecules is referred to as the MPT. The molecular composition of the mPTP is not yet clear, but several proteins have been shown to be components that participate in mPTP activity, including VDAC [67], ANT [68], PiC [69], PPIF [70, 71], TSPO [72], HKII [73] and several members of the Bcl-2 family [74, 76, 133].

Ca^{2+} ions, prooxidant and proapoptotic proteins, a decrease in the mitochondrial membrane potential, pH variations and adenine nucleotides all sensitize the opening of the pore [25, 77].

MPT resulting from mPTP opening is usually considered a transducer event in between Ca^{2+} or oxidative signal and different type of cell death [78, 79]. Nonetheless several observations have suggested that mPTP is a component of the Ca^{2+} efflux mechanism [80, 81, 134, 135] proposing a physiological role for this ambiguous complex. Unfortunately a different amount of studies have proposed the exact opposite [82, 83] leaving this supposition still unresolved. Therefore, we focused on the role of the mPTP in mitochondrial Ca^{2+} homeostasis under non-pathological conditions. Recently, we suggested that, similar to PPIF, the c subunit of the F_O ATP synthase constitutes a critical component of the mPTP and that it is required for the MPT, mitochondrial fragmentation and cell death induced by oxidative stress or mitochondrial Ca^{2+} overload [21]. A concept further confirmed by two different groups [136, 137].

By modulating c subunit expression and using pharmacological approaches, we revealed the important finding that the mPTP is not necessary for mitochondrial Ca^{2+} release; therefore, it does not participate in mitochondrial Ca^{2+} homeostasis in a non-pathological context at least in HeLa cells.

Results and discussion

Results

To study the contribution of mPTP in mitochondrial Ca^{2+} homeostasis, we have investigated the kinetics of the mitochondrial and cytosolic Ca^{2+} influx and efflux. We have recently suggested that the c subunit of the F_O ATP synthase is a component of the mPTP that is required for the MPT-driven mitochondrial fragmentation that is induced by cytosolic Ca^{2+} overload and oxidative stress [21]. Therefore, we decided to modulate mPTP activity by genetically manipulating the expression of the c subunit in the HeLa human cervical carcinoma cell line. The mammalian ATP synthase c subunit is encoded by three different nuclear genes (ATP5G1, ATP5G2 and ATP5G3) that produce three different proteic products. These products differ in their mitochondrial localization sequence, but results in the same mature protein after cleavage of the localization peptide [121]. As previously shown, we used a mix of three commercially validated small-interfering RNAs (siRNAs) to silence the three different genes that code for the c subunit (ATP5G1, ATP5G2 and ATP5G3). Analysis of mRNA levels for the three genes by Real Time PCR indicates that silencing strategy produces an approximate reduction of 75 % for ATP5G1, 53 % for ATP5G2 and 20 % for ATP5G3 (**Fig. 19Ai**). This also results in a reduction close to 70 % of total protein levels as indicated by western blot analysis (**Fig. 19Aii**). To monitor the effective state of the mPTP, we used the calcein-Co^{2+} assay during c subunit silencing (**Fig. 19B**). As previously reported, ATP5G silencing ablated the mPTP activity and resulted in increased fluorescence of mitochondrial calcein (**Fig. 19C**).

By taking advantage of aequorin technology [91], we first measured the mitochondrial and cytosolic Ca^{2+} concentrations after stimulation with 100 μM histamine in HeLa cells that were transfected with a control siRNA (siSCR) or a mix of siRNAs that targeted ATP5G1, ATP5G2 and ATP5G3 (siATP5G) for 48 h (**Fig. 19C**). Silencing of the c subunit [siATP5G] caused a non-significant reduction in Ca^{2+} uptake by the mitochondria (peak amplitude: 67.35 ± 4.41 μM vs. 71.08 ± 3.33 μM [siSCR]; $p > 0.05$) and in the Ca^{2+} uptake rate, but no significant variations in the rate of Ca^{2+} release from the mitochondria (**Fig. 19D**). Further no significant differences in the cytosolic Ca^{2+} levels (peak amplitude: 2.13 ± 0.09 μM vs. 2.32 ± 0.08 μM [siSCR]; $p > 0.05$) (**Fig. 19E**) or in the kinetics of Ca^{2+} influx and efflux (**Fig. 19F**) were detected.

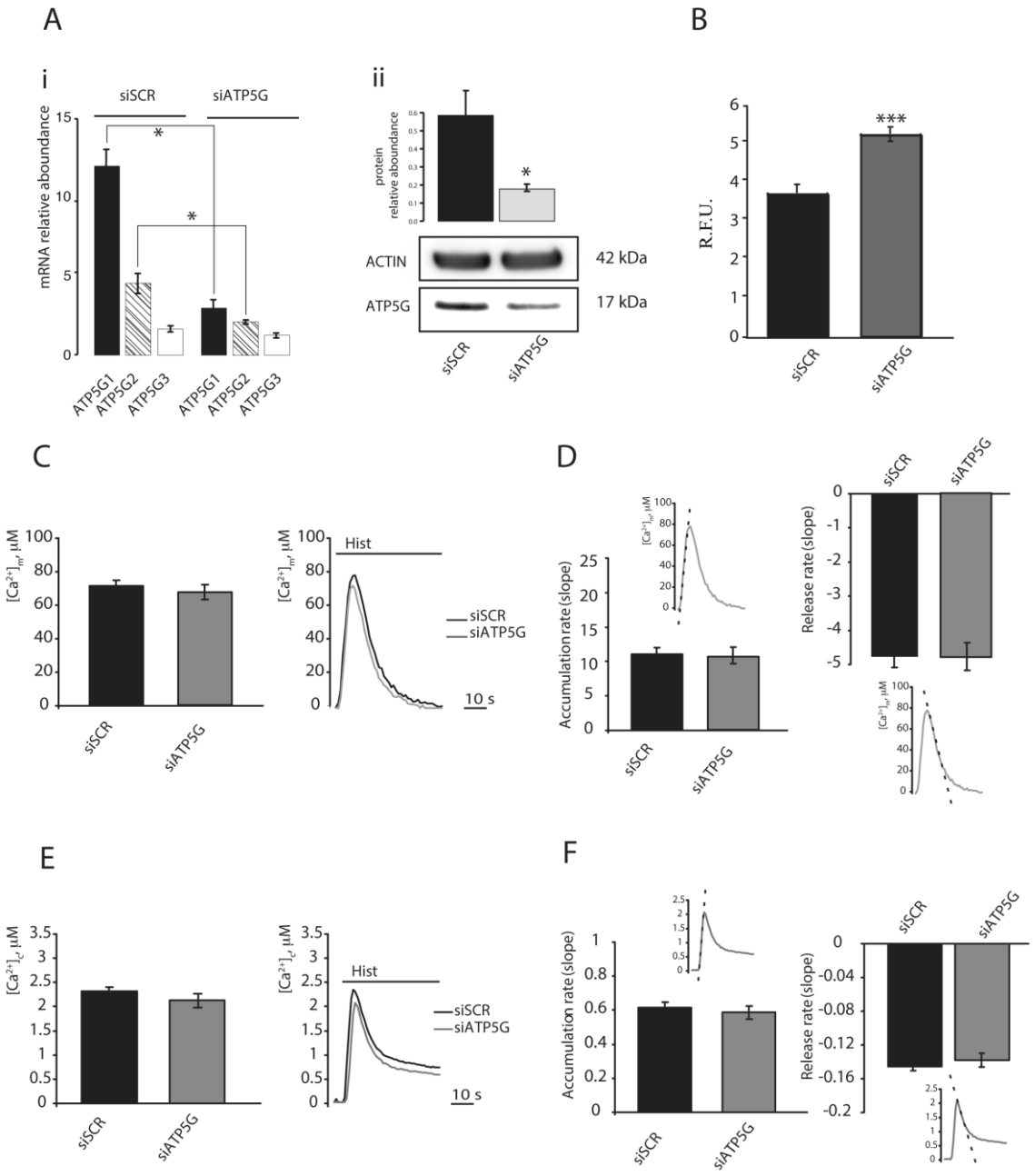

Figure 19: Calcium signaling during F1/FO ATP synthase c subunit silencing in HeLa cells. The mRNA relative aboundance of ATP5G1, ATP5G2 and ATP5G3 (Ai) and the protein relative aboundance of ATP5G (Aii) after Human cervical carcinoma (HeLa) cells transfection with a scrambled siRNA (siSCR) or a mix of siRNAs targeting ATP5G1, ATP5G2 and ATP5G3 (siATP5G) for 48 h. Fluorescence intensity levels in the Calcein-Co^{2+} assay (B). HeLa cells were transfected as in (A) but in a combination with a plasmid encoding a mitochondrial red fluorescent protein (mtDsRED). These cells were monitored using fluorescence microscopy to assess the Calcein signal.

HeLa cells were transfected as in (A) but in a combination with a plasmid coding for a mitochondrial (C) (n=30 from 6 indipendent experiments) or cytosolic (E) (n=10 from 3 indipendent experiments) aequorin and then stimulated with 100 µM histamine (Hist).

The rates of mitochondrial (D) and cytosolic (F) Ca^{2+} accumulation and release and a schematic representation of the meaning of the indexes are shown. The data are presented as means ± SEM *p < 0.05,*p < 0.001.**

To confirm the experimental method, mitochondrial Ca^{2+} dynamics were monitored in the presence of a well-established blocker of the mitochondrial Ca^{2+} efflux system, CGP37157, which is an inhibitor of the mitochondrial Na^{+}/Ca^{2+} exchanger [138].

HeLa cells were exposed to CGP37157 (10 μM) for 2 min, and Ca^{2+} uptake was induced with histamine (100 μM) in the continuous presence of the inhibitor.

CGP37157 caused an expected increase in Ca^{2+} uptake by the mitochondria (peak amplitude: 109.2 ± 15.52 μM vs. 68.6 ± 6.81 μM [MOCK]; $p < 0.05$) **(Fig. 20A**) and a significant decrease of 31% in the rate of Ca^{2+} release from the mitochondria due to inhibition of the mitochondrial Na^{+}/Ca^{2+} exchanger (**Fig. 20B**). The absence of significant differences between the cytosolic Ca^{2+} levels (peak amplitude: 2.84 ± 0.06 μM vs. 2.77 ± 0.33 μM [siSCR]; $p > 0.05$) (**Fig. 20C**) and Ca^{2+} influx and efflux kinetics (**Fig. 20D**) confirmed the specificity of CGP37157.

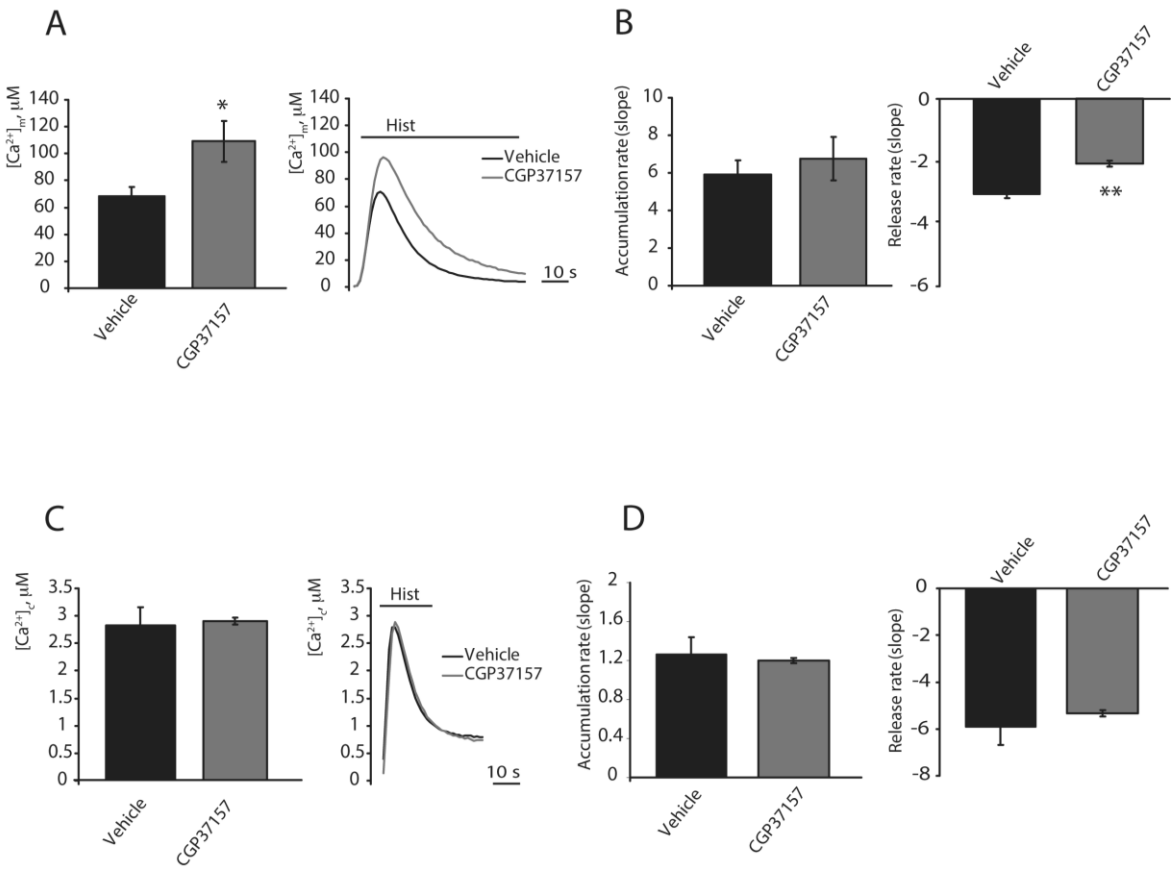

Figure 20: Inhibition of mitochondrial Ca^{2+} efflux by CGP37157. HeLa cells were transfected with a plasmid coding for a mitochondrial (A and B) (n=9 from 3 indipendent experiments) or cytosolic (C and D) (n=9 from 3 indipendent experiments) aequorin and treated with 10 μM CGP37157 for 2 min. The cells were then stimulated with 100 μM histamine (Hist) in the continuous presence of the inhibitor (A and C). Rates of mitochondrial (B) or cyctosolic (D) Ca^{2+} accumulation and release. The data are presented as means ± SEM *p < 0.05, **p<0.01.

In our experimental settings, HeLa cells appear to display higher RNA levels of ATP5G1 compared to its omologous. We thus decided to overexpress a Myc-tagged ATP5G1, which was under the control of the cytomegalovirus immediate early promoter and verify its effect on mitochondrial calcium homeostasis.

Overexperession levels were assessed by western blot and results in dramatic increase in levels of c subunit (**Fig. 21A**). As expected, ATP5G1 overexpression was sufficient to induce the opening of the mPTP, as confirmed by the calcein-Co^{2+} assay (**Fig. 21B**).

Overexpression of the c subunit induces a tendency in lower the mitochondrial Ca^{2+} uptake (peak amplitude: 82.34 ± 5.4 μM vs. 93.89 ± 10.6 μM [MOCK]; $p > 0.05$), without significantly affect the kinetics of Ca^{2+} influx and efflux (**Fig. 21C and 21D**) or cytosolic Ca^{2+} levels (peak amplitude: 3.03 ± 0.08 μM vs. 2.94 ± 0.07 μM [siSCR]; $p > 0.05$) (**Fig. 21E and 21F**).

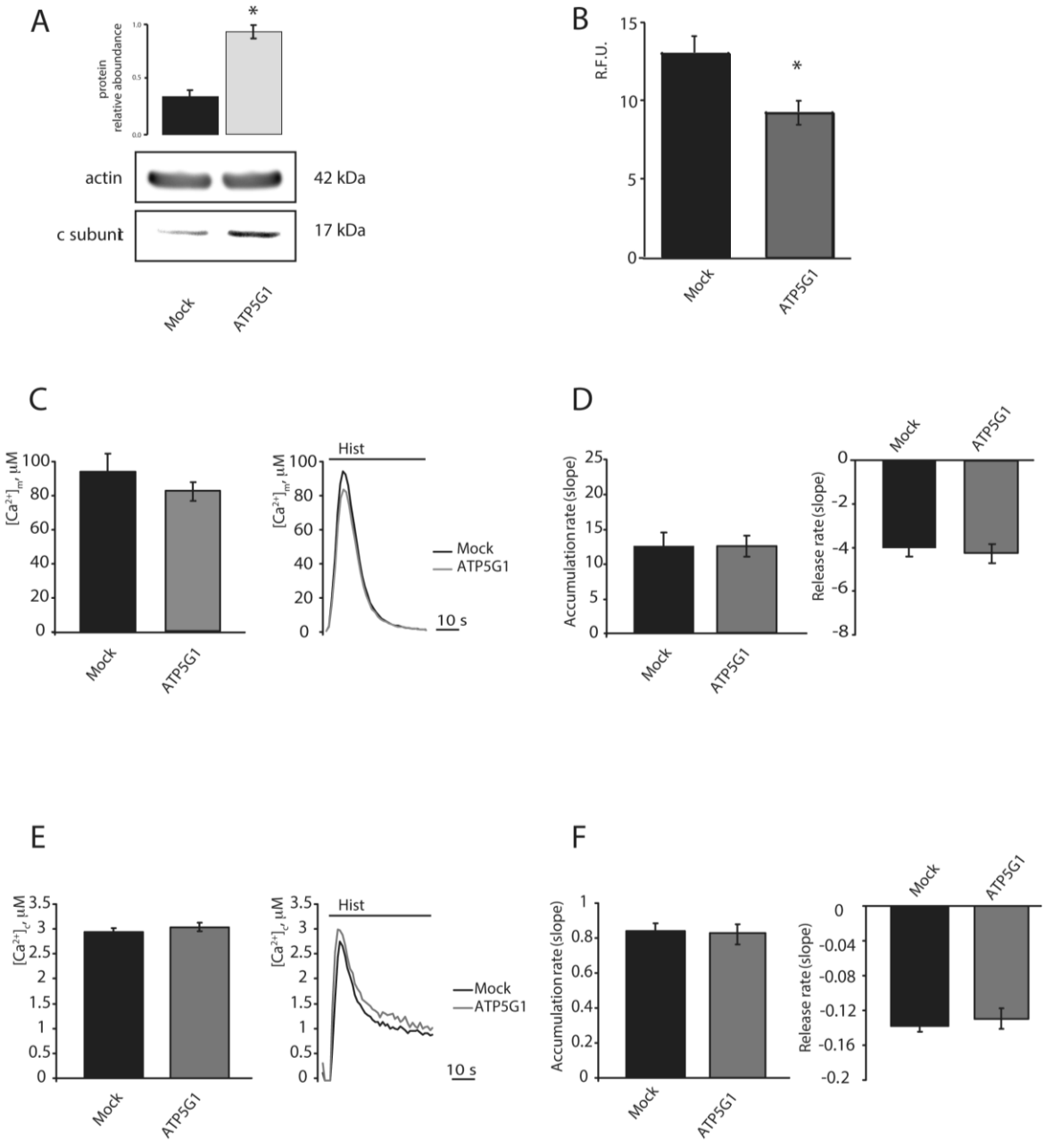

Figure 21. Calcium signaling during F1/FO ATP synthase c subunit overexpression in HeLa cells. The protein relative aboundance of HeLa cells mock transfected or transfected for 48 h with a plasmid encoding MYC-tagged ATP5G1 (A). Fluorescence intensity levels in the Calcein-Co2+ assay (B). HeLa cells were transfected as in (A) but in a combination with a plasmid encoding a mitochondrial red fluorescent protein (mtDsRED) (B), or in a combination with a plasmid coding for a mitochondrial (C) (n=16 from 4 indipendent experiments) or cytosolic (E) (n=10 from 3 indipendent experiments) aequorin, and then, the cells were stimulated with 100 µM histamine (Hist). Rates of mitochondrial (D) and cytosolic (F) Ca^{2+} accumulation and release. The data are presented as means ± SEM **p < 0.01.

To confirm the absence of an effect of mPTP modulation on Ca^{2+} efflux, we used a pharmacological approach; specifically, Cyclosporine A (CsA) and hydrogen peroxide (H_2O_2) were used as an inhibitor of the mPTP [139] and an inducer of mPTP opening, respectively [140].

CsA (1 μM) was added to HeLa cells 30 min before stimulation with histamine (100 μM) and measurements of $[Ca^{2+}]_m$. As previously reported [21], CsA induced a significant increase in Ca^{2+} uptake (peak amplitude: 82.63 ± 2.82 μM vs. 70.2 ± 2.65 μM [VEHICLE]; $p < 0.05$) (**Fig. 22A**) and in the rate of Ca^{2+} accumulation in the mitochondria due to an increase in the mitochondrial membrane potential, which is the driving force for Ca^{2+} accumulation. In contrast, no differences in Ca^{2+} efflux kinetics (**Fig. 22B**) were observed. The closed state of the mPTP was confirmed using the calcein-Co^{2+} assay (**Fig. 22C**).

In contrast, to pharmacologically induce mPTP opening, HeLa cells were exposed to H_2O_2 (500 μM) 30 min before stimulation with histamine (100 μM). As expected, in the presence of H_2O_2, a significant decrease in Ca^{2+} uptake by the mitochondria was induced (peak amplitude: 36.52 ± 3.34 μM vs. 70.2 ± 2.65 μM [VEHICLE]; $p < 0.001$) (**Fig. 22D**).

Regarding the Ca^{2+} influx/efflux kinetics, a significant reduction of 33% in the rate of Ca^{2+} accumulation into the mitochondria and a significant reduction of 22% in the rate of Ca^{2+} release from the mitochondria in the presence of H_2O_2 (500 μM) occurred (**Fig. 22E**).

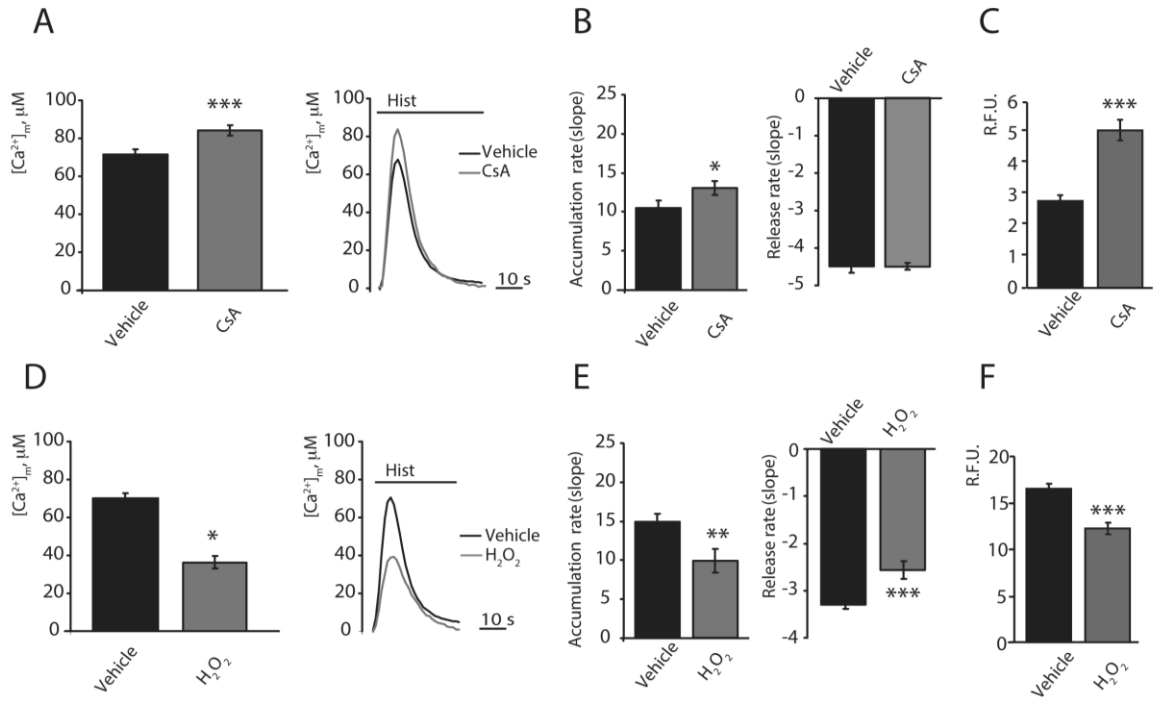

Figure 22: Modulation of the Ca^{2+} influx/efflux rates by CsA or H_2O_2 treatment. HeLa cells were transfected with a plasmid coding for a mitochondrially targeted aequorin and treated with 1 µM CsA for 30 min. The cells were then stimulated with 100 µM histamine (Hist) (A) (n=16 from 4 indipendent experiments).. Rates of mitochondrial (B) Ca^{2+} accumulation and release. Fluorescence intensity levels in the Calcein-Co^{2+} assay (C). HeLa cells were transfected as in (A) but in a combination with a plasmid encoding a mitochondrial red fluorescent protein (mtDsRED). The cells were monitored by fluorescence microscopy to assess the calcein signal. HeLa cells were transfected with a plasmid coding for a mitochondrial aequorin and treated with 500 µM H_2O_2 for 30 min (D and E). The cells were then stimulated with 100 µM histamine (Hist) (D) (n=10 from 3 indipendent experiments). Rates of mitochondrial (E) Ca^{2+} accumulation and release. Fluorescence intensity levels in the Calcein-Co2+ assay (F). HeLa cells were transfected with a plasmid encoding a mitochondrial red fluorescent protein (mtDsRED). The cells were monitored by fluorescence microscopy to assess the calcein signal. The data are presented as means ± SEM *p < 0.05, **p < 0.01, ***p < 0.001.

To confirm the specificity of the effect of H_2O_2 on mPTP opening and Ca^{2+} handling, we combined H_2O_2 (500 μM) and CsA (1 μM) before stimulation with histamine (100 μM) (**Fig. 23A**). In such condition, histamine challenging display a partial recovering in both $[Ca^{2+}]_m$ (peak amplitude: 32.59 ± 5.79 μM [Vehicle] vs. 51.6 ± 10.3 μM [CsA]; $p < 0.05$) and uptake rate, while no significant reduction in the Ca^{2+} efflux kinetic were observed (**Fig. 23B**). Silencing of ATP5G results in protection of mPTP opening during challenging with the prooxidant H_2O_2, in an extent comparable with treatment of CsA [21]. As expected HeLa cells depleted of ATP5G display a $[Ca^{2+}]_m$ protected from H_2O_2 in both amplitude (peak amplitude: 32.6 ± 5.79 μM [siSCR] vs. 57.3 ± 4.96 μM [siATP5G]; $p < 0.01$) and uptake speed while no significant differences were observed in the recovery phase of the peak (**Fig. 23C and 23D**). On opposite the ATP5G1 overexpression results in a promotion of H_2O_2 induced suppression of mitochondrial Ca^{2+} uptake (peak amplitude: 47.9 ± 5.19 μM [Mock] vs. 29.2 ± 2.22 μM [ATP5G1]; $p < 0.01$), with a parallel inhibition of the uptake and release kinetics (**Fig. 23E and 23F**).

Overall, the data shown that the mPTP pharmacological opening inversely correlate with amplitude and influx rate $[Ca^{2+}]_m$ but do not affect efflux rates in living cells.

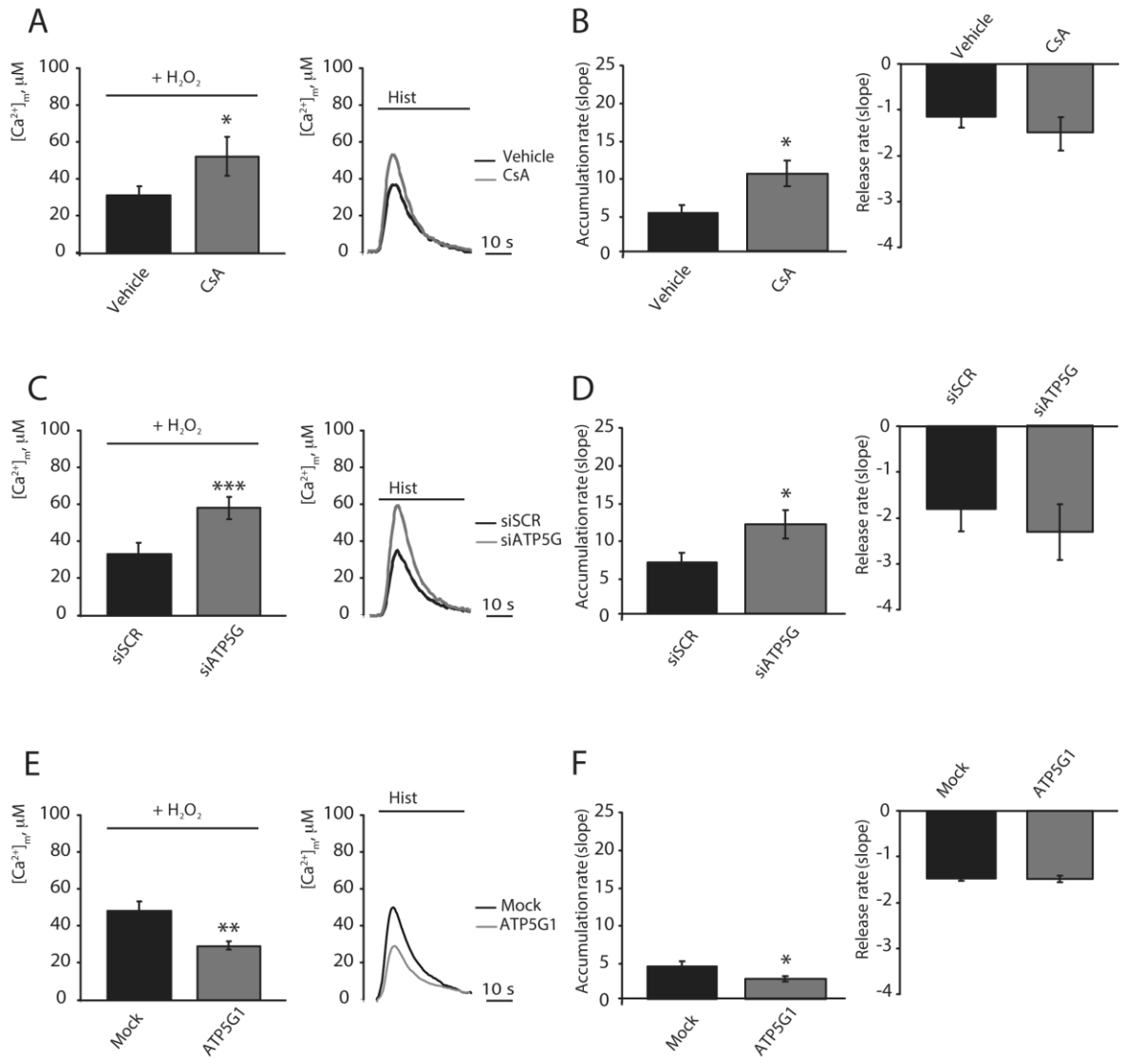

Figure 23: Modulation of the mPTP activity by c subunit silencing, c subunit overexpression and CsA treatment in combination with H_2O_2 treatment. HeLa cells were transfected with a plasmid coding for a mitochondrially targeted aequorin, treated with 1 µM CsA for 30 min and then treated with 500 µM H2O2 for 30 min (A and B). The cells were then stimulated with 100 µM histamine (Hist) (A) (n=10 from 3 indipendent experiments). Rates of mitochondrial (B) Ca^{2+} accumulation and release.

HeLa cells were transfected with a scrambled siRNA (siSCR) or a mix of siRNAs targeting ATP5G1, ATP5G2 and ATP5G3 (siATP5G) in a combination with a plasmid coding for a mitochondrial aequorin for 48 h and treated with 500 µM H_2O_2 for 30 min (C and D). The cells were then stimulated with 100 µM histamine (Hist) (C). (n=10 from 3 indipendent experiments). Rates of mitochondrial (D) Ca^{2+} accumulation and release.

HeLa cells were mock transfected or transfected for 48 h with a plasmid encoding MYC-tagged ATP5G1 in a combination with a plasmid coding for a mitochondrial aequorin and treated with 500 µM H_2O_2 for 30 min (E and F). The cells were then stimulated with 100 µM histamine (Hist) (E) (n=10 from 3 indipendent experiments). Rates of mitochondrial (F) Ca^{2+} accumulation and release.

The data are presented as means ± SEM *p < 0.05, ***p < 0.001.

Multiple authors proposed that the mPTP exerts a significant effect on the mitochondrial Ca^{2+} efflux only during saturation of the Ca^{2+} export system [141]. To explore this, we monitored the effect of genetic manipulation of ATP5G by blocking the mitochondrial Na^{+}/Ca^{2+} exchanger.

As previously shown (**Fig. 20**) exposure to CGP37157 induce significant increase in $[Ca^{2+}]_m$ during agonist stimulation with concomitant reduction of efflux rate. If mPTP opening extrude Ca^{2+} only during saturations of other efflux systems then c subunit depletion should results in a strengthened inhibition of efflux rate. In spite to this hypothesis, silencing of ATP5G in HeLa cells exposed to CGP37157 did not display any significant differences in peak amplitude when compared to siSCR-treated cells (**Fig. 24A,** peak amplitude: 86.2 ± 17.2 μM [siSCR] vs. 85.7 ± 15.93 μM [siATP5G]; $p > 0.05$) as also in uptake or release speed (**Fig. 24B**).

An analogous situation was observed by ATP5G1 overexpression. As we proposed that ATP5G1 overexpression sensitize MPT induction, the threshold for mPTP opening should be reached faster by the saturation of efflux systems. Nonetheless exposure to CGP37157 did not induce any significant variations in any of the measured indicators of mitochondrial Ca^{2+} homeostasis (**Fig. 24C and 24D,** peak amplitude: 95.23 ± 12.44 μM [Mock] vs. 81.27 ± 18.91 μM [ATP5G1]; $p > 0.05$).

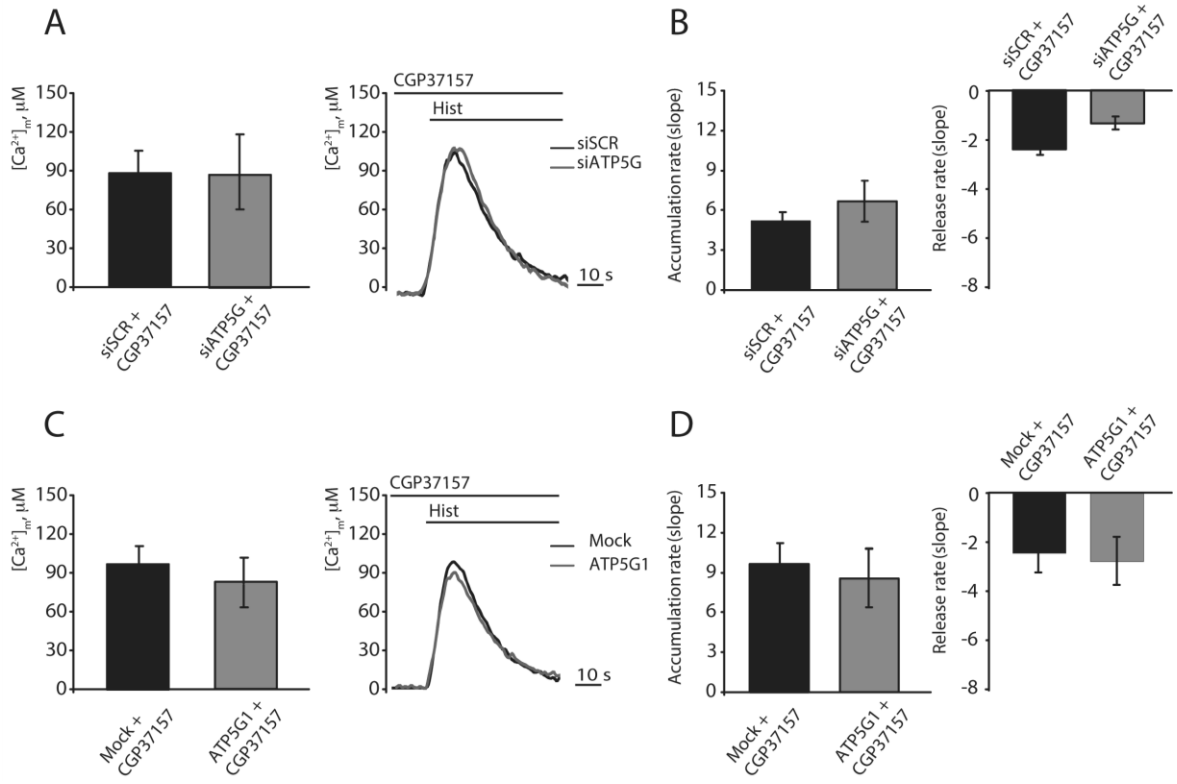

Figure 24: Modulation of the mPTP activity by combined CGP37157 and c subunit silencing or c subunit overexpression. HeLa cells were transfected with a scrambled siRNA (siSCR) or a mix of siRNAs targeting ATP5G1, ATP5G2 and ATP5G3 (siATP5G) in a combination with a plasmid coding for a mitochondrial aequorin for 48 h and treated with 10 µM CGP37157 added 2 min before stimulation with histamine, which was done in the continuous presence of CGP37157. (A and B). The cells were then stimulated with 100 µM histamine (Hist) (A) (n=10 from 3 indipendent experiments). Rates of mitochondrial (B) Ca^{2+} accumulation and release. HeLa cells were mock transfected or transfected for 48 h with a plasmid encoding MYC-tagged ATP5G1 in a combination with a plasmid coding for a mitochondrial aequorin and treated with 10 µM CGP37157 added 2 min before stimulation with histamine, which was done in the continuous presence of CGP37157. (C and D). The cells were then stimulated with 100 µM histamine (Hist) (C) (n=10 from 3 indipendent experiments). Rates of mitochondrial (D) Ca^{2+} accumulation and release. The data are presented as means ± SEM.

To avoid any aspecific effect related to modulation of ATP5G expression effect of efflux system saturation was tested by pharmacological inhibition of mPTP by CsA. HeLa cell exposed to GCP37157 display peak amplitude much lower compared to the double-treated cells (**Fig. 25A,** peak amplitude: 132.2 ± 29.53 µM [CsA + CGP37157] vs. 75.84 ± 8.00 µM [CGP37157]; $p < 0.05$). This also reflects in a dramatic increase in uptake rate (**Fig. 25B**). In spite of the different amount of Ca^{2+} available, CsA do not induce the hypothesized reduction in efflux rate, but only a barely increase (**Fig. 25B**).

Furthermore, as alternative route to saturation $[Ca^{2+}]_m$, we forced an increase in $[Ca^{2+}]_m$ by overexpressing the MCU. HeLa cells overexpressing the mitochondrial Ca^{2+} uniporter

displayed a dramatic increase in mitochondrial Ca^{2+} uptake (peak amplitude: 62.74 ± 3.69 µM vs. 112.14 ± 10.27 µM [MOCK]; $p < 0.01$), which was near 100% (**Fig. 25A**). As expected, a significant stimulation of Ca^{2+} influx was observed (approximately 97%); however, no significant variations in efflux were detectable (**Fig. 25B**). MCU overexpression was then combined with mPTP inhibition by CsA. Cells that were exposed to CsA (1 µM) and overexpressing MCU display a tendency in reduction of maximal $[Ca^{2+}]_m$, (peak amplitude: 112.2 ± 10.27 µM [MCU] vs. 98.9 ± 13.57 µM [MCU + CsA]; $p > 0.05$) in contrast to what was observed in mock-transfected cells (**Fig. 25C and 25A**). Nonetheless no differences were detected in the Ca^{2+} efflux rates (**Fig. 25D**).

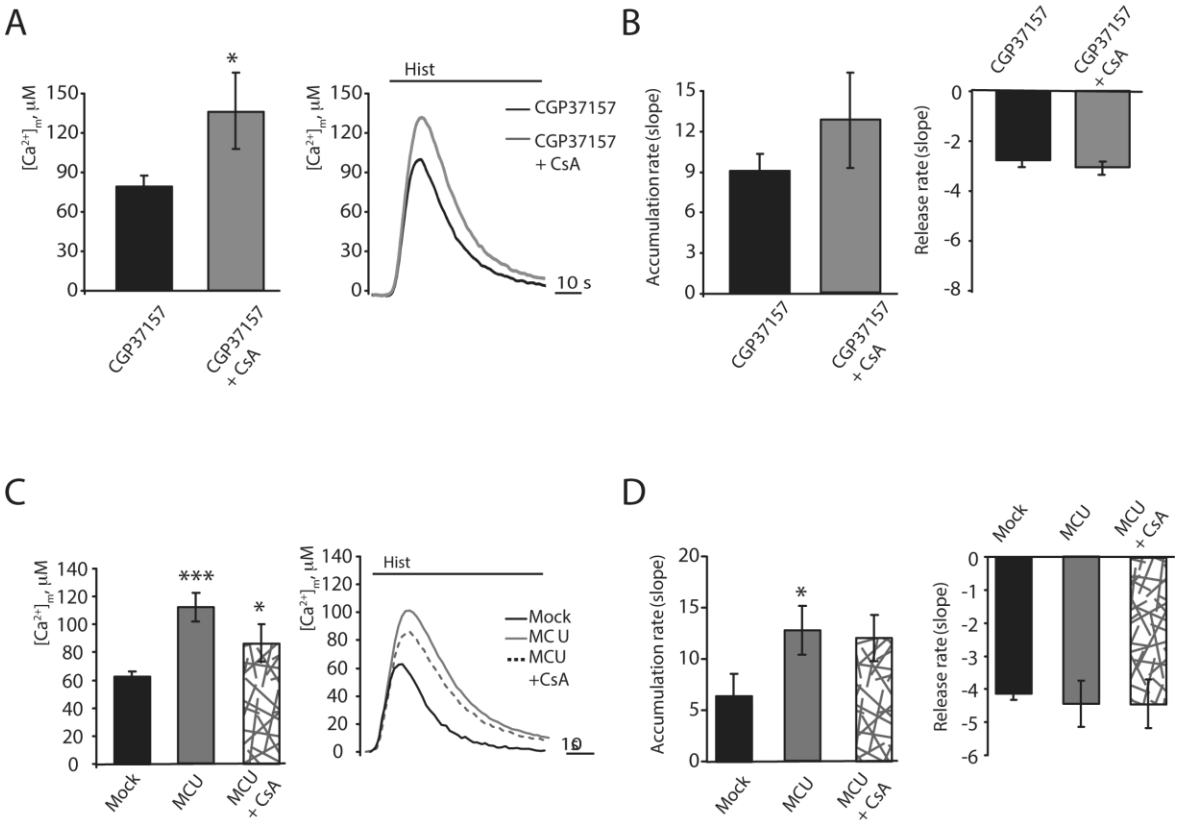

Figure 25: Modulation of the mPTP activity by CsA treatment in combination with CGP37157 treatment or MCU overexpression. HeLa cells were transfected for 48 h with a plasmid coding for a mitochondrial aequorin and treated with 10 µM CGP37157 for 2 min, in absence or presence of 1 µM CsA for 30 min. (A and B). The cells were then stimulated with 100 µM histamine (Hist) (A) (n=9 from 3 indipendent experiments). Rates of mitochondrial (B) Ca^{2+} accumulation and release. HeLa cells were mock transfected or transfected for 48 h with a plasmid encoding MCU-FLAG in a combination with a plasmid coding for a mitochondria-targeted aequorin in absence or presence of 1 µM CsA for 30 min (C and D). The cells were then stimulated with 100 µM histamine (Hist) (C) (n=9 from 3 indipendent experiments). Rates of mitochondrial (D) Ca^{2+} accumulation and release. The data are presented as means ± SEM *p < 0.05, ***p < 0.001.

The efficiency of the mitochondrial Ca^{2+} efflux system has been proposed to be dependent upon $[Ca^{2+}]_m$. Some previously described conditions cause variations in the maximal $[Ca^{2+}]_m$. To avoid data misinterpretation due to this effect, we measured mitochondrial Ca^{2+} accumulation and release in permeabilized cells that were exposed to the same $[Ca^{2+}]$. For this purpose, HeLa cells were perfused with a solution mimicking the intracellular milieu (IB) supplemented with 2 mM EGTA, the cells were then permeabilized with digitonin 30 for 1 min. The perfusion buffer was then changed to IB, which had an EGTA-buffered $[Ca^{2+}]$ of 1 μM. The cells were finally perfused with IB that was supplemented with Ruthenium Red (RuR), which is an inhibitor of the mitochondrial Ca^{2+} uniporter, and deprived of free Ca^{2+} to induce a maximal rate of Ca^{2+} release from the mitochondria. The same experiment was performed during modulation of c subunit expression or in the presence of CsA (1 μM), which was added 30 min before the beginning of the measurement. Exposure of permeabilized cells transfected with scrambled siRNA to external $[Ca^{2+}]$ (1 μM) induced a rapid increase in $[Ca^{2+}]_m$ that was stabilized at a value of 3.09 ± 0.24, analogous to the $[Ca^{2+}]_m$ that was reached in cells transfected with siATP5G (**Fig. 26A,** plateau 2.89 ± 0.22 μM). The switch to a Ca^{2+}-free condition in the presence of RuR induced a dramatic decrease in the $[Ca^{2+}]_m$, and the rate at which this occurred appeared to be identical between cells transfected with scrambled siRNA or depleted in ATP5G (**Fig. 26B**). Negligible variations in both plateau levels or Ca^{2+} efflux rates were detected also when overexpressing ATP5G1 (**Fig. 26C and 26D,** plateau level: 2.03 ± 0.26 μM [Mock] vs. 2.34 ± 0.43 μM [ATP5G1]; $p > 0.05$) or during exposure to CsA (**Fig. 24E and 24F,** plateau level: 1.72 ± 0.28 μM [Vehicle] vs. 1.65 ± 0.74 μM [CsA]; $p > 0.05$). This confirmed that mPTP does not affect maximal mitochondrial Ca^{2+} efflux rate in standardized $[Ca^{2+}]_m$.

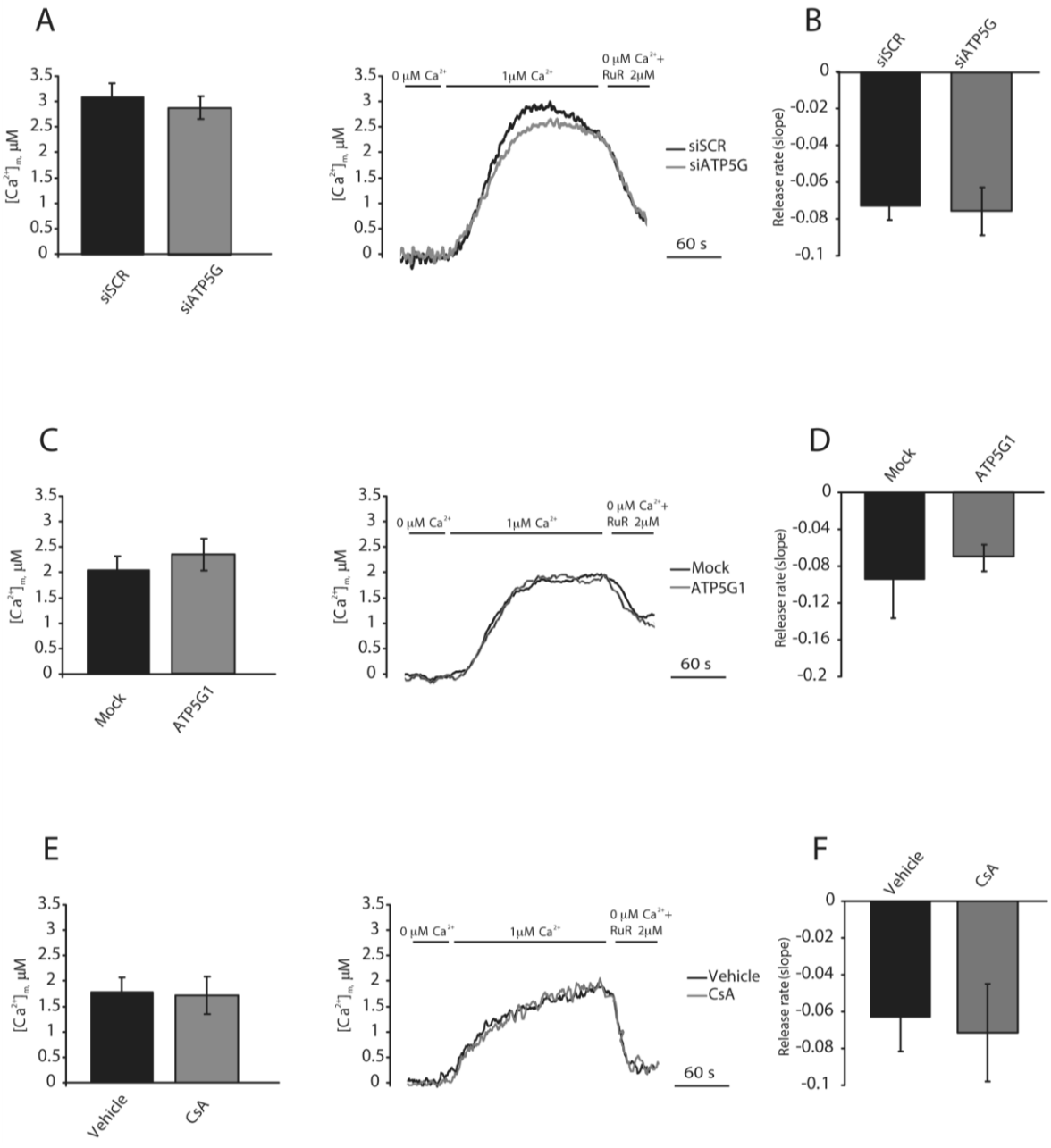

Figure 26: Modulation of the mPTP activity by c subunit silencing, c subunit overexpression and CsA treatment in permeabilized cells. HeLa cells were transfected with a scrambled siRNA (siSCR) or a mix of siRNAs targeting ATP5G1, ATP5G2 and ATP5G3 (siATP5G) in a combination with a plasmid coding for a mitochondrial aequorin for 48 h (A and B) (n=9 from 3 indipendent experiments); HeLa cells were mock transfected or transfected for 48 h with a plasmid encoding MYC-tagged ATP5G1 in a combination with a plasmid coding for a mitochondrial aequorin (C and D) (n=10 from 3 indipendent experiments); HeLa cells were transfected with a plasmid coding for a mitochondria-targeted aequorin and treated with 1 µM CsA for 30 min or Vehicle (E and F) (n=10 from 3 indipendent experiments). The cells were then digitonin-permeabilized and stimulated with 1 µM [Ca^{2+}] in EGTA-buffered buffer. Calcium efflux was stimulated by a calcium-free buffer supplemented with Ruthenium Red (RuR). Rate of mitochondrial Ca^{2+} release after Ca^{2+} deprivation and RuR perfusion (B, D and F)). The data are presented as means ± SEM.

Nonetheless in such experimental conditions a possible effect of mPTP in efflux kinetic could be overcome by the activity of mNCX and the Ca^{2+}/H+ antiporter. Ca^{2+} efflux rates where monitored in presence of the mitochondrial Na^{+}/Ca^{2+} exchanger CGP37157 elicited by 2 μM RuR and in presence of external Ca^{2+}. The presence of CGP37157 dramatically increase mitochondrial Ca^{2+} uptake causing fast aequorin consumption when external Ca^{2+} 1 μM was added ($[Ca^{2+}]_m$ > 14 μM data not show). In this second group of permeabilized cells Ca^{2+} uptake was then elicited by external Ca^{2+} 0.5 μM. Administration of RuR induce slow (but not absent) Ca^{2+} release from mitochondrial matrix in scrambled, siRNA-trasfected HeLa cells. Interestingly cells transfected with siRNA for ATP5G1 display the same $[Ca^{2+}]_m$ at the plateau while the efflux speed, in presence of RuR was consistently (but not significantly) reduced suggesting a possible role for mPTP in Ca^{2+} efflux in this condition (data not shown). According to this hypotesys the efflux rate in HeLa overexpressing ATP5G1 display a strong (but not significant) increase (**Fig. 27A and 27B**). Finally when cells were pretreated with CsA (**Fig. 27C and 27D**) the extrusion rate appear completely identical to the once measured in untreated cells, indicating that mPTP was not responsible for remaining Ca^{2+} leak from mitochondrial matrix.

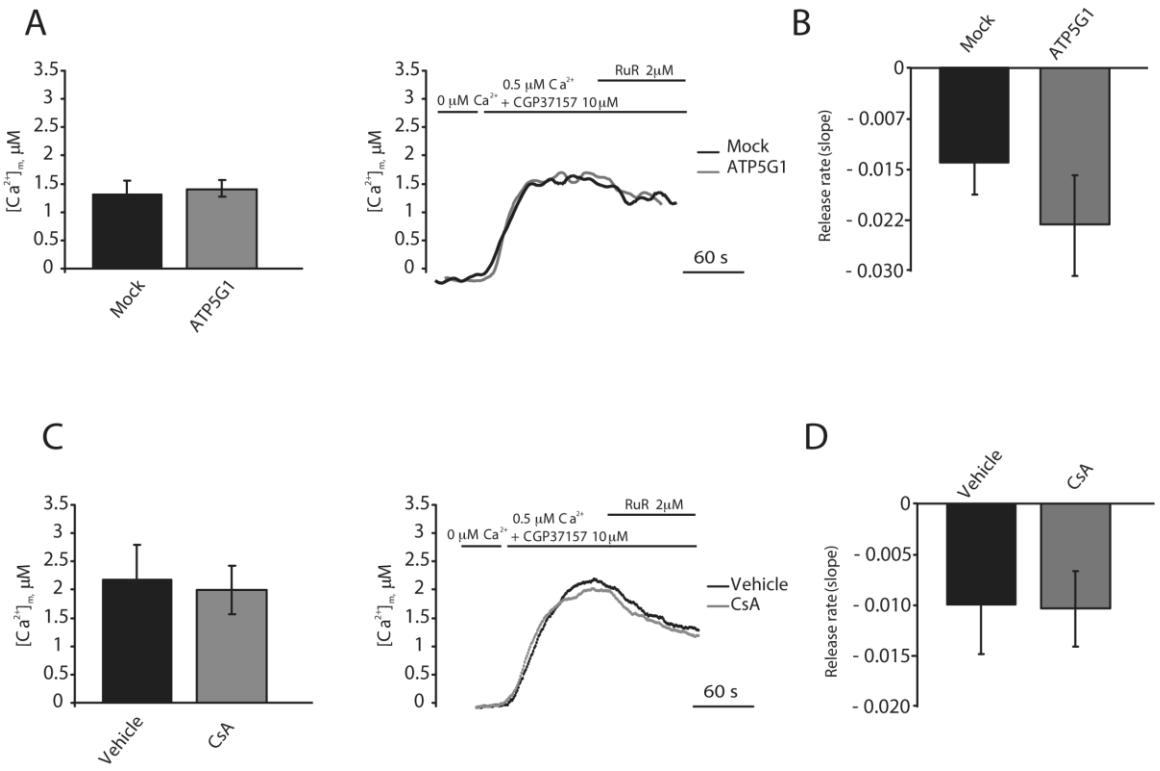

Figure 27: Modulation of the mPTP activity by combined CGP37157 and c subunit overexpression or CsA treatment in permeabilized cells. HeLa cells were mock transfected or transfected for 48 h with a plasmid encoding MYC-tagged ATP5G1 in a combination with a plasmid coding for a mitochondrial aequorin (A and B) (n=9 from 3 indipendent experiments); HeLa cells were transfected with a plasmid coding for a mitochondria-targeted aequorin and treated with 1 µM CsA for 30 min or Vehicle (C and D) (n=9 from 3 indipendent experiments). The cells were then digitonin-permeabilized and stimulated with 0.5 µM [Ca^{2+}] in EGTA-buffered buffer and in presence of CGP37157 10 µM. Calcium efflux was stimulated by 2 µM Ruthenium Red (RuR).

Rate of mitochondrial Ca^{2+} release after Ca^{2+} deprivation and RuR perfusion (B and D). The data are presented as means ± SEM.

Discussion

Correct Ca^{2+} uptake into the mitochondria is essential for mitochondrial oxidative phosphorylation, but excessive Ca^{2+} uptake leads to cell death [142]. Therefore, the balance between Ca^{2+} influx and efflux is fundamental for correct intracellular homeostasis and is extensively regulated by influx (through the mitochondrial Ca^{2+} uniporter) and efflux (through the Na^{+}/Ca^{2+} or H^{+}/Ca^{2+} exchanger) systems [82].

Some authors have proposed that the mPTP is a component of the Ca^{2+} efflux system due to the non-specific channel properties that were observed during its opening [45, 81]. These reports are based mainly on pharmacological inhibition of the mPTP by cyclosporine A (CsA, which targets PPIF) or by knocking down PPIF, which causes typical alterations in mitochondrial Ca^{2+} homeostasis that could be associated with alterations in the mitochondrial Ca^{2+} efflux (especially alterations in the maximal $[Ca^{2+}]_m$ and Ca^{2+} extrusion rates). On the other hand, several other reports have indicated the opposite [82, 83], which suggests a different function for CsA in affecting Ca^{2+} homeostasis.

Driven by our recent work suggesting that the c subunit of the $F1/F_O$ ATP synthase is a component of the mPTP, we have focused our attention on the involvement of the mPTP in mitochondrial Ca^{2+} homeostasis under non-pathological conditions. The novelty of our study lies in the regulation of mPTP activity by manipulating the c subunit of the $F1/F_O$ ATP synthase and measuring the $[Ca^{2+}]_m$ and $[Ca^{2+}]_c$ using the pH-independent, luminescent, Ca^{2+}-sensitive probe, aequorin [91].

Measurements of $[Ca^{2+}]_m$ revealed a minimum reduction in mitochondrial Ca^{2+} loading after c subunit silencing but no variations in the rate of Ca^{2+} release from the mitochondria were observed. Furthermore, no changes in the cytosolic Ca^{2+} levels were observed. As previously shown in this condition, we forced the closing of the mPTP, and the cells were protected from damage.

An analogous situation occurs when the c subunit is overexpressed, which forces the opening of the mPTP. In this case, mitochondrial Ca^{2+} accumulation is reduced, but no changes in the rate of Ca^{2+} influx and efflux occur.

In both cases the observed variations in peak amplitude correlates with the decrease in the mitochondrial membrane potential that is induced by c subunit silencing or overexpression, which we recently reported [91]. The overall modulation of c subunit expression suggested that, under physiological conditions in HeLa cells, mPTP is not directly involved in the Ca^{2+} efflux mechanism, and an indirect effect could be hypothesized instead.

We previously reported that, in this cell line, c subunit silencing generates a moderate reduction of the MMP, which is the opposite of the significant depolarization that occurs upon c subunit overexpression. Variations in ψ_m, which is the driving force for Ca^{2+} accumulation in the mitochondrial matrix, could produce the exact effects on $[Ca^{2+}]_m$ and uptake rate that were observed in this model. To validate these results, we took advantage of the well-known PPIF inhibitor CsA that was reported to be capable of increasing the ψ_m and $[Ca^{2+}]_m$ [143, 144]. After CsA treatment, a significant increase in mitochondrial Ca^{2+} uptake and the peak amplitude occurred, but, again, no differences in the rate of mitochondrial Ca^{2+} efflux were observed (which was in accordance with the observation of c subunit silencing).

However, we cannot completely ignore the several respectable reports proposing that there is an effect of the mPTP on mitochondrial Ca^{2+} efflux. Most of these reports were based on PPIF inhibition or knock out. It could then be speculated that PPIF could somehow affect other participants of the Ca^{2+} efflux system, as proposed by Wei and co-workers [82], and possibly generate a conformational rearrangement upon interaction with other proteins due to its peptidyl-prolyl isomerase activity.

It could be argued that c subunit overexpression did not lead to an mPTP opening event sufficient to generate a detectable Ca^{2+} efflux. To test this hypothesis, we induced mPTP opening through the use of the prototypic, pro-oxidant H_2O_2. Exposure to this stress agent results in mPTP opening with consequent reduction in the maximal $[Ca^{2+}]_m$ after agonist exposure, and an increase in Calcein quenching by cobalt. In this condition a decrease in the mitochondrial Ca^{2+} influx and efflux were observed, in agreement with the reduced driving force, while the model of an opened aspecific Ca^{2+} channel (as the mPTP would be) should produced a significant increase in Ca^{2+} efflux rate.

Nonetheless, although the $[Ca^{2+}]_m$ is partially recovered, in cells silenced for ATP5G or pretreated with CsA, protection from mPTP does not modify the Ca^{2+} efflux kinetics. As opposite the ATP5G1 overexpression promotes the H_2O_2 induced mPTP opening causing a further reduction in maximal $[Ca^{2+}]_m$ under agonist stimulation. In spite of this, the efflux rate do not display a significant stimulation, but rather a bare inhibition. These observations provide strong confirmation that, even following a potent induction of its opening, the mPTP does not participate in Ca^{2+} efflux. We previously confirmed that, induction of mPTP by H_2O_2 cause a slow ψ_m dissipation (probably due to the induction of the low conductance mode of mPTP) [21, 145]. During protection or induction of mPTP opening, $[Ca^{2+}]_m$ recovering phase seem to correlate with the levels of ψ_m previously

observed in such conditions [21], strengthening the hypothesis that a possible modulation of $[Ca^{2+}]_m$ by mPTP should indirectly occurs, due to regulation of ψ_m.

It was proposed that the effects of the mPTP on Ca^{2+} efflux kinetics could be relevant as a "safe valve" only in mitochondria with a saturated Ca^{2+} efflux system [141], which is analogous to what was observed in Ca^{2+} retention capacity experiments that largely used isolated mitochondria to determine the threshold for mPTP opening. To challenge this hypothesis in living cells, we combined the c subunit expression with the blockade of mitochondrial Na^+/ Ca^{2+} antiporter through the use of CGP37157. Interestingly all the tendencies previously observed while silencing or overexpressing c subunit were completely masked by the use of CGP37157, suggesting that sustained $[Ca^{2+}]_m$ levels are not sufficient to induce a calcium efflux through mPTP. Further an effect of on $[Ca^{2+}]_m$ was still observable, while blocking mNCX, as an increase in $[Ca^{2+}]_m$ and in influx rate (characters dependent on ψ_m), nonetheless efflux rate was, still, not affected.

An alternative Ca^{2+} overload approach was proposed. Recently several components of the mitochondrial calcium uptake machinery has been revealed [64]. Core element of the MCU system is the proteic channel product of the CCDC109a gene (MCUa [40, 41]. Overexpressing the MCU, as expected, resulted in an extraordinary increase in the Ca^{2+} influx rate and $[Ca^{2+}]_m$. Such an increase was not further stimulated by the mPTP opening inhibition through treatment with CsA, which suggested that the mitochondrial network was near its maximal uptake capacity. Interestingly MCUa overexpression also resulted in a reproducible tendency in increase also the Ca^{2+} efflux rate. Treatment with CsA did not generate any significant effects on calcium efflux rates of MCUa-overexpressing cells. Overall these results clearly indicates that overload of $[Ca^{2+}]_m$, in our cell model, is not sufficient to induce a mPTP dependent Ca^{2+} efflux.

The Ca^{2+} efflux system is dependent upon $[Ca^{2+}]_m$, which is exposed; and modulation of the expression of the c subunit as well as exposure to CsA results in alterations of the $[Ca^{2+}]_m$.

To avoid misinterpretation of the data due to different values of $[Ca^{2+}]_m$, Ca^{2+} efflux measurements were performed in permeabilized cells that had been stimulated with external Ca^{2+} (1 μM) to obtain a stable level of $[Ca^{2+}]_m$ in the control mitochondria compared. After that plateau was reached, the external Ca^{2+} was removed, and the MCU inhibitor Ruthenium Red was added to avoid Ca^{2+} reuptake. The rate of Ca^{2+} release from the mitochondria under these conditions has to be considered as the maximum efflux speed that could be reach and revealed no significant differences after mPTP inhibition with CsA as also during ATP5G silencing or its overexpression. It is reasonable to assume that, being

mitochondria in permeabilized cells energized by addition of ADP, pyruvate and succinate, the efflux rate is driven mostly by the mNCX and to the H^+/Ca^{2+} exchangers.

Nonetheless a further induction of efflux system saturation by inhibition of mitochondrial Na^+/ Ca^{2+} antiporter (in the presence of external Ca^{2+}) and MCU inhibition (by RuR) generate a Ca^{2+} leak from mitochondrial matrix independent on mPTP inhibition (by ATP5G silencing or CsA administration) as also to its stimulation (by ATP5G1 overexpression) thus ascribable only to the H^+/Ca^{2+} exchanger excluding the possible involvement of the mPTP as a component of the Ca^{2+} efflux system even when standardized Ca^{2+} concentrations where achieved.

The presented results suggest that, in spite of what can be observed in isolated mitochondria, the mPTP has a Ca^{2+}-induction threshold that is too high to be reached in living cells, and this is most likely due to the high efficiency of the Na^+/ Ca^{2+} and H^+/Ca^{2+} exchangers, which can could compete with and overcome the mPTP. It should also be considered that the Ca^{2+} efflux from mitochondria is an energetically unfavorable process due to the strong electrochemical gradient, which is negative in the matrix. This allows for passive import into the matrix, as occurs during MCU. If the current model for the mPTP, which states that it forms a nonspecific channel, is correct, then its partial opening even in the presence of a reduced ψ_m (as it apparently occurs in its low conductance mode) should favor import instead of efflux. In contrast, efflux through a channel would be expected on de-energized mitochondria, as was reported for the MCU [146]. Still has to be considered that inhibition of mPTP induce increase in Ca^{2+} loading capacity that can lead to generation of toxic Ca^{2+} phosphorous rich precipitates [147]. Present results do not exclude mPTP participation in this phenomenon, but it would suggest that it could be indirectly involved. Opening of mPTP do not directly allow Ca^{2+} transport, but rather would dissipated mitochondrial membrane potential facilitating Ca^{2+} efflux from conventional Ca^{2+} efflux system or by inverse transportation through MCU.

Altogether, these data demonstrate that, under physiological conditions, the mPTP is a dispensable element for mitochondrial Ca^{2+} homeostasis and, especially, for mitochondrial Ca^{2+} release at least in our cell model.

Materials and methods

Cell culture and transfection.

Mouse embryonic fibroblast (MEFs) were maintained in a humidified 5% CO_2, 37°C incubator in Dulbecco's modified Eagle's medium (DMEM) supplemented with 10% fetal bovine serum (FBS; Life technologies, 10270) 100 U/ml penicillin (EuroClone, 3001D), 100 mg/ml streptomycin (EuroClone, 3000D) were infected by recombinant adenovirus expressing mitochondrially or cytosolic aequorin, mtGFP and MCU-GFP. For aequorin measurements, the cells were seeded before transfection onto 13mm glass coverslips and allowed to grow to 50% confluence. For mitochondrial membrane potential analysis by fluorescence microscopy cells were seeded on 24mm glass coverslip. For immunoblotting analysis, cells were seeded on 6 well plates in the same conditions of growth.

HeLa cells were grown in Dulbecco's Modified Eagle's Medium (DMEM) (Euroclone), supplemented with 10% fetal bovine serum (FBS, Gibco) and penicillin/streptomycin (Gibco), in atmosphere of 5% (v/v) carbon dioxide in air at 37 °C. Cells were seeded 24 h before transfection onto glass coverslips (13mm in diameter for aequorin experiments or 24mm for microscopy experiments), or on 10cm Petri dishes for immunoblotting and cell death experiments.

Cortical/hippocampal neurons were prepared from 1- to 3-day-old newborn rats, [148], and neurons were resuspended in Neurobasal A Medium (Gibco) with supplement B-27 (Gibco), GlutaMax (Gibco) and penicillin/streptomycin (Gibco) rigorously at 37°C and plated onto glass coverslips, coated with poly-D-lysine (Sigma).

HeLa were allowed reach 50% confluence before transfection. Cultured neurons were transfected at 3 days in vitro (DIV 3). RNA interference experiments were performed by transfecting cells with a commercial control siRNA (AllStars RNAi Controls, herein referred to as siSCR), with a validated siRNA specific for ATP5A1 (siATP5A1, sense 5'-GGC UGG AUU UGA AGC UUA AdTdT-3') or with a mix of siRNAs targeting ATP5G1 (5'-GCU CUG AUC CGC UGU UGU AdTdT-3'), ATP5G1 (5'-CGG AGA UAC UGA CAG AUG AdTdT-3') and ATP5G3 (5'-AGG GCU CUA CGG UAU UUA AdTdT-3'), all purchased from Qiagen. siRNAs were transfected by means of the HiPerfect® transfection reagent, as per manufacturer's instructions [149]. For transient overexpression experiments, a pCMV6 entry- based plasmid coding for a MYC-tagged variant of ATP5G1 under the control of the CMV immediate early promoter (RC200292) was obtained from OriGene. A pcDNA3 based plasmid coding for MCU-flag tagged was gift from prof.

Rosario Rizzuto from University of Padua, pcDNA3 empty vector was used as Mock. For the quantification of mitochondrial ATP levels, a VR1012-based construct encoding a mitochondrially targeted variant of the Photinus pyralis luciferase under the control of the CMV immediate early promoter was employed [120]. For the study of mitochondrial morphology, a pcDNA3-based plasmid coding for a mitochondrially targeted variant of GFP (mtGFP) under the control of the CMV immediate early promoter was used [150]. For the quantification of cell death in neurons, a pcDNA3-based construct coding for GFP under the control of the CMV immediate early promoter was used [151]. Plasmid transfections were performed via the standard Ca^{2+} phosphate procedure [152].

MEFs cells synchronization protocol. MEFs cells were subjected to a synchronization protocol by the use of Serum Starvation (SS). Cells are seeded in the wells and then subjected to SS, in particular with DMEM high glucose supplemented with only 0.1% FBS (the total absence of serum leads cells to autophagy) for 48-72 h. After this time cells are in G0 phase. Cells are then washed with PBS and subsequently additioned with complete medium (Serum Readdition (SR)). After 8 h of SR cells are in G1 phase, after 24 h in G1/S phase, after 28 h in S phase. For the remaining phases, the addition of Nocodazole 100 ng/ml induces cell cycle progression, by microtubules depolymerization. After 24 h of SR plus 4 or 8 h of Nocodazole treatment (in SR medium) cells are in G2 and M phase respectively.

RNA extraction and gene expression analyses. For the expression analysis of *ATP5G1*, *ATP5G2*, and *ATP5G3* silencing, total RNA was purified from HeLa cells transfected with scrambled or ATP5G1 siRNAs (siATP5G1, 2 and 3), for 48 h following the standard TRIzol protocol. To analyze mRNA expression, qRT-PCR was performed on 500 ng of total RNA using oligo dT (Fermentas) and random primers (Gibco). Quantitative PCR reaction was performed using Qiagen Taq DNA Polymerase and EvaGreen (Biotium Inc). The following oligonucleotides were used as primers for the qPCR reaction:
ATP5G1-fw, 5'-GCTGAGACCAAGGGCTAAAG-3';
ATP5G1-rv, 5'-CGGATCAGAGCTGGAGAAATG-3';
ATP5G2-fw, 5'-TGGAACTGTGTTTGGGAGC-3';
ATP5G2-rv, 5'-TGGCAAAGAGGATGAGAAAGG-3';
ATP5G3-fw, 5'-TGGTTCTGGTGCTGGTATTG-3';
ATP5G3-rv, 5'-GAGACCCATAGCTTCAGACAAG-3'.

Reactions were incubated in a 96-well PCR plate at 95°C for 15 min, followed by 40 cycles of 95° C for 30 sec and 58°C for 1 min, on Bio-Rad-Chromo4 Real Time thermal Cycler.
(available at http://fiji.sc/) and the parallel iterative deconvolution plugin.

Aequorin measurements. Probes used are chimeric aequorins targeted to the cytosol (cytAEQ) and mitochondria (mtAEQmut). "AEQ" refers to wild-type aequorin, and "AEQmut" refers to a low affinity D119A mutant of aequorin. For the experiments with cytAEQ and mtAEQmut, MEFs cells were incubated with 50 mM coelenterazine (Fluka, 7372) for 1–2 h in complete DMEM high glucose. HeLa cells were incubated with 5 mM coelenterazine (Fluka, 7372) for 1–2 h in Krebs-Ringer buffer (KRB). A coverslip with transfected cells was placed in a perfused thermostated chamber located in close proximity to a low-noise photomultiplier with a built-in amplifier/discriminator. All aequorin measurements were performed in KRB supplemented with 1 mM $CaCl_2$. Agonist was added to the same medium as specified in figure legends. All experiments were terminated by lysing cells with 100 μM Triton in a hypotonic Ca^{2+}-containing solution (10 mM $CaCl_2$ in H_2O) thus discharging the remaining aequorin pool. The output of the discriminator was captured by a Thorn EMI photon-counting board and stored in an IBM-compatible computer for further analyses. The aequorin luminescence data were calibrated offline into $[Ca^{2+}]$ values using a computer algorithm based on the Ca^{2+} response curve of wild-type and mutant aequorins. In the experiments with permeabilized cells, a buffer mimicking the cytosolic ionic composition, (intracellular buffer) was used: 130 mM KCl, 10 mM NaCl, 2 mM K_2HPO_4, 5 mM succinic acid, 5 mM malic acid, 1 mM $MgCl_2$, 20 mM HEPES, 1 mM pyruvate, 0.5 mM ATP (pH 7 at 37 °C). Intracellular buffer was supplemented with 2 mM EGTA and 2 mM HEDTA-buffered $[Ca^{2+}]$ 1 μM or 0.5 μM (intracellular buffer/Ca^{2+}), calculated with the Chelator software [153]. HeLa cells were permeabilized by a 1-min perfusion with 50 μM digitonin (added to intracellular buffer/EGTA) during luminescence measurements. Mitochondrial Ca^{2+} uptake rate was calculated as the first derivative by using Microsoft Excel (Microsoft Co.); all the slopes were calculated at the same $[Ca^{2+}]_m$ to ensure comparable activity of efflux system.

Quantification of cell death. Dead cells were quantified by virtue of their ability to take up propidium iodide (PI), reflecting the breakdown of the plasma membrane [154, 155]. To this aim, HeLa cells were processed as indicated in the Tali® Apoptosis Kit (Molecular Probes-Life Technologies) and analyzed on a Tali® Image-Based cytometer (Invitrogen-

Life Technologies). Conversely, rat neurons were stained with 1 μM PI (Molecular Probes-Life Technologies) for 5 min at room temperature (RT), then fixed with 4% paraformaldehyde (PFA) and stained with 1 μM Hoechst 33342 (Molecular Probes-Life Technologies) for 20 min at RT. Coverslips were then mounted on slides and analyzed on an Axiovert 200M microscope (Carl Zeiss) equipped with a 40× water immersion objective (N.A. 1.2, from Carl Zeiss) and a CoolSnap HQ CCD camera (Photometrics). Fifty random fields per condition were acquired in MetaMorph® (Molecular Devices) and images were analyzed with CellProfiler (Broad Institute) using a customized pipeline for the quantification of PI^+ GFP^+ cells.

Calcein-Co^{2+} assays. HeLa Cells were loaded with 1 mM calcein acetoxymethyl ester and Co2+ as instructed by the Image-IT® LIVE Mitochondrial Transition Pore Assay Kit (Molecular Probes-Life Technologies). Cells were then imaged by means of 490 ± 20 nm excitation and 525 nm longpass emission filters on a Axiovert 200M fluorescence microscope equipped with a 40× water immersion objective (N.A. 1.2, from Carl Zeiss). Finally, images were analyzed with MetaMorph® and quenching rates were determined as the slopes of the fluorescence trace over a period of 60 sec post-stimulation.

Quantification of Δψ. Cells were loaded with 1 nM tetramethylrhodamine methyl ester (TMRM, from Molecular Probes-Life Technologies) in complete DMEM high glucose for MEFs cells and in Krebs-Ringer buffer supplemented with 250 μM sulfinpyrazone for HeLa cells, then placed in a humidified chamber at 37°C and imaged with a LiveScan Swept Field Confocal Microscope (Nikon Instruments Inc.) equipped with a 60× oil immersion (N.A. 1.4, from Nikon Instruments Inc.) every 30 sec for 30 min. TMRM fluorescence was analyzed by means of the NIS Elements software package (Nikon Instruments Inc.), and depolarization rates were defined as the slopes of the fluorescence trace over a period of 10 min post-stimulation.

Quantification of mitochondrial ATP. HeLa cells expressing a mitochondrially targeted variant of the Photinus pyralis lucifer- ase were perfused with a modified Krebs-Ringer buffer containing 125 mM NaCl, 5 mM KCl, 1 mM Na_3PO_4, 1 mM $MgSO_4$, 1 mM $CaCl_2$, 20 μM luciferin and 20 mM HEPES buffer (pH 7.4 at 37°C), and luciferin-dependent luminescence was moni- tored with a customized luminometer (Elettrofor), as previously described [120].

Analysis of mitochondrial morphology. HeLa cells expressing a mitochondrially targeted variant of GFP [151] were imaged with an IX-81 automated epifluorescence microscope (Olympus) equipped with a 60× oil immersion objective (N.A. 1.35, from Olympus) and an ORCA-R CCD camera (Hamamatsu Photonics K.K.). Selected cells were followed over time, and z-stacks were subjected to digital deconvolution by means of a Wiener deconvolution filter and a theoretical point-spread function provided by the Xcellence software (Olympus). GFP+ objects were quantified with the "3D object counter" plug-in of the open-source Fiji software (freely available at http://fiji.sc/), whereas 3D representations were obtained with the "3D Viewer" plug-in.

Immunofluorescence microscopy. Immunofluorescence microscopy was performed according to standard procedures [156]. Briefly, cells were fixed in 4% PFA for 20 min at RT, washed three times in PBS and permeabilized with 0.1% Triton X-100 (v:v in PBS) for 5 min at RT. Thereafter, unspecific binding sites were blocked by incubating cells in 2% powdered milk (w:v in PBS) for 1 h at RT. Cells were then incubated overnight at 4°C with primary antibodies specific for HSPD1 (1:100 in blocking buffer) or MYC (1:25 in blocking buffer) (both from Abcam). Finally, primary antibodies were revealed by means of appropri- ate AlexaFluor 488® and AlexaFluor 594® conjugates (Molecular Probes-Life Technologies). Images were acquired on an Axiovert 220 M microscope equipped with a 100× oil immersion Plan Neofluar® objective (N.A. 1.3, from Carl Zeiss) and a CoolSnap HQ CCD camera. Each field was acquired over 21 z-planes spaced by 0.5 μm, and z-stacks were deconvoluted with the "Parallel Iterative Deconvolution" plug-in of Fiji.

Immunoblotting. To obtain whole-cell extracts, cells were washed, harvested and lysed in RIPA buffer (50 mM TRIS-HCl pH 7.8, 150 mM NaCl, 1% IGEPAL CA-630, 0.5% sodium deoxycholate, 0.1% SDS, 1 mM dithiothreitol) supplemented with 2 mM Na_3VO_4, 2 mM NaF, 1 mM phenylmethylsulfonyl fluoride and Complete Protease Inhibitor Cocktail® (Roche Diagnostics Corp.). Alternatively, cytosolic extracts were obtained by digitonin permeabilization, as previously described.74 Thereafter, protein extracts (30 μg/lane) were separated on precast 4–12% SDS-PAGE gels (Life Sciences), electrotransfered onto PVDF membranes (Bio-Rad) and probed with antibodies specific for Cyclin A (non-commercial), pHH3 (Millipore), MCU (Sigma), p27 (BD Biosciences), the F_O a subunit (Abcam), the F_O c subunit (Abcam), the F1 α subunit (Abcam), cytochrome c (BD Biosciences) and VDAC1 (Abcam). An antibody specific for β actin (Sigma-Aldrich) and for Skp1 (Santa Cruz) were used to monitor equal lane loading. Finally, membranes

were incubated with appropriate horseradish peroxidase-conjugated secondary antibodies (Southern Biotech), followed by chemiluminescence detection with the SuperSignal West Pico® reagent and CL-XPosure® X-ray films (both from Thermo Scientific-Pierce).

Cell cycle analysis by Tali® Image-Based Cytometer. It is a 3-channel (bright field, green fluorescence, red fluorescence) benchtop assay platform that uses state-of-the-art optics and image analysis to perform assays for cells in suspension, including GFP and RFP expression, apoptosis, cell viability (live, dead, and total cells), cell counting and cell cycle assays.

Cells previously infected with an adenovirus expressing mtGFP or MCU-GFP and cells not infected were collected in a tube and centrifuged 250 x g for 5 min at 4 ° C, resuspended in an appropriate volume of medium and counted. At this point, it is taken a number of cells in a range between 1 x 10^5 and 5 x 10^6. Cells are centrifuged 500 x g for 5 min at 4 °C, the pellet is resuspended in PBS and centrifuged again. PBS is removed and cells are resuspended in 70% of cold ethanol and are stored at -20 °C at least for 24 h. Cells are then centrifuged 500 x g for 5 min at 4 °C and the pellet resuspended in 1 ml of PBS. After another centrifugation 500 x g for 10 min at 4 °C pellet is resuspended in 200 µl of Tali® Cell Cycle Solution (containing Propidium Iodide (PI) and RNAse) and in 30 min at RT cells are ready to be analyzed.

Cell cycle analysis by FACS (Fluorescence-Activated Cell Sorting). Samples were prepared as previously described for cell cycle analysis by Tali® Image-Based Cytometer, but at the end cells were resuspended in a solution home made containing PI and RNAse.

Statistical procedures. Unless otherwise indicated, assays were performed in triplicate independent instances, yielding comparable results. Data, which are presented as means ± SEM, were analyzed with Microsoft Excel (Microsoft Co.). Statistical significance was determined by means of ANOVA followed by two-tailed unpaired Student's t-tests. p values < 0.05 were considered statistically significant.

REFERENCES

[1] S.D. Dyall, M.T. Brown, P.J. Johnson, Ancient invasions: from endosymbionts to organelles, Science, 304 (2004) 253-257.

[2] T.G. Frey, C.A. Mannella, The internal structure of mitochondria, Trends Biochem Sci, 25 (2000) 319-324.

[3] F. Vogel, C. Bornhovd, W. Neupert, A.S. Reichert, Dynamic subcompartmentalization of the mitochondrial inner membrane, J Cell Biol, 175 (2006) 237-247.

[4] G. Benard, R. Rossignol, Ultrastructure of the mitochondrion and its bearing on function and bioenergetics, Antioxid Redox Signal, 10 (2008) 1313-1342.

[5] G.M. Cereghetti, L. Scorrano, The many shapes of mitochondrial death, Oncogene, 25 (2006) 4717-4724.

[6] A. Santel, M.T. Fuller, Control of mitochondrial morphology by a human mitofusin, J Cell Sci, 114 (2001) 867-874.

[7] D.I. James, P.A. Parone, Y. Mattenberger, J.C. Martinou, hFis1, a novel component of the mammalian mitochondrial fission machinery, J Biol Chem, 278 (2003) 36373-36379.

[8] E. Smirnova, L. Griparic, D.L. Shurland, A.M. van der Bliek, Dynamin-related protein Drp1 is required for mitochondrial division in mammalian cells, Mol Biol Cell, 12 (2001) 2245-2256.

[9] Y. Yoon, E.W. Krueger, B.J. Oswald, M.A. McNiven, The mitochondrial protein hFis1 regulates mitochondrial fission in mammalian cells through an interaction with the dynamin-like protein DLP1, Mol Cell Biol, 23 (2003) 5409-5420.

[10] T. Yu, J.L. Robotham, Y. Yoon, Increased production of reactive oxygen species in hyperglycemic conditions requires dynamic change of mitochondrial morphology, Proc Natl Acad Sci U S A, 103 (2006) 2653-2658.

[11] G. Csordas, G. Hajnoczky, SR/ER-mitochondrial local communication: calcium and ROS, Biochim Biophys Acta, 1787 (2009) 1352-1362.

[12] H.A. Krebs, L.V. Eggleston, The oxidation of pyruvate in pigeon breast muscle, Biochem J, 34 (1940) 442-459.

[13] D.O. Lambeth, K.N. Tews, S. Adkins, D. Frohlich, B.I. Milavetz, Expression of two succinyl-CoA synthetases with different nucleotide specificities in mammalian tissues, J Biol Chem, 279 (2004) 36621-36624.

[14] S. Amemori, R. Iwakiri, H. Endo, A. Ootani, S. Ogata, T. Noda, S. Tsunada, H. Sakata, H. Matsunaga, M. Mizuguchi, Y. Ikeda, K. Fujimoto, Oral dimethyl sulfoxide for

systemic amyloid A amyloidosis complication in chronic inflammatory disease: a retrospective patient chart review, J Gastroenterol, 41 (2006) 444-449.

[15] M. Bonora, S. Patergnani, A. Rimessi, E. De Marchi, J.M. Suski, A. Bononi, C. Giorgi, S. Marchi, S. Missiroli, F. Poletti, M.R. Wieckowski, P. Pinton, ATP synthesis and storage, Purinergic Signal, 8 (2012) 343-357.

[16] P.J. Quinn, R.M. Dawson, Interactions of cytochrome c and [14C], Biochem J, 115 (1969) 65-75.

[17] P. Mitchell, Keilin's respiratory chain concept and its chemiosmotic consequences, Science, 206 (1979) 1148-1159.

[18] P.D. Boyer, Catalytic site forms and controls in ATP synthase catalysis, Biochim Biophys Acta, 1458 (2000) 252-262.

[19] S.J. Ferguson, ATP synthase: from sequence to ring size to the P/O ratio, Proc Natl Acad Sci U S A, 107 (2010) 16755-16756.

[20] Y. Zhuo, H. Luo, K. Zhang, Leber hereditary optic neuropathy and oxidative stress, Proc Natl Acad Sci U S A, 109 (2012) 19882-19883.

[21] M. Bonora, A. Bononi, E. De Marchi, C. Giorgi, M. Lebiedzinska, S. Marchi, S. Patergnani, A. Rimessi, J.M. Suski, A. Wojtala, M.R. Wieckowski, G. Kroemer, L. Galluzzi, P. Pinton, Role of the c subunit of the FO ATP synthase in mitochondrial permeability transition, Cell Cycle, 12 (2013) 674-683.

[22] M.R. Duchen, Mitochondria in health and disease: perspectives on a new mitochondrial biology, Mol Aspects Med, 25 (2004) 365-451.

[23] S. DiMauro, E.A. Schon, Mitochondrial respiratory-chain diseases, N Engl J Med, 348 (2003) 2656-2668.

[24] S. Anderson, A.T. Bankier, B.G. Barrell, M.H. de Bruijn, A.R. Coulson, J. Drouin, I.C. Eperon, D.P. Nierlich, B.A. Roe, F. Sanger, P.H. Schreier, A.J. Smith, R. Staden, I.G. Young, Sequence and organization of the human mitochondrial genome, Nature, 290 (1981) 457-465.

[25] G. Kroemer, L. Galluzzi, C. Brenner, Mitochondrial membrane permeabilization in cell death, Physiol Rev, 87 (2007) 99-163.

[26] C. Garrido, L. Galluzzi, M. Brunet, P.E. Puig, C. Didelot, G. Kroemer, Mechanisms of cytochrome c release from mitochondria, Cell Death Differ, 13 (2006) 1423-1433.

[27] M.M. Hill, C. Adrain, S.J. Martin, Portrait of a killer: the mitochondrial apoptosome emerges from the shadows, Mol Interv, 3 (2003) 19-26.

[28] J.F. Turrens, Mitochondrial formation of reactive oxygen species, J Physiol, 552 (2003) 335-344.

[29] P. Pinton, A. Rimessi, S. Marchi, F. Orsini, E. Migliaccio, M. Giorgio, C. Contursi, S. Minucci, F. Mantovani, M.R. Wieckowski, G. Del Sal, P.G. Pelicci, R. Rizzuto, Protein kinase C beta and prolyl isomerase 1 regulate mitochondrial effects of the life-span determinant p66Shc, Science, 315 (2007) 659-663.

[30] M. Giorgio, E. Migliaccio, F. Orsini, D. Paolucci, M. Moroni, C. Contursi, G. Pelliccia, L. Luzi, S. Minucci, M. Marcaccio, P. Pinton, R. Rizzuto, P. Bernardi, F. Paolucci, P.G. Pelicci, Electron transfer between cytochrome c and p66Shc generates reactive oxygen species that trigger mitochondrial apoptosis, Cell, 122 (2005) 221-233.

[31] E. De Marchi, F. Baldassari, A. Bononi, M.R. Wieckowski, P. Pinton, Oxidative stress in cardiovascular diseases and obesity: role of p66Shc and protein kinase C, Oxid Med Cell Longev, 2013 (2013) 564961.

[32] P. Pinton, R. Rizzuto, Bcl-2 and Ca2+ homeostasis in the endoplasmic reticulum, Cell Death Differ, 13 (2006) 1409-1418.

[33] N.N. Danial, S.J. Korsmeyer, Cell death: critical control points, Cell, 116 (2004) 205-219.

[34] C. Giorgi, D. De Stefani, A. Bononi, R. Rizzuto, P. Pinton, Structural and functional link between the mitochondrial network and the endoplasmic reticulum, Int J Biochem Cell Biol, 41 (2009) 1817-1827.

[35] J.E. Vance, Phospholipid synthesis in a membrane fraction associated with mitochondria, J Biol Chem, 265 (1990) 7248-7256.

[36] M.J. Berridge, P. Lipp, M.D. Bootman, The versatility and universality of calcium signalling, Nat Rev Mol Cell Biol, 1 (2000) 11-21.

[37] C.S. Rossi, A.L. Lehninger, Stoichiometric relationships between mitochondrialion accumulation and oxidative phosphorylation, Biochem Biophys Res Commun, 11 (1963) 441-446.

[38] C. Giorgi, A. Romagnoli, P. Pinton, R. Rizzuto, Ca2+ signaling, mitochondria and cell death, Curr Mol Med, 8 (2008) 119-130.

[39] D.G. Nicholls, Mitochondria and calcium signaling, Cell Calcium, 38 (2005) 311-317.

[40] D. De Stefani, A. Raffaello, E. Teardo, I. Szabo, R. Rizzuto, A forty-kilodalton protein of the inner membrane is the mitochondrial calcium uniporter, Nature, 476 (2011) 336-340.

[41] J.M. Baughman, F. Perocchi, H.S. Girgis, M. Plovanich, C.A. Belcher-Timme, Y. Sancak, X.R. Bao, L. Strittmatter, O. Goldberger, R.L. Bogorad, V. Koteliansky, V.K. Mootha, Integrative genomics identifies MCU as an essential component of the mitochondrial calcium uniporter, Nature, 476 (2011) 341-345.

[42] R. Palty, W.F. Silverman, M. Hershfinkel, T. Caporale, S.L. Sensi, J. Parnis, C. Nolte, D. Fishman, V. Shoshan-Barmatz, S. Herrmann, D. Khananshvili, I. Sekler, NCLX is an essential component of mitochondrial Na+/Ca2+ exchange, Proc Natl Acad Sci U S A, 107 (2010) 436-441.
[43] P. Castaldo, M. Cataldi, S. Magi, V. Lariccia, S. Arcangeli, S. Amoroso, Role of the mitochondrial sodium/calcium exchanger in neuronal physiology and in the pathogenesis of neurological diseases, Prog Neurobiol, 87 (2009) 58-79.
[44] A. Villa, M.I. Garcia-Simon, P. Blanco, B. Sese, E. Bogonez, J. Satrustegui, Affinity chromatography purification of mitochondrial inner membrane proteins with calcium transport activity, Biochim Biophys Acta, 1373 (1998) 347-359.
[45] P. Bernardi, V. Petronilli, The permeability transition pore as a mitochondrial calcium release channel: a critical appraisal, J Bioenerg Biomembr, 28 (1996) 131-138.
[46] L. Santella, E. Ercolano, G.A. Nusco, The cell cycle: a new entry in the field of Ca2+ signaling, Cell Mol Life Sci, 62 (2005) 2405-2413.
[47] K.A. Skelding, J.A. Rostas, N.M. Verrills, Controlling the cell cycle: the role of calcium/calmodulin-stimulated protein kinases I and II, Cell Cycle, 10 (2011) 631-639.
[48] C.R. Kahl, A.R. Means, Regulation of cell cycle progression by calcium/calmodulin-dependent pathways, Endocr Rev, 24 (2003) 719-736.
[49] A. Raffaello, D. De Stefani, R. Rizzuto, The mitochondrial Ca(2+) uniporter, Cell Calcium, 52 (2012) 16-21.
[50] M. Bragadin, T. Pozzan, G.F. Azzone, Kinetics of Ca2+ carrier in rat liver mitochondria, Biochemistry, 18 (1979) 5972-5978.
[51] B. Moreau, C. Nelson, A.B. Parekh, Biphasic regulation of mitochondrial Ca2+ uptake by cytosolic Ca2+ concentration, Curr Biol, 16 (2006) 1672-1677.
[52] M. Trenker, R. Malli, I. Fertschai, S. Levak-Frank, W.F. Graier, Uncoupling proteins 2 and 3 are fundamental for mitochondrial Ca2+ uniport, Nat Cell Biol, 9 (2007) 445-452.
[53] P.S. Brookes, N. Parker, J.A. Buckingham, A. Vidal-Puig, A.P. Halestrap, T.E. Gunter, D.G. Nicholls, P. Bernardi, J.J. Lemasters, M.D. Brand, UCPs--unlikely calcium porters, Nat Cell Biol, 10 (2008) 1235-1237; author reply 1237-1240.
[54] F. Perocchi, V.M. Gohil, H.S. Girgis, X.R. Bao, J.E. McCombs, A.E. Palmer, V.K. Mootha, MICU1 encodes a mitochondrial EF hand protein required for Ca(2+) uptake, Nature, 467 (2010) 291-296.
[55] M. Patron, A. Raffaello, V. Granatiero, A. Tosatto, G. Merli, D. De Stefani, L. Wright, G. Pallafacchina, A. Terrin, C. Mammucari, R. Rizzuto, The mitochondrial

calcium uniporter (MCU): molecular identity and physiological roles, J Biol Chem, 288 (2013) 10750-10758.
[56] S. Marchi, L. Lupini, S. Patergnani, A. Rimessi, S. Missiroli, M. Bonora, A. Bononi, F. Corra, C. Giorgi, E. De Marchi, F. Poletti, R. Gafa, G. Lanza, M. Negrini, R. Rizzuto, P. Pinton, Downregulation of the mitochondrial calcium uniporter by cancer-related miR-25, Curr Biol, 23 (2013) 58-63.
[57] K. Mallilankaraman, P. Doonan, C. Cardenas, H.C. Chandramoorthy, M. Muller, R. Miller, N.E. Hoffman, R.K. Gandhirajan, J. Molgo, M.J. Birnbaum, B.S. Rothberg, D.O. Mak, J.K. Foskett, M. Madesh, MICU1 is an essential gatekeeper for MCU-mediated mitochondrial Ca(2+) uptake that regulates cell survival, Cell, 151 (2012) 630-644.
[58] G. Csordas, T. Golenar, E.L. Seifert, K.J. Kamer, Y. Sancak, F. Perocchi, C. Moffat, D. Weaver, S. de la Fuente Perez, R. Bogorad, V. Koteliansky, J. Adijanto, V.K. Mootha, G. Hajnoczky, MICU1 controls both the threshold and cooperative activation of the mitochondrial Ca(2)(+) uniporter, Cell Metab, 17 (2013) 976-987.
[59] M. Plovanich, R.L. Bogorad, Y. Sancak, K.J. Kamer, L. Strittmatter, A.A. Li, H.S. Girgis, S. Kuchimanchi, J. De Groot, L. Speciner, N. Taneja, J. Oshea, V. Koteliansky, V.K. Mootha, MICU2, a paralog of MICU1, resides within the mitochondrial uniporter complex to regulate calcium handling, PLoS One, 8 (2013) e55785.
[60] A. Raffaello, D. De Stefani, D. Sabbadin, E. Teardo, G. Merli, A. Picard, V. Checchetto, S. Moro, I. Szabo, R. Rizzuto, The mitochondrial calcium uniporter is a multimer that can include a dominant-negative pore-forming subunit, EMBO J, 32 (2013) 2362-2376.
[61] F. Fieni, S.B. Lee, Y.N. Jan, Y. Kirichok, Activity of the mitochondrial calcium uniporter varies greatly between tissues, Nat Commun, 3 (2012) 1317.
[62] K. Mallilankaraman, C. Cardenas, P.J. Doonan, H.C. Chandramoorthy, K.M. Irrinki, T. Golenar, G. Csordas, P. Madireddi, J. Yang, M. Muller, R. Miller, J.E. Kolesar, J. Molgo, B. Kaufman, G. Hajnoczky, J.K. Foskett, M. Madesh, MCUR1 is an essential component of mitochondrial Ca2+ uptake that regulates cellular metabolism, Nat Cell Biol, 14 (2012) 1336-1343.
[63] Y. Sancak, A.L. Markhard, T. Kitami, E. Kovacs-Bogdan, K.J. Kamer, N.D. Udeshi, S.A. Carr, D. Chaudhuri, D.E. Clapham, A.A. Li, S.E. Calvo, O. Goldberger, V.K. Mootha, EMRE is an essential component of the mitochondrial calcium uniporter complex, Science, 342 (2013) 1379-1382.
[64] S. Marchi, P. Pinton, The mitochondrial calcium uniporter complex: molecular components, structure and physiopathological implications, J Physiol, 592 (2014) 829-839.

[65] M. Patron, V. Checchetto, A. Raffaello, E. Teardo, D. Vecellio Reane, M. Mantoan, V. Granatiero, I. Szabo, D. De Stefani, R. Rizzuto, MICU1 and MICU2 Finely Tune the Mitochondrial Ca Uniporter by Exerting Opposite Effects on MCU Activity, Mol Cell, (2014).
[66] C. Brenner, S. Grimm, The permeability transition pore complex in cancer cell death, Oncogene, 25 (2006) 4744-4756.
[67] I. Szabo, V. De Pinto, M. Zoratti, The mitochondrial permeability transition pore may comprise VDAC molecules. II. The electrophysiological properties of VDAC are compatible with those of the mitochondrial megachannel, FEBS Lett, 330 (1993) 206-210.
[68] G. Beutner, A. Ruck, B. Riede, D. Brdiczka, Complexes between porin, hexokinase, mitochondrial creatine kinase and adenylate translocator display properties of the permeability transition pore. Implication for regulation of permeability transition by the kinases, Biochim Biophys Acta, 1368 (1998) 7-18.
[69] P. Varanyuwatana, A.P. Halestrap, The roles of phosphate and the phosphate carrier in the mitochondrial permeability transition pore, Mitochondrion, 12 (2012) 120-125.
[70] E. Basso, L. Fante, J. Fowlkes, V. Petronilli, M.A. Forte, P. Bernardi, Properties of the permeability transition pore in mitochondria devoid of Cyclophilin D, J Biol Chem, 280 (2005) 18558-18561.
[71] A.C. Schinzel, O. Takeuchi, Z. Huang, J.K. Fisher, Z. Zhou, J. Rubens, C. Hetz, N.N. Danial, M.A. Moskowitz, S.J. Korsmeyer, Cyclophilin D is a component of mitochondrial permeability transition and mediates neuronal cell death after focal cerebral ischemia, Proc Natl Acad Sci U S A, 102 (2005) 12005-12010.
[72] J. Sileikyte, V. Petronilli, A. Zulian, F. Dabbeni-Sala, G. Tognon, P. Nikolov, P. Bernardi, F. Ricchelli, Regulation of the inner membrane mitochondrial permeability transition by the outer membrane translocator protein (peripheral benzodiazepine receptor), J Biol Chem, 286 (2011) 1046-1053.
[73] F. Chiara, D. Castellaro, O. Marin, V. Petronilli, W.S. Brusilow, M. Juhaszova, S.J. Sollott, M. Forte, P. Bernardi, A. Rasola, Hexokinase II detachment from mitochondria triggers apoptosis through the permeability transition pore independent of voltage-dependent anion channels, PLoS One, 3 (2008) e1852.
[74] M.G. Vander Heiden, X.X. Li, E. Gottleib, R.B. Hill, C.B. Thompson, M. Colombini, Bcl-xL promotes the open configuration of the voltage-dependent anion channel and metabolite passage through the outer mitochondrial membrane, J Biol Chem, 276 (2001) 19414-19419.

[75] S. Shimizu, M. Narita, Y. Tsujimoto, Bcl-2 family proteins regulate the release of apoptogenic cytochrome c by the mitochondrial channel VDAC, Nature, 399 (1999) 483-487.
[76] N. Zamzami, C. El Hamel, C. Maisse, C. Brenner, C. Munoz-Pinedo, A.S. Belzacq, P. Costantini, H. Vieira, M. Loeffler, G. Molle, G. Kroemer, Bid acts on the permeability transition pore complex to induce apoptosis, Oncogene, 19 (2000) 6342-6350.
[77] H.K. Baumgartner, J.V. Gerasimenko, C. Thorne, P. Ferdek, T. Pozzan, A.V. Tepikin, O.H. Petersen, R. Sutton, A.J. Watson, O.V. Gerasimenko, Calcium elevation in mitochondria is the main Ca2+ requirement for mitochondrial permeability transition pore (mPTP) opening, J Biol Chem, 284 (2009) 20796-20803.
[78] C. Giorgi, F. Baldassari, A. Bononi, M. Bonora, E. De Marchi, S. Marchi, S. Missiroli, S. Patergnani, A. Rimessi, J.M. Suski, M.R. Wieckowski, P. Pinton, Mitochondrial Ca(2+) and apoptosis, Cell Calcium, 52 (2012) 36-43.
[79] C. Chinopoulos, V. Adam-Vizi, Calcium, mitochondria and oxidative stress in neuronal pathology. Novel aspects of an enduring theme, FEBS J, 273 (2006) 433-450.
[80] R.A. Altschuld, C.M. Hohl, L.C. Castillo, A.A. Garleb, R.C. Starling, G.P. Brierley, Cyclosporin inhibits mitochondrial calcium efflux in isolated adult rat ventricular cardiomyocytes, Am J Physiol, 262 (1992) H1699-1704.
[81] J.W. Elrod, R. Wong, S. Mishra, R.J. Vagnozzi, B. Sakthievel, S.A. Goonasekera, J. Karch, S. Gabel, J. Farber, T. Force, J.H. Brown, E. Murphy, J.D. Molkentin, Cyclophilin D controls mitochondrial pore-dependent Ca(2+) exchange, metabolic flexibility, and propensity for heart failure in mice, J Clin Invest, 120 (2010) 3680-3687.
[82] A.C. Wei, T. Liu, S. Cortassa, R.L. Winslow, B. O'Rourke, Mitochondrial Ca2+ influx and efflux rates in guinea pig cardiac mitochondria: low and high affinity effects of cyclosporine A, Biochim Biophys Acta, 1813 (2011) 1373-1381.
[83] O. Eriksson, P. Pollesello, E. Geimonen, Regulation of total mitochondrial Ca2+ in perfused liver is independent of the permeability transition pore, Am J Physiol, 276 (1999) C1297-1302.
[84] R. Rizzuto, A.W. Simpson, M. Brini, T. Pozzan, Rapid changes of mitochondrial Ca2+ revealed by specifically targeted recombinant aequorin, Nature, 358 (1992) 325-327.
[85] O. Shimomura, F.H. Johnson, Y. Saiga, Extraction, purification and properties of aequorin, a bioluminescent protein from the luminous hydromedusan, Aequorea, J Cell Comp Physiol, 59 (1962) 223-239.

[86] M. Brini, R. Marsault, C. Bastianutto, J. Alvarez, T. Pozzan, R. Rizzuto, Transfected aequorin in the measurement of cytosolic Ca2+ concentration ([Ca2+]c). A critical evaluation, J Biol Chem, 270 (1995) 9896-9903.
[87] N.J. Watkins, A.K. Campbell, Requirement of the C-terminal proline residue for stability of the Ca(2+)-activated photoprotein aequorin, Biochem J, 293 (Pt 1) (1993) 181-185.
[88] R. Rizzuto, M. Brini, T. Pozzan, Targeting recombinant aequorin to specific intracellular organelles, Methods Cell Biol, 40 (1994) 339-358.
[89] J.P. Hendrick, P.E. Hodges, L.E. Rosenberg, Survey of amino-terminal proteolytic cleavage sites in mitochondrial precursor proteins: leader peptides cleaved by two matrix proteases share a three-amino acid motif, Proc Natl Acad Sci U S A, 86 (1989) 4056-4060.
[90] M. Brini, L. Pasti, C. Bastianutto, M. Murgia, T. Pozzan, R. Rizzuto, Targeting of aequorin for calcium monitoring in intracellular compartments, J Biolumin Chemilumin, 9 (1994) 177-184.
[91] M. Bonora, C. Giorgi, A. Bononi, S. Marchi, S. Patergnani, A. Rimessi, R. Rizzuto, P. Pinton, Subcellular calcium measurements in mammalian cells using jellyfish photoprotein aequorin-based probes, Nat Protoc, 8 (2013) 2105-2118.
[92] R.E. Shackelford, W.K. Kaufmann, R.S. Paules, Cell cycle control, checkpoint mechanisms, and genotoxic stress, Environ Health Perspect, 107 Suppl 1 (1999) 5-24.
[93] A.W. Murray, Recycling the cell cycle: cyclins revisited, Cell, 116 (2004) 221-234.
[94] M. Malumbres, M. Barbacid, Mammalian cyclin-dependent kinases, Trends Biochem Sci, 30 (2005) 630-641.
[95] J.V. Harper, G. Brooks, The mammalian cell cycle: an overview, Methods Mol Biol, 296 (2005) 113-153.
[96] K. Vermeulen, D.R. Van Bockstaele, Z.N. Berneman, The cell cycle: a review of regulation, deregulation and therapeutic targets in cancer, Cell Prolif, 36 (2003) 131-149.
[97] M.D. Bootman, P. Lipp, M.J. Berridge, The organisation and functions of local Ca(2+) signals, J Cell Sci, 114 (2001) 2213-2222.
[98] M. Murgia, C. Giorgi, P. Pinton, R. Rizzuto, Controlling metabolism and cell death: at the heart of mitochondrial calcium signalling, J Mol Cell Cardiol, 46 (2009) 781-788.
[99] L. Lu, M.S. Ladinsky, T. Kirchhausen, Cisternal organization of the endoplasmic reticulum during mitosis, Mol Biol Cell, 20 (2009) 3471-3480.
[100] R. Rizzuto, M. Brini, M. Murgia, T. Pozzan, Microdomains with high Ca2+ close to IP3-sensitive channels that are sensed by neighboring mitochondria, Science, 262 (1993) 744-747.

[101] R.A. Haworth, D.R. Hunter, The Ca2+-induced membrane transition in mitochondria. II. Nature of the Ca2+ trigger site, Arch Biochem Biophys, 195 (1979) 460-467.
[102] M. Crompton, A. Costi, A heart mitochondrial Ca2(+)-dependent pore of possible relevance to re-perfusion-induced injury. Evidence that ADP facilitates pore interconversion between the closed and open states, Biochem J, 266 (1990) 33-39.
[103] I. Szabo, M. Zoratti, The giant channel of the inner mitochondrial membrane is inhibited by cyclosporin A, J Biol Chem, 266 (1991) 3376-3379.
[104] J.E. Kokoszka, K.G. Waymire, S.E. Levy, J.E. Sligh, J. Cai, D.P. Jones, G.R. MacGregor, D.C. Wallace, The ADP/ATP translocator is not essential for the mitochondrial permeability transition pore, Nature, 427 (2004) 461-465.
[105] C.P. Baines, R.A. Kaiser, T. Sheiko, W.J. Craigen, J.D. Molkentin, Voltage-dependent anion channels are dispensable for mitochondrial-dependent cell death, Nat Cell Biol, 9 (2007) 550-555.
[106] L.A. Shchepina, O.Y. Pletjushkina, A.V. Avetisyan, L.E. Bakeeva, E.K. Fetisova, D.S. Izyumov, V.B. Saprunova, M.Y. Vyssokikh, B.V. Chernyak, V.P. Skulachev, Oligomycin, inhibitor of the F0 part of H+-ATP-synthase, suppresses the TNF-induced apoptosis, Oncogene, 21 (2002) 8149-8157.
[107] G. Santamaria, M. Martinez-Diez, I. Fabregat, J.M. Cuezva, Efficient execution of cell death in non-glycolytic cells requires the generation of ROS controlled by the activity of mitochondrial H+-ATP synthase, Carcinogenesis, 27 (2006) 925-935.
[108] S. Matsuyama, Q. Xu, J. Velours, J.C. Reed, The Mitochondrial F0F1-ATPase proton pump is required for function of the proapoptotic protein Bax in yeast and mammalian cells, Mol Cell, 1 (1998) 327-336.
[109] S.A. Novgorodov, T.I. Gudz, G.P. Brierley, D.R. Pfeiffer, Magnesium ion modulates the sensitivity of the mitochondrial permeability transition pore to cyclosporin A and ADP, Arch Biochem Biophys, 311 (1994) 219-228.
[110] M.B. Murataliev, P.D. Boyer, Interaction of mitochondrial F1-ATPase with trinitrophenyl derivatives of ATP and ADP. Participation of third catalytic site and role of Mg2+ in enzyme inactivation, J Biol Chem, 269 (1994) 15431-15439.
[111] M. Crompton, S. Virji, J.M. Ward, Cyclophilin-D binds strongly to complexes of the voltage-dependent anion channel and the adenine nucleotide translocase to form the permeability transition pore, Eur J Biochem, 258 (1998) 729-735.
[112] C.P. Baines, R.A. Kaiser, N.H. Purcell, N.S. Blair, H. Osinska, M.A. Hambleton, E.W. Brunskill, M.R. Sayen, R.A. Gottlieb, G.W. Dorn, J. Robbins, J.D. Molkentin, Loss

of cyclophilin D reveals a critical role for mitochondrial permeability transition in cell death, Nature, 434 (2005) 658-662.
[113] V. Giorgio, E. Bisetto, M.E. Soriano, F. Dabbeni-Sala, E. Basso, V. Petronilli, M.A. Forte, P. Bernardi, G. Lippe, Cyclophilin D modulates mitochondrial F0F1-ATP synthase by interacting with the lateral stalk of the complex, J Biol Chem, 284 (2009) 33982-33988.
[114] K.N. Alavian, H. Li, L. Collis, L. Bonanni, L. Zeng, S. Sacchetti, E. Lazrove, P. Nabili, B. Flaherty, M. Graham, Y. Chen, S.M. Messerli, M.A. Mariggio, C. Rahner, E. McNay, G.C. Shore, P.J. Smith, J.M. Hardwick, E.A. Jonas, Bcl-xL regulates metabolic efficiency of neurons through interaction with the mitochondrial F1FO ATP synthase, Nat Cell Biol, 13 (2011) 1224-1233.
[115] J.C. Greie, T. Heitkamp, K. Altendorf, The transmembrane domain of subunit b of the Escherichia coli F1F(O) ATP synthase is sufficient for H(+)-translocating activity together with subunits a and c, Eur J Biochem, 271 (2004) 3036-3042.
[116] I. Masgras, A. Rasola, P. Bernardi, Induction of the permeability transition pore in cells depleted of mitochondrial DNA, Biochim Biophys Acta, 1817 (2012) 1860-1866.
[117] J.E. McGeoch, G. Guidotti, A 0.1-700 Hz current through a voltage-clamped pore: candidate protein for initiator of neural oscillations, Brain Res, 766 (1997) 188-194.
[118] T.S. Azarashvili, J. Tyynela, I.V. Odinokova, P.A. Grigorjev, M. Baumann, Y.V. Evtodienko, N.E. Saris, Phosphorylation of a peptide related to subunit c of the F0F1-ATPase/ATP synthase and relationship to permeability transition pore opening in mitochondria, J Bioenerg Biomembr, 34 (2002) 279-284.
[119] A. De Grassi, C. Lanave, C. Saccone, Evolution of ATP synthase subunit c and cytochrome c gene families in selected Metazoan classes, Gene, 371 (2006) 224-233.
[120] L.S. Jouaville, P. Pinton, C. Bastianutto, G.A. Rutter, R. Rizzuto, Regulation of mitochondrial ATP synthesis by calcium: evidence for a long-term metabolic priming, Proc Natl Acad Sci U S A, 96 (1999) 13807-13812.
[121] C. Vives-Bauza, J. Magrane, A.L. Andreu, G. Manfredi, Novel role of ATPase subunit C targeting peptides beyond mitochondrial protein import, Mol Biol Cell, 21 (2010) 131-139.
[122] G. Benard, N. Bellance, D. James, P. Parrone, H. Fernandez, T. Letellier, R. Rossignol, Mitochondrial bioenergetics and structural network organization, J Cell Sci, 120 (2007) 838-848.
[123] V. Petronilli, G. Miotto, M. Canton, R. Colonna, P. Bernardi, F. Di Lisa, Imaging the mitochondrial permeability transition pore in intact cells, Biofactors, 8 (1998) 263-272.

[124] E. Basso, V. Petronilli, M.A. Forte, P. Bernardi, Phosphate is essential for inhibition of the mitochondrial permeability transition pore by cyclosporin A and by cyclophilin D ablation, J Biol Chem, 283 (2008) 26307-26311.
[125] J.P. Abrahams, A.G. Leslie, R. Lutter, J.E. Walker, Structure at 2.8 A resolution of F1-ATPase from bovine heart mitochondria, Nature, 370 (1994) 621-628.
[126] A.F. Schinder, E.C. Olson, N.C. Spitzer, M. Montal, Mitochondrial dysfunction is a primary event in glutamate neurotoxicity, J Neurosci, 16 (1996) 6125-6133.
[127] M.R. Duchen, A. Verkhratsky, S. Muallem, Mitochondria and calcium in health and disease, Cell Calcium, 44 (2008) 1-5.
[128] S. Patergnani, S. Marchi, A. Rimessi, M. Bonora, C. Giorgi, K.D. Mehta, P. Pinton, PRKCB/protein kinase C, beta and the mitochondrial axis as key regulators of autophagy, Autophagy, 9 (2013) 1367-1385.
[129] C. Brenner, M. Moulin, Physiological roles of the permeability transition pore, Circ Res, 111 (2012) 1237-1247.
[130] S. Marchi, S. Patergnani, P. Pinton, The endoplasmic reticulum-mitochondria connection: One touch, multiple functions, Biochim Biophys Acta, 1837 (2014) 461-469.
[131] S. Patergnani, J.M. Suski, C. Agnoletto, A. Bononi, M. Bonora, E. De Marchi, C. Giorgi, S. Marchi, S. Missiroli, F. Poletti, A. Rimessi, J. Duszynski, M.R. Wieckowski, P. Pinton, Calcium signaling around Mitochondria Associated Membranes (MAMs), Cell Commun Signal, 9 (2011) 19.
[132] J.B. Parys, J.P. Decuypere, G. Bultynck, Role of the inositol 1,4,5-trisphosphate receptor/Ca2+-release channel in autophagy, Cell Commun Signal, 10 (2012) 17.
[133] S. Shimizu, A. Konishi, T. Kodama, Y. Tsujimoto, BH4 domain of antiapoptotic Bcl-2 family members closes voltage-dependent anion channel and inhibits apoptotic mitochondrial changes and cell death, Proc Natl Acad Sci U S A, 97 (2000) 3100-3105.
[134] S.S. Smaili, J.T. Russell, Permeability transition pore regulates both mitochondrial membrane potential and agonist-evoked Ca2+ signals in oligodendrocyte progenitors, Cell Calcium, 26 (1999) 121-130.
[135] A. Barsukova, A. Komarov, G. Hajnoczky, P. Bernardi, D. Bourdette, M. Forte, Activation of the mitochondrial permeability transition pore modulates Ca2+ responses to physiological stimuli in adult neurons, Eur J Neurosci, 33 (2011) 831-842.
[136] V. Giorgio, S. von Stockum, M. Antoniel, A. Fabbro, F. Fogolari, M. Forte, G.D. Glick, V. Petronilli, M. Zoratti, I. Szabo, G. Lippe, P. Bernardi, Dimers of mitochondrial ATP synthase form the permeability transition pore, Proc Natl Acad Sci U S A, 110 (2013) 5887-5892.

[137] T. Azarashvili, I. Odinokova, A. Bakunts, V. Ternovsky, O. Krestinina, J. Tyynela, N.E. Saris, Potential role of subunit c of F0F1-ATPase and subunit c of storage body in the mitochondrial permeability transition. Effect of the phosphorylation status of subunit c on pore opening, Cell Calcium, 55 (2014) 69-77.
[138] D.A. Cox, L. Conforti, N. Sperelakis, M.A. Matlib, Selectivity of inhibition of Na(+)-Ca2+ exchange of heart mitochondria by benzothiazepine CGP-37157, J Cardiovasc Pharmacol, 21 (1993) 595-599.
[139] K.M. Broekemeier, M.E. Dempsey, D.R. Pfeiffer, Cyclosporin A is a potent inhibitor of the inner membrane permeability transition in liver mitochondria, J Biol Chem, 264 (1989) 7826-7830.
[140] R. Assaly, A. de Tassigny, S. Paradis, S. Jacquin, A. Berdeaux, D. Morin, Oxidative stress, mitochondrial permeability transition pore opening and cell death during hypoxia-reoxygenation in adult cardiomyocytes, Eur J Pharmacol, 675 (2012) 6-14.
[141] P. Bernardi, S. von Stockum, The permeability transition pore as a Ca(2+) release channel: new answers to an old question, Cell Calcium, 52 (2012) 22-27.
[142] A.P. Halestrap, P. Pasdois, The role of the mitochondrial permeability transition pore in heart disease, Biochim Biophys Acta, 1787 (2009) 1402-1415.
[143] M. Crompton, H. Ellinger, A. Costi, Inhibition by cyclosporin A of a Ca2+-dependent pore in heart mitochondria activated by inorganic phosphate and oxidative stress, Biochem J, 255 (1988) 357-360.
[144] D.S. Cassarino, R.H. Swerdlow, J.K. Parks, W.D. Parker, Jr., J.P. Bennett, Jr., Cyclosporin A increases resting mitochondrial membrane potential in SY5Y cells and reverses the depressed mitochondrial membrane potential of Alzheimer's disease cybrids, Biochem Biophys Res Commun, 248 (1998) 168-173.
[145] M. Saotome, H. Katoh, Y. Yaguchi, T. Tanaka, T. Urushida, H. Satoh, H. Hayashi, Transient opening of mitochondrial permeability transition pore by reactive oxygen species protects myocardium from ischemia-reperfusion injury, Am J Physiol Heart Circ Physiol, 296 (2009) H1125-1132.
[146] F. Rigoni, Y. Mathien-Shire, R. Deana, Effect of ruthenium red on calcium efflux from rat liver mitochondria, FEBS Lett, 120 (1980) 255-258.
[147] T. Kristian, N.B. Pivovarova, G. Fiskum, S.B. Andrews, Calcium-induced precipitate formation in brain mitochondria: composition, calcium capacity, and retention, J Neurochem, 102 (2007) 1346-1356.

[148] L. Pasti, T. Pozzan, G. Carmignoto, Long-lasting changes of calcium oscillations in astrocytes. A new form of glutamate-mediated plasticity, The Journal of biological chemistry, 270 (1995) 15203-15210.
[149] L. Galluzzi, E. Morselli, I. Vitale, O. Kepp, L. Senovilla, A. Criollo, N. Servant, C. Paccard, P. Hupe, T. Robert, H. Ripoche, V. Lazar, A. Harel-Bellan, P. Dessen, E. Barillot, G. Kroemer, miR-181a and miR-630 regulate cisplatin-induced cancer cell death, Cancer Res, 70 (2010) 1793-1803.
[150] R. Rizzuto, P. Pinton, W. Carrington, F.S. Fay, K.E. Fogarty, L.M. Lifshitz, R.A. Tuft, T. Pozzan, Close contacts with the endoplasmic reticulum as determinants of mitochondrial Ca2+ responses, Science, 280 (1998) 1763-1766.
[151] F. De Giorgi, Z. Ahmed, C. Bastianutto, M. Brini, L.S. Jouaville, R. Marsault, M. Murgia, P. Pinton, T. Pozzan, R. Rizzuto, Targeting GFP to organelles, Methods Cell Biol, 58 (1999) 75-85.
[152] P. Pinton, D. Ferrari, P. Magalhaes, K. Schulze-Osthoff, F. Di Virgilio, T. Pozzan, R. Rizzuto, Reduced loading of intracellular Ca(2+) stores and downregulation of capacitative Ca(2+) influx in Bcl-2-overexpressing cells, J Cell Biol, 148 (2000) 857-862.
[153] T.J. Schoenmakers, G.J. Visser, G. Flik, A.P. Theuvenet, CHELATOR: an improved method for computing metal ion concentrations in physiological solutions, Biotechniques, 12 (1992) 870-874, 876-879.
[154] O. Kepp, L. Galluzzi, M. Lipinski, J. Yuan, G. Kroemer, Cell death assays for drug discovery, Nat Rev Drug Discov, 10 (2011) 221-237.
[155] L. Galluzzi, M.C. Maiuri, I. Vitale, H. Zischka, M. Castedo, L. Zitvogel, G. Kroemer, Cell death modalities: classification and pathophysiological implications, Cell Death Differ, 14 (2007) 1237-1243.
[156] J. Hoffmann, I. Vitale, B. Buchmann, L. Galluzzi, W. Schwede, L. Senovilla, W. Skuballa, S. Vivet, R.B. Lichtner, J.M. Vicencio, T. Panaretakis, G. Siemeister, H. Lage, L. Nanty, S. Hammer, K. Mittelstaedt, S. Winsel, J. Eschenbrenner, M. Castedo, C. Demarche, U. Klar, G. Kroemer, Improved cellular pharmacokinetics and pharmacodynamics underlie the wide anticancer activity of sagopilone, Cancer Res, 68 (2008) 5301-5308.